Journal of Quantitative Spectroscopy & Radiative Transfer 326 (2024) 109083

Contents lists available at ScienceDirect

Journal of Quantitative Spectroscopy and Radiative Transfer

journal homepage: www.elsevier.com/locate/jqsrt

The 2024 release of the ExoMol database: Molecular line lists for exoplanet and other hot atmospheres

Jonathan Tennyson [a,*], Sergei N. Yurchenko [a], Jingxin Zhang [a], Charles A. Bowesman [a], Ryan P. Brady [a], Jeanna Buldyreva [g], Katy L. Chubb [b], Robert R. Gamache [h], Maire N. Gorman [b,j], Elizabeth R. Guest [a], Christian Hill [e], Kyriaki Kefala [a], A.E. Lynas-Gray [a,c,d], Thomas M. Mellor [a], Laura K. McKemmish [f], Georgi B. Mitev [a], Irina I. Mizus [k], Alec Owens [a], Zhijian Peng [a], Armando N. Perri [a], Marco Pezzella [a,i], Oleg L. Polyansky [a,k], Qianwei Qu [a], Mikhail Semenov [a], Oleksiy Smola [a], Andrei Solokov [a], Wilfrid Somogyi [a], Apoorva Upadhyay [a], Samuel O.M. Wright [a], Nikolai F. Zobov [k]

[a] Department of Physics and Astronomy, University College London, Gower Street, London WC1E 6BT, UK
[b] School of Physics, HH Wills Physics Laboratory, Tyndall Avenue, Bristol, BS8 1TL, UK
[c] Department of Physics, University of Oxford, Keble Road, Oxford OX1 3RH, UK
[d] Department of Physics and Astronomy, University of the Western Cape, Private Bag X17, Bellville 7535, South Africa
[e] Nuclear Data Section, International Atomic Energy Agency, Vienna A-1400, Austria
[f] School of Chemistry, University of New South Wales, 2052 Sydney, Australia
[g] Institut UTINAM UMR CNRS 6213, Université de Franche-Comté, 16 Route de Gray, 25030 Besançon cedex, France
[h] Department of Environmental, Earth, and Atmospheric Sciences University of Massachusetts Lowell, Lowell, MA 01854, USA
[i] Dipartimento di Fisica e Geologia, Universitá di Perugia, Via Pascoli SNC, 06123 Perugia, Italy
[j] School of Mathematical and Physical Sciences, University of Sussex, Brighton, BN1 9QH, UK
[k] Institute of Applied Physics, Russian Academy of Sciences, 46 Ulyanov Street, Nizhny Novgorod, 603950, Russia

ARTICLE INFO

Dataset link: www.exomol.com, https://github.com/ExoMol/

Keywords:
Infrared
Visible
Einstein *A* coefficients
Transition frequencies
Partition functions
Cooling functions
Lifetimes
Cross-sections
k coefficients
Pressure broadening
Photodissociation
Ultraviolet

ABSTRACT

The ExoMol database (www.exomol.com) provides molecular data for spectroscopic studies of hot atmospheres. These data are widely used to model atmospheres of exoplanets, cool stars and other astronomical objects, as well as a variety of terrestrial applications. The 2024 data release reports the current status of the database which contains recommended line lists for 91 molecules and 224 isotopologues giving a total of almost 10^{12} individual transitions. New features of the database include extensive "MARVELization" of line lists to allow them to be used for high resolutions studies, extension of several line lists to ultraviolet wavelengths, provision of photodissociation cross-sections and extended provision of broadening parameters. Some of the in-house data specifications have been rewritten in JSON and moved for conformity with other international standards. Data products, including specific heats, a database of lifetimes for plasma studies, and the ExoMolHR web app which allows exclusively high resolution data to be extracted, are discussed.

1. Introduction

The ExoMol project was founded in 2011 to provide molecular line lists for exoplanet and other atmospheres [1] with a particular emphasis on providing results for elevated temperatures which are not adequately covered by databases such as HITRAN [2] or GEISA [3]. ExoMol has followed the practice of providing data release papers every four years with the first two in 2016 [4] and 2020 [5]; the present paper is the third such release. A short review of the first decade of activity by the ExoMol project has been given by the project founders Tennyson and Yurchenko [6].

* Corresponding author.
E-mail address: j.tennyson@ucl.ac.uk (J. Tennyson).

https://doi.org/10.1016/j.jqsrt.2024.109083
Received 21 April 2024; Received in revised form 10 June 2024; Accepted 10 June 2024
Available online 27 June 2024

Since the launch of the project, ExoMol has created line lists for 67 molecules (approaching 150 isoptopologues) details of which are given below. Also discussed below are line lists created by other teams, which are included in the database to ensure coverage of key molecular species as far as possible. A major goal of the original ExoMol project was to provide line lists which were as complete as possible as these have been shown to be essential for correctly reproducing broad band spectra [7] and also opacities. Since that time, high resolution Doppler-shift cross-correlation spectroscopy has been pioneered as a very successful tool for detecting atoms and molecules in exoplanet atmospheres [8–10]. Key line lists constructed with an emphasis on completeness lacked the necessary accuracy for these high resolution studies [11,12], see also Yurchenko et al. [13], thus addressing the needs of high resolution observation led to a significant extension in the scope of the ExoMol project.

The tension between completeness and accuracy in providing hot line lists for astronomical modelling is well known [14]. ExoMol has developed techniques based on the use of the MARVEL (measured active vibration–rotation energy levels) algorithm [15] to provide empirical energy levels from high resolution laboratory spectra. High accuracy energy levels plus extrapolation from them [16] can be used to provide accurate transitions while retaining the completeness of the computed line lists. These procedures are discussed in Section 2.1.

The ExoMol project has continued to provide line lists for new species and has updated and/or extended existing line lists for a number of other molecules. The database has also developed in other directions: notably there has been increasing provision for photoabsorption at shorter wavelengths. Extending the database to ultraviolet wavelengths has led to the need to consider not only line absorption at these wavelengths but also continuum absorption, line broadening due to predissociation and photodissociation rates. As a result we have had to both develop new methods for treating photodissociation [17], predissociation [18–20] and continuum absorption [19], and to extend the ExoMol data model to allow for these processes [21].

Since the ExoMol 2020 release, ExoMol line lists have been used extensively in the modelling of gas giant atmospheres, such as sub-Neptunes [22–37], Neptune-like exoplanets [38–42], so-called Hycean planets [43–45], Saturn-like exoplanets [46–59], young Jupiters [60], cool Jupiters [61], warm Jupiters [27,62–66], hot Jupiters [29,67–132] and ultra-hot Jupiters [12,133–168]. They have also been employed in characterising the atmospheres of terrestrial planets [169–179], particularly hot rocky exoplanets [180–188], those containing volatiles [189] and those undergoing photoevaporation [190,191]. Within our Solar System, they have been used to study the Venusian atmosphere [192, 193], volcanic plumes on Io [194] and comets [195]. In all kinds of planetary atmospheres they have been utilised in the modelling of clouds and hazes [22,26,54,71,102,104,115,196–203] and photochemistry [204]. ExoMol line lists have been used to test the detection capabilities of current and future space based telescopes [27, 178,205–213] and have frequently been incorporated in a variety of radiative transfer, forward-modelling, spectral synthesis and opacity codes [95,214–224]. They have also been employed to study the detectability of biosignatures [225] and prebiosignatures [175]. In stars, ExoMol line lists have also aided in the study of molecular species in the atmospheres of main sequence dwarfs [226–232], giants [233–235], brown dwarfs [60,200,202,236–254], eruptive Young Stellar Objects [255], in stellar winds from Oxygen-rich [256–258] and Carbon-rich [259,260] Asymptotic Giant Branch stars, in cool Carbon stars [261,262], in supergiants [256], in stellar merger remnants [263,264] and modelling supernova ejecta [265]. They have also been used to look at molecules in the interstellar medium (ISM) [266,267] and to study the isotope exchange rates of molecules important in those environments [268]. Outside of astronomy, ExoMol line lists have been employed in laser absorption spectroscopy [269–272], laser induced breakdown spectroscopy [273,274], laser fragmentation [275], laser induced fluorescence [276], plasma stoichiometry [277], fusion plasmas [278], the design of gas sensors [279], combustion [280] and explosions [281]. ExoMol line lists are often used as a benchmark in *ab initio* calculations [282–287] and to compare line strengths [288–295].

The ExoMol database is complete enough to be used to generate other data products. Examples include the creation of the Lifetimes DataBase (LiDB) of vibronic state lifetimes, primarily for use in plasma modelling [296], see Section 8.2; a database of NASA polynomial fits to specific heats generated from ExoMol data [297] and a database of high resolution transitions suitable for spectral assignment [298], see Section 8.1. Importantly ExoMol line lists have been used to give molecular opacities in the ExoMolOP database [299] discussed below; opacities based on ExoMol data have also been generated by several other groups [137,218,248,300–309]. The generation of opacities, see Section 3.5, requires treatment of line broadening, progress on this topic for the ExoMol project is discussed in Section 4. ExoMol is providing input to JWST (James Webb Space Telescope) through the MAESTRO (Molecules and Atoms in Exoplanet Science: Tools and Resources for Opacities) database, see https://science.data.nasa.gov/opacities/ and the exoplanet characterisation Ariel Space Mission [310], which is due to launch in 2029.

Of course ExoMol is not the only source of spectroscopic data for studies of atmospheres. HITRAN [311] is a well established database [312] which is designed for use at temperatures in the region of 296 K and contains molecules of importance in the Earth's atmosphere. HITEMP [313] extends HITRAN to higher temperatures, albeit currently for only eight molecules. Where appropriate the extension of HITRAN or HITEMP is based on ExoMol data [314], and ExoMol uses HITRAN line lists for the diatomic molecules HF, HCl, HBr and CO for which the HITRAN compilation is appropriate for use at higher temperatures. The TheoReTS database [315] contains very extensive computed line lists for nine polyatomic molecules with five or more atoms; not all of these line lists are suitable for high temperature studies. The NASA Ames group provides very extensive line lists for 6 molecules; 5 triatomics plus ammonia. Their CO_2 line lists, which include isotopologues, are designed for use at temperatures up to 3000 K [316]. The SO_2 ExoMol line list [317] was produced in collaboration with the NASA Ames group. The MoLLIST [318] data base due to Bernath and co-workers provides empirical line lists designed for use at higher temperatures for 26 diatomics, ammonia and methane as well as cross-sections for eight polyatomic molecules with six or more atoms. A number of the MoLLIST diatomic line lists are also available from the ExoMol database, see Section 2.6. The VALD [319] and Kurucz [320] databases, which are largely aimed at stellar atmospheres, contain data on some diatomic species.

As discussed in Section 6, with this release ExoMol has started providing temperature-dependent photodissociation cross-sections. The main current provider of photodissociation cross-sections for astronomical studies is the Leiden VUV cross-section database [321] whose data are largely designed for use in studies of the (cold) interstellar medium. Thus far Leiden have not considered the temperature of the molecule in their photodissociation cross sections as the data are largely aimed for use at temperatures of 300 K or below.

2. Line lists

Table 1 summarises the recommended ExoMol line lists present in the database. Note that a number of ExoMol line lists have been replaced by either extended and/or improved upon line lists for the same species; these older line lists are no longer recommended and are not listed in the table although they are still available via the ExoMol website. The 2020 data release introduced the use of uncertainties in the energies given in the `.states` file to allow high resolution transitions to be identified. This feature has now been introduced for all ExoMol-generated recommended line lists, although uncertainties are generally not provided for old line lists or those provided from other sources. At the same time, the previously optional lifetime column in

the `.states` file has been made mandatory and all `.states` files for recommended line lists include lifetimes; this feature is important for modelling line-broadening effects due to predissociation [21].

Below, specific notes for some individual line lists are given. Those line lists which were included in the 2020 release and have not been updated are not explicitly discussed; please refer to the 2020 manuscript or the cited original line list paper for further details. An overview of the temperature-dependent cross-sections for earlier ExoMol line lists is already available [322] and below we give similar plots for many of the newly computed line lists. Before discussing individual line lists we discuss our strategy for improving the accuracy of calculated line positions.

2.1. MARVELization

In terms of the resolving power, defined via wavelength λ and its uncertainty $\Delta\lambda$ as $R = \frac{\lambda}{\Delta\lambda}$, calculated ExoMol line lists are generally of sufficient accuracy to be useful for $R < 10\,000$. This is sufficient for current spaceborne observations of exoplanets, for example JWST has a maximum $R = 3000$. However, ground based observations, and in particular high resolution Doppler-shift cross-correlation spectroscopy, work at much higher resolutions, typically $R = 100\,000$ or even higher. It is clear that the standard theoretical method, even using empirical data to improve the spectroscopy model [377], struggles to approach the level of accuracy required for this resolution. A different approach has therefore been adopted based on the explicit use of empirically derived energy levels.

To provide empirical energy levels we used the MARVEL algorithm [15]. Originally developed to improve representations of water vibration–rotation spectra [378,379], the MARVEL methodology is actually agnostic about the type of spectra being studied and we have applied it widely to rovibronic problems as well as, for VO, to hyperfine-resolved spectra [380]. In essence MARVEL takes a list of assigned high resolution transitions with uncertainties and inverts them to give a list of empirical energies with associated uncertainties. MARVEL does this by constructing a spectroscopic network [381] composed of (all available) assigned, measured transitions with uncertainties; this network is inverted using the so-called X-matrix method [382] to give empirical energy levels each with an associated uncertainty.

The ExoMol data structure gives a single set of energy levels in the `.states` file and a set of Einstein A coefficients in the transitions (`.trans`) file, which are processed together to compute transition wavenumbers and intensities. This structure lends itself to straightforward improvement by replacing calculated energy levels with empirical ones, increasing the accuracy of predicted transition wavenumbers. This approach has the advantage over simply replacing computed transition wavenumbers with measured ones because it produces accurate predictions for the transition wavenumbers of many yet to be observed transitions. For example, Al-Derzi et al. [383] performed a MARVEL project for formaldehyde (H_2CO) which used a network of 16 403 unique transitions to determine 5029 energy levels. Substituting these 5029 energies into the AYTY ExoMol H_2CO line list [326] resulted in 367 779 transitions whose wavenumbers were determined using these empirical energies. We refer to this process as MARVELization. In practice there are a number of ways of improving on the energy levels provided by the variational calculations as discussed by McKemmish et al. [16]. Even so, it is usually only possible to MARVELize a small proportion of the energy levels (for example the AYTY line list contains over 12 billion transitions) although in general the MARVELized levels include the ones involved in the strongest transitions. We note that the A in MARVEL stands for active which means that MARVEL datasets can be actively updated when new high resolution measurements become available. Thus, for example, a new optical frequency comb Fourier transform spectrum of formaldehyde by Germann et al. [384] was recently used to update the MARVEL results of Al-Derzi et al. [383] and the AYTY line list; use of this very high resolution spectrum added a further 82 new energy levels to the MARVEL compilation and, perhaps more importantly, substantially improved the accuracy of many of the energy levels. Line lists that have been MARVELized are identified by ✔ marks in Table 1.

To use the uncertainties in the energy levels it is assumed that the uncertainty in the transition wavenumber, $\Delta\omega$, is given by

$$\Delta\omega = \sqrt{(\Delta E')^2 + (\Delta E'')^2}, \tag{1}$$

where $\Delta E'$ and $\Delta E''$ are the uncertainties in the upper and lower state energy levels, respectively. Note that on occasion this uncertainty will be an overestimate as there are situations where a precisely determined transition has been measured between two states whose energies are both less well determined. However, we suggest that the current implementation should be adequate for most practical purposes. As part of this data release we have ensured that all ExoMol-generated recommended datasets contain uncertainties in their energy levels and the source of these energies are marked using the codes given below in Section 3.1. For cases where these levels have not been MARVELized, these uncertainties can be quite large. Conversely, transitions between two states with MARVELized energies should be accurate enough to use in high resolution studies. Our post-processing codes, ExoCross [385] and PyExoCross [386], give the option of generating spectra or cross-sections only using transitions with low uncertainties and our new web portal ExoMolHR, see Section 8, provides a database of high resolution transitions which can be interrogated interactively.

An underlying assumption of the MARVELization process is that the relatively small shifts in the line positions do not significantly influence the line intensities. In most cases this is probably a reasonable assumption but there is one set of circumstances where things are more complicated. Resonances caused by the accidental interaction of levels in different vibrational or vibronic states can lead to severe perturbations of the intensities caused by so-called intensity stealing between transitions. This effect is known to be very sensitive to the details the calculation; Lodi and Tennyson [387] designed a method for identifying those transitions which are sensitive to these interactions by performing repeat calculations with different potential energy and dipole moment surfaces. This method has proved important for high accuracy calculations [388]. However, the Lodi-Tennyson method requires the generation of, at least, four line lists for given species and thus far has not been employed for the large and usually expensive ExoMol line lists.

2.2. Diatomics

2.2.1. AlO, paper XVIII

The ATP line list for aluminium monoxide, AlO, has been updated using MARVEL [389]. AlO has been detected in a number of objects such as hot Jupiter exoplanets WASP-43b [390] and HAT-P-41b [77], as well as in eruptive young stellar objects (YSOs) [255] using the ATP line list. The ATP line list has also been used in plasma studies [274, 391,392].

2.2.2. NO, papers XXI and XLII

The full rovibronic $^{14}N^{16}O$ XABC line list [356] replaces the ground state NONname [393] line list. A MARVEL study was undertaken as part of the XABC line list construction. However, NONname should still be used for the minor isotopologues of NO.

The XABC line list gives thorough coverage of the so-called γ, β and δ band systems, which correspond, respectively, to the A $^2\Sigma^+$ – X $^2\Pi$, B $^2\Pi$ – X $^2\Pi$ and C $^2\Pi$ — X $^2\Pi$ electronic bands. We note that the γ band system has recently been proposed as a potential biomarker in exoplanetary atmospheres [394]. Cross-sections for NO computed using XAB are shown in Fig. 1.

Table 1
Datasets created by the ExoMol project and included in the ExoMol database: recommended line lists only. Line lists denoted with a ✔ are suitable for high resolution studies.

Paper	Molecule	N_{iso}	T_{max}	N_{elec}	N_{lines} [a]	DSName		Reference
III	HCN/HNC	1[a]	4000	1	34 418 408	Harris	✔	[323]
V	NaCl	2	3000	1	702 271	Barton		[324]
V	KCl	4	3000	1	1 326 765	Barton		[324]
VII	PH_3	1	1500	1	16 803 703 395	SAlTY		[325]
VIII	H_2CO	1	1500	1	12 688 112 669	AYTY	✔	[326]
IX	AlO	4	8000	3	4 945 580	ATP	✔	[327]
X	NaH	2	7000	2	79 898	Rivlin		[328]
XI	HNO_3	1	500	1	6 722 136 109	AlJS		[329]
XII	CS	8	3000	1	548 312	JnK	✔	[330]
XIII	CaO	1	5000	5	21 279 299	VBATHY	✔	[331]
XIV	SO_2	1	2000	1	1 300 000 000	ExoAmes	✔	[317]
XV	H_2O_2	1	1250	1	20 000 000 000	APTY		[332]
XVI	H_2S	1	2000	1	115 530 373	AYT2	✔	[333]
XVII	SO_3	1	800	1	21 413 927 818	UYT2	✔	[334]
XIX	$H_2{}^{17,18}O$	2	3000	1	519 461 789	HotWat78	✔	[335]
XX	H_3^+	1	3000	1	127 542 657	MiZATeP	✔	[336]
XXII	SiH_4	1	1200	1	62 690 449 078	OYT2		[337]
XXIII	PO	1	5000	1	2 096 289	POPS		[338]
XXIII	PS	1	5000	3	30 394 544	POPS		[338]
XXIV	SiH	4	5000	3	1 724 841	SiGHTLY		[339]
XXV	SiS	12	5000	1	91 715	UCTY		[340]
XXVI	NS	6	5000	1	3 479 067	SNaSH		[341]
XXVII	C_2H_4	1	700	1	49 841 085 051	MaYTY		[342]
XXIX	CH_3Cl	2	1200	1	166 279 593 333	OYT		[343]
XXX	$H_2{}^{16}O$	1	5000	1	5 745 071 340	POKAZATEL	✔	[344]
XXXI	C_2	3	5000	8	6 080 920	8states	✔	[345]
XXXII	MgO	5	5000	5	72 833 173	LiTY	✔	[346]
XXXIII	TiO	5	5000	13	58 983 952	Toto	✔	[347]
XXXIV	PH	1	4000	2	65 055	LaTY	✔	[348]
XXXV	NH_3	1	1500	1	16 941 637 250	CoYuTe	✔	[349]
XXXVI	SH	2	3000	2	572 145	GYT	✔	[350]
XXXVII	HCCH	1	2000	1	4 347 381 911	aCeTY	✔	[351]
XXXVIII	SiO_2	1	3000	1	32 951 275 437	OYT3		[352]
XXXIX	CO_2	1	3000	1	7 996 570 390	UCL-4000	✔	[353]
XL	H_3O^+	1	1500	1	2 089 331 073	eXeL	✔	[354]
XLI	KOH	1	3500	1	38 362 078 911	OYT4		[355]
XLI	NaOH	1	3500	1	49 663 923 092	OYT5		[355]
XLII	NO	1	3500	4	4 596 666	XABC	✔	[356]
XLIII	NaO	1	2500	2	4 726 283	NaOUCMe	✔	[357]
XLIV	SiO	1	3500	10	91 395 763	SiOUVenIR	✔	[358]
XLV	CaH	1	5000	3	293 151	XAB	✔	[359]
XLV	MgH	3	5000	3	88 575	XAB	✔	[359]
XLVI	SiN	4	3000	6	43 646 806	SiNful	✔	[359]
XLVII	CaOH	1	3000	3	24 215 753 701	OYT6	✔	[359]
XLVIII	H_2CS	1	2000	1	4 356 116 660	MOTY	✔	[360]
XLIX	AlCl	2	5000	4	4 722 048	YNAT	✔	[361]
L	H_3^+	4	3000	1	–	MiZo	✔	[362]
LI	LiOH	2	3000	1	331 274 717	OYT7		[363]
LII	CH^+	2	5000	2	34 194	PYT		[364]
LIII	YO	3	5000	6	60 678 140	BRYTS		[365]
LIV	AlH	4	5000	2	36 152	AloHa	✔	[19]
LV	VO	1	5400	15	58 904 173 243	HyVO	✔	[366]
LVI	SO	1	5000	8	7 008 190	SOLIS	✔	[367]
LVII	CH_4	1	2000	1	50 395 644 806	MM	✔	[368]
LVIII	OCS	1	2000	1	2 482 380 391	OYT8	✔	[369]
LIX	N_2O	5	2000	1	1 360 351 722	TYM	✔	[370]
LX	$^{15}NH_3$	1	1000	1	929 795 249	CoYuTe-15	✔	[371]
LXI	OH	1	5000	8	1 685 102	MYTHOS	✔	[372]
LXII	C_3	3	3000	1	5 481 690 507	AtLast	✔	[373]
LXIII	HDO	1	3000	1	3 000 000	TBD	✔	[374]
LXIV	PN	1	5000	1	634 243	PaiN	✔	[375]

Paper: Number in series published in Mon. Not. R. Astron. Soc.; N_{iso}: the number of isotopologues considered; T_{max}: maximum temperature for which the line list is complete; N_{elec}: number of electronic states considered; N_{lines}: number of lines, the value is for the main (parent) isotopologue.

[a] The Larner line list [376] for $H^{13}CN/HN^{13}C$ is recommended.

2.2.3. AlH, papers XXI and XLIV

Pavlenko et al. [395] used the AlHambra line list [396] to analyse the spectrum of AlH in our nearest star, Proxima Cen. While the line list reproduced the majority of the observed spectrum well, it did not reproduce the predissociative lines accurately either in their position or their widths. As a result it was decided to implement procedures [18] and data structures [21] to represent line broadening due to predissociation within the project. A new line list, AloHa [19], superseded the AlHambra line list. AloHa has been MARVELized for both AlH and AlD, and also provides an accurate representation of the predissociation

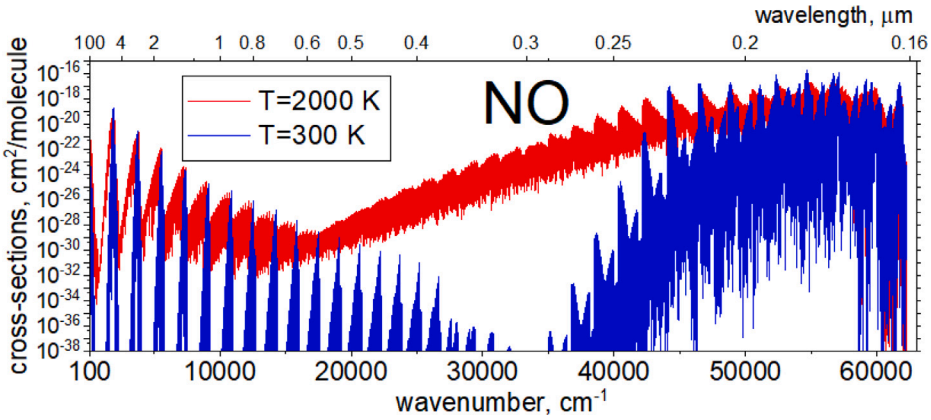

Fig. 1. Cross-sections generated using the ExoMol line list XAB for NO at $T = 300$ K and 2000 K.

lifetime. The line list also provides continuum absorption cross-sections describing photoabsorption, i.e. absorption to continuum (unbound) states. The structure of the continuum absorption cross sections is introduced in Section 3.3.

2.2.4. MgO, paper XXXII

The LiTY line list [346] for magnesium monoxide, MgO, has been updated for the four lowest electronic states using MARVEL [16]. Additionally, the Predicted Shift (PS) methodology was used to improve the calculated energies and estimate energy uncertainties [16]. The updated line list was used to update the line lists for the $^{24}Mg^{17}O$, $^{24}Mg^{18}O$, $^{25}Mg^{16}O$, and $^{26}Mg^{16}O$ isotopologues with the isotopologue extrapolation procedure (IE) [16]. MgO has been suggested as one of the constituents of the so-called lava planets [181,397].

2.2.5. TiO, paper XXXIII

The Toto line list for TiO [347] has been widely used. Notably, Toto was successfully used by Pavlenko et al. [398] to extract Ti isotopic abundances using band heads of ^{50}TiO, ^{49}TiO, ^{48}TiO, and ^{47}TiO in the spectra of M dwarfs. This work provides endorsement of the isotopologue extrapolation procedure (IE) [16] used to improve the line lists for minor isotopologues by using data from the main isotopologue. The Toto line list has recently been updated using new MARVEL energy levels derived incorporating recent laboratory measurements [16]. The `.states` file was updated using the Predicted Shift (PS) methodology [16]. Toto has been used for the detection of TiO in a number of exoplanets, such as the ultra-hot Jupiter WASP-189b [145], WASP-33b [141], WASP-76b [399] and WASP-77Ab [126].

2.2.6. SH, paper XXXVI

The GYT linelist [400] remains as the recommended ExoMol linelist for the mercapto radical and is recommended for all applications [5]. As in hydroxyl (Section 2.2.13), SH exhibits strong and complex predissociation due to spin-orbit interactions between the $A\,^2\Sigma^+$ state and the dissociative, $1\,^2\Sigma^-$, $1\,^4\Sigma^-$, and $1\,^4\Pi$ states. SH/SD predissociation lifetimes will be released soon [18] and lifetimes in the GYT linelist will be updated as per Section 5.

2.2.7. NaO, paper XLIII

A new line list for NaO called NaOUCMe [357] has been provided; there is very limited high resolution spectroscopic data on NaO so the line list is not suitable for high resolution studies.

2.2.8. SiO, paper XLIV

A new line list for silicon monoxide, SiO, called SiOUVenIR, has been provided [358] and replaces the well-used EJBT rovibrational line list [401]. The new line list has been MARVELized and also provides much broader wavelength coverage as it also covers rovibronic transitions. Like MgO, SiO has been suggested as one of the important sources of opacity in lava planets as well as sub-Neptunes [181,186,189,190,397,402,403]. Cross-sections for SiO computed using SiOUVenIR are shown in Fig. 2.

2.2.9. CaH and MgH, paper XLV

New rovibronic line lists for CaH and MgH called XAB have been computed [359]. The line lists have been MARVELized and consider the important isotopologues of both species. The line lists replace the more restricted rovibrational Yadin line lists [404]. As MARVELized line lists for BeH, as well as BeD and BeT, are also available [405], the Yadin linelists [404] for these alkaline earth monohydrides are no longer recommended. Cross-sections of MgH computed using the XAB line list are shown in Fig. 3.

2.2.10. VO, paper XLV

The new HyVO line list for Vanadium monoxide [366] replaces the previous ExoMol VOMYT line list [406]. VOMYT was built on a relatively crude theoretical model and known to be inadequate for high resolution studies [12]. The spectrum of VO shows significant splittings due to the hyperfine structure induced by the high spin ($I = \frac{7}{2}$) and large magnetic moment of the ^{51}V nucleus. To create a VO line list suitable for high resolution studies, it was necessary to perform a MARVEL study which explicitly considered hyperfine effects where possible [380], extend our diatomic variational nuclear motion code Duo to include hyperfine effects [407] and then perform extensive model building studies [408,409]. HyVO is a fully hyperfine-resolved line list which contains nearly 59 billion transitions, a huge number for a diatomic molecule. The new HyVO line list has been used to detect VO in the atmosphere of WASP-76b via high-resolution cross-correlation spectroscopy [168], strengthening the findings of the previous study of this planet which utilised the old VOMYT line list [159].

2.2.11. SO, paper LVI

The new SOLIS line list for the main sulfur monoxide isotopologue $^{32}S^{16}O$ has been computed and MARVELized [367]. The electronic structure of SO exhibits non-adiabatic behaviour where an earlier study [410] builds a quasi-diabatic spectroscopic *ab initio* model before refinement to MARVEL data.

SO is expected to be abundant within exoplanets whose atmospheres undergo warm chemistry or have regions with prolific photochemical reactions. It was recently detected in a JWST MIR transmission spectrum of WASP-39b, a Saturn-mass exoplanet, using the SOLIS line list [130].

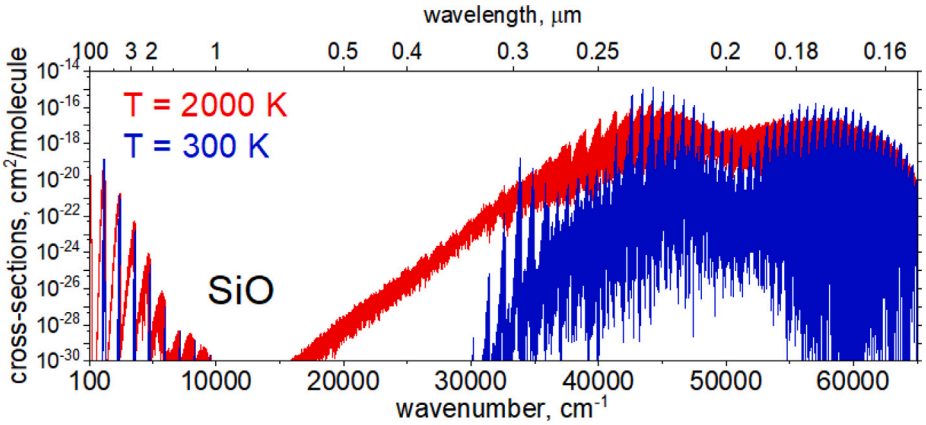

Fig. 2. Cross-sections generated using the ExoMol line list SiOUVenIR for SiO at $T = 300$ K and 2000 K.

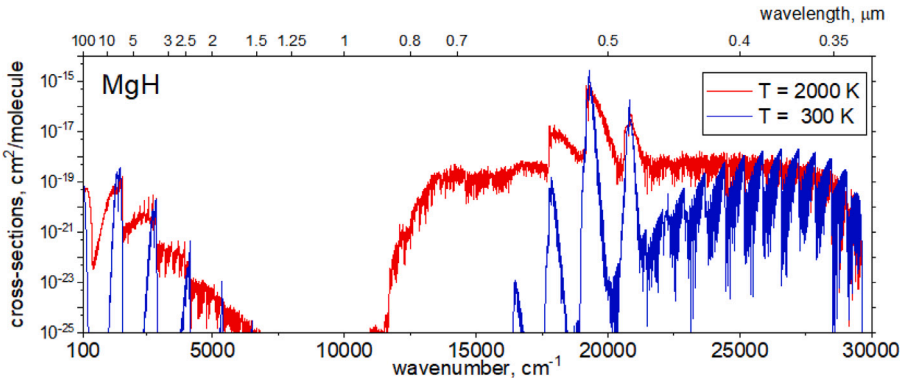

Fig. 3. Cross-sections of MgH generated using the ExoMol line list XAB at $T = 300$ K and 2000 K.

2.2.12. SiN, paper XLVI

A new line list for silicon mononitride, SiN, called Sinful, has been computed [359] for the main isotopologues, $^{28}Si^{14}N$, $^{29}Si^{14}N$, $^{30}Si^{14}N$, $^{28}Si^{15}N$. The line list includes 6 lowest-lying electronic states. The line list has been MARVELized and is in good agreement with previously reported spectra. SiN is considered to be a good indicator for planet-metallicity [411] and has been detected in different media in space [412–418].

2.2.13. OH, paper LXI

The new MYTHOS OH line list [372] replaces the one provided by MoLLIST [419] as the recommended ExoMol line list. The rovibronic line list considers transitions within the ground X $^2\Pi$ electronic state to the A $^2\Sigma^+$, B $^2\Sigma^+$ and C $^2\Sigma^+$ states which all support bound states. The model also includes four dissociative states, 1 $^2\Sigma^-$, 1 $^4\Sigma^-$, 1 $^4\Pi$, and 1 $^2\Delta$, the first three of which causes significant predissociation broadening of levels within the A $^2\Sigma^+$ state [20]; the lifetime broadening effects are explicitly allowed for in the line list. Transitions from the ground state to the dissociative 1 $^2\Sigma^-$ and 1 $^2\Delta$ states are also calculated here and are included in the temperature dependent photoabsorption cross-sections. The line list is of a high accuracy having used the empirical energies from a previous MARVEL study [420]. Two datasets are made available: a state bound-to-bound line list and temperature dependent photoabsorption cross sections which include the continuum transitions. Temperature-dependent photodissociation cross-sections for OH are currently being computed.

2.2.14. PN, paper LXIV

A rovibrational line list for phosphorus nitride, named YYLT, was computed early in the ExoMol project [421]. A new, MARVELized robvibronic line list PaiN [375] covering the A–X band system and providing improvements for the X–X transitions has been constructed starting from the *ab initio* spectroscopic model of Semenov et al. [422]. PaiN has replaced YYLT as the recommended line list. We note the PN is likely to be hard to detect in exoplanet atmospheres because it has a strong vibrational fundamental in the 10 μm region, which is a wavelength to long for current observational capabilities, and the A–X band system lies in the UV around 250 nm which is also hard to observe and unlikely to be important around cool stars.

2.2.15. Other new diatomic line lists

New line lists are provided for AlCl (YNAT [361]), CH^+ (PYT [364]) and YO (BRYTS [365]), all of which include rovibronic transitions as well as rotation-vibration transitions.

2.3. Triatomics

2.3.1. H_3^+, papers XX and L

Bowesman et al. [362] updated the MiZATeP H_3^+ line list [336] and the ST line list for H_2D^+ [423] using MARVEL. New MiZo line lists for D_2H^+ and D_3^+ were generated [362]; the MiZo D_2H^+ line list also uses MARVEL energy levels while the energy levels of the more limited D_3^+ line list were improved using effective Hamiltonian data. All the line lists are suitable for high resolution studies at long wavelengths. A review of the role of H_3^+ in astrophysics has been provided by Miller et al. [424].

2.3.2. Water, papers XIX, XXX and LXIII

POKAZATEL [344] remains the recommended line list for $H_2^{16}O$, it has been widely and successfully used. Water is of course widely observed in exoplanet spectra and several other line lists including BT2 [425], HITEMP 2010 [313] which is based on BT2, and the

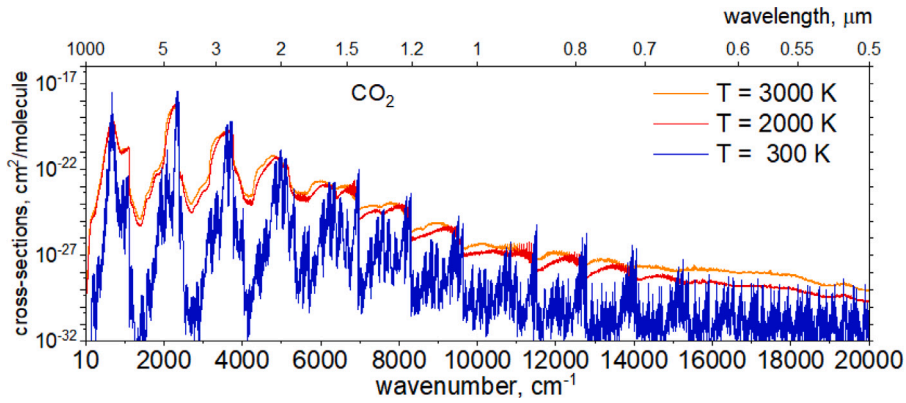

Fig. 4. Cross-sections generated using the ExoMol line list UCL-4000 for CO_2 at $T = 300$ K, 2000 K and 3000 K.

pioneering but now dated Partridge and Schwenke [426]. We strongly recommend the adoption of POKAZATEL over these older, less complete and less accurate line lists for this key molecule. Indeed a near infrared laboratory high temperature ($T = 1723$ K) comparison suggested that POKAZATEL reproduced the observed spectrum roughly six times better than BT2 [427].

Isotopologues $H_2{}^{17}O$ and $H_2{}^{18}O$ are represented by the HotWat78 line lists [335]. While POKAZATEL is very complete and should give a good representation of water absorption up to at least 5000 K, the Hotwat78 line lists are only complete up to 3000 K. We plan to extend the temperature range covered for $H_2{}^{17}O$ and $H_2{}^{18}O$.

All H_2O line lists discussed above have been MARVELized [428,429] and are therefore suitable for high accuracy studies.

A new line list TBD has been computed for deuterated water, HDO [374]. This replaces the old VTT line list [430]. TBD is more complete than VTT. In particular, the potential energy surface (PES) used in the line list calculations was obtained by fitting to the data [431] up to 35 000 cm^{-1}. Energies up to 41 000 cm^{-1} were used in the linelist calculations. Unlike VTT, the TBD energy levels have been MARVELized using energies from an IUPAC study [432]; we note that a MARVEL project to update these energy levels is in progress which will lead to the release of an updated version of TBD. The spectrum of HDO is significantly different from that of H_2O and the TBD line list should be suitable for use in high resolution studies.

In addition, room temperature line lists for the isotopologues $H_2^{14}O$ [433], $H_2^{15}O$ [434] and $H_2^{19}O$ [435] have recently been added to the databases. These isotopologues, in which the radioactive oxygen atom has a half-life in the region of a minute, may form in thunderstorms [436], in water cooled nuclear and fusion reactors, and as a result of using isotopes in medical procedures.

2.3.3. CO_2, paper XXXIX

The UCL-4000 line list [353] for carbon dioxide has been produced using an accurate PES AMES-1 [437] and a high-level *ab initio* dipole moment surface [438] of CO_2 using the TROVE variational program [439]. UCL-4000 has been widely used but suffers from two issues. It is only for the parent, $^{12}C^{16}O_2$, isotopologue and at visible wavelengths it was found to overestimate transition intensities at higher wavenumbers, a problem found with other hot CO_2 line lists [440]. We are therefore in the process of constructing an improved hot line list for this important molecule which will consider all important isotopologues and be MARVELized [441,442]. Cross-sections for CO_2 generated using the UCL-4000 line list are illustrated in Fig. 4.

The same methodology used for UCL-4000 was subsequently used to produce an electric quadrupole (E2) line list for CO_2 [443]. The theoretical E2 transitions were validated experimentally using in the 3.3 μm region [444] and used to detect E2 lines in the Martian atmospheric spectra from the ExoMars ACS observations [445].

2.3.4. LiOH, NaOH, KOH, papers XLI and LI

New line lists for the alkali metal hydoxides KOH, NaOH and LiOH named OYT4 [355], OYT5 [355] and OYT7 [363], respectively, have been calculated. There is a lack of high resolution spectroscopic data for these systems so these are not MARVELized and therefore not suitable for high resolution studies. Cross-sections for LiOH generated using the OYT7 line list are illustrated in Fig. 5.

2.3.5. CaOH, paper XLVII

A new line list called OYT6 is provided for calcium monohydroxide, CaOH [359]. This is the first rovibronic line list for a triatomic molecule which includes consideration of the important $\tilde{A}\,^2\Pi - \tilde{X}\,^2\Sigma^+$ electronic band system as well as ground state rotation-vibration transitions. This line list was built on a MARVEL study [446], then constructed a spectroscopic model [447] using the rovibronic nuclear motion code for triatomics EVEREST [448]. CaOH is known to be an important component of the atmosphere of cool stars [449]; the OYT6 line list has been used as a thermometer in combustion and explosion applications [281]. Cross-sections for CaOH computed using the OYT6 line list are shown in Fig. 6.

2.3.6. OCS, paper LVIII

A new line list called OYT8 is provided for carbonyl sulfide, OCS [369]; this line list uses a previous MARVEL study [450] and therefore should be suitable for high resolution studies. Given that CO [451], CO_2 [51], SO_2 [53,130], and now SO have been detected by JWST in exoplanetary atmospheres, the presence of OCS would also appear likely. Major studies are already searching for its spectroscopic signature [56,452].

2.3.7. N_2O, paper LIX

A new line list for nitrous oxide, N_2O, has been computed [370]. N_2O is prominent in the Earth's atmosphere and considered to be an observable potential biomarker on exoplanets [453–455]. Five isotopologues are considered, $^{14}N_2{}^{16}O$, $^{15}N^{14}N^{16}O$, $^{14}N^{15}N^{16}O$, $^{14}N_2{}^{17}O$ and $^{14}N_2{}^{18}O$. The parent isotopologue $^{14}N_2{}^{16}O$ was MARVELized using the MARVEL energies of Tennyson et al. [456]. MARVEL studies on the four isotopologues arising from substituting a single atom are in progress.

2.3.8. C_3, paper LXII

A new line list for C_3 has been calculated, which considers rovibrational transitions within the ground state. Three isotopologues are considered: $^{12}C_3$, $^{12}C^{13}C^{12}C$ and the asymmetric $^{12}C^{12}C^{13}C$. The $^{12}C_3$ line list was MARVELized using results from a previous MARVEL study [457].

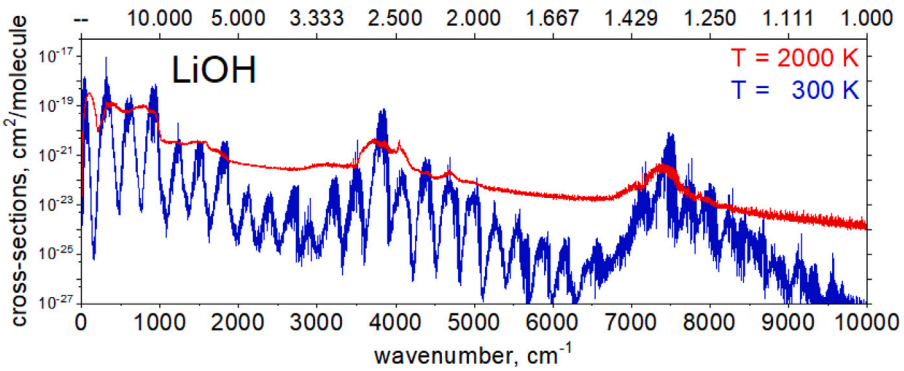

Fig. 5. Cross-sections for LiOH generated using the ExoMol line list OYT7 at $T = 300$ K and 2000 K.

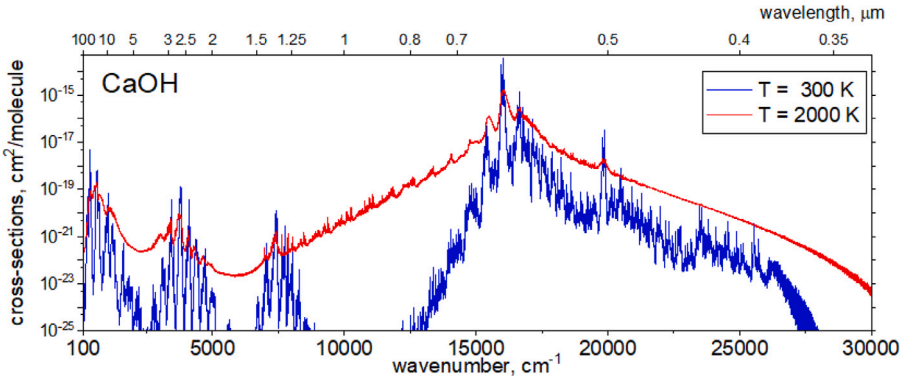

Fig. 6. Cross-sections for CaOH generated using the ExoMol line list OYT6 at $T = 300$ K and 2000 K.

2.4. Tetratomics

2.4.1. H_2CO, paper VIII

The AYTY line list for formaldehyde [326], $H_2{}^{12}C^{16}O$, has been updated using MARVEL [383,384] by replacing the calculated AYTY energy levels with MARVEL ones. Based on this update, 373 160 transition frequencies with experimental accuracy were determined. These are illustrated in Fig. 7, where they are compared to 40 670 transitions of $H_2{}^{12}C^{16}O$ in HITRAN 2020. A line list for $H_2{}^{13}CO$ is under construction.

2.4.2. NH_3, papers XXXV and LX

The CoYuTe line list for $^{14}NH_3$ ammonia [349] has been updated using new MARVEL data [458]. The CoYuTe line list has been and is continuing to be used to assign ammonia spectra in the near-infrared and to analyse plasma emissions spectra [459]. Laboratory spectra of ammonia need to be analysed in this region and into the visible not least because pronounced ammonia features are observed in Jupiter in the near-infrared and visible. In particular, the feature at 6474 Å is modelled by CoYuTe [460,461] better than other available compilations but for which CoYuTe still shows a noticeable shift in wavelength compared to the observations.

A new $^{15}NH_3$ line list called CoYuTe-15 was generated using the same procedure as for the $^{14}NH_3$ CoYuTe line list [349], including MARVELization; it replaces the previous room-temperature $^{15}NH_3$ line list [462] which is also less accurate and not MARVELized. The recent detection of $^{15}NH_3$ in the atmosphere of a cool brown dwarf [247] suggests that this isotopologue could also be detected in the atmospheres of exoplanets.

2.4.3. HCCH, paper XXXVII

The aCeTY line list for acetylene, C_2H_2, has been updated using MARVEL [463].

2.4.4. H_2CS, paper XLVIII

A new line list for thioformaldehyde, H_2CS, called MOTY has been computed by Mellor et al. [360]; the energy levels were on the basis of a MARVEL study [464] to make it suitable for high resolution studies. Fig. 8 illustrates the cross-sections for H_2CS computed using MOTY.

2.5. Pentatomics

2.5.1. CH_4, paper LVII

A completely new line list for methane, CH_4, called MM [465] replaces the previous ExoMol methane line lists 10to10 [466] and 30to10 [467]. MM is based on the use of improved theory, an improved potential energy surface plus extensive MARVELization based on a comprehensive, parallel MARVEL study [368]. Line lists for hot methane are also available from TheoReTS [468,469] and HITEMP [470]. MM is broadly comparable with the TheoReTS line list but at high temperatures (>1000 K) is significantly more complete than the HITEMP line list. Cross-sections of CH_4 generated using the MM line list are illustrated in Fig. 9.

There are many unassigned or partially assigned published high resolution spectra of methane available [368]. We are actively using MM to assign these spectra [471]. Any new assignments we make, or indeed new high resolution spectra, will be used in an extended MARVEL study, the results of which can be used to re-MARVELize and further improve the accuracy of the MM line list.

2.6. Other line lists

Table 2 gives an overview of recommended line lists available through the ExoMol website but not generated by the ExoMol project. As for Table 1, an indication is given as to whether the data as presented are appropriate for high resolution studies. For Table 2 this information may be less useful because while most of the sources do

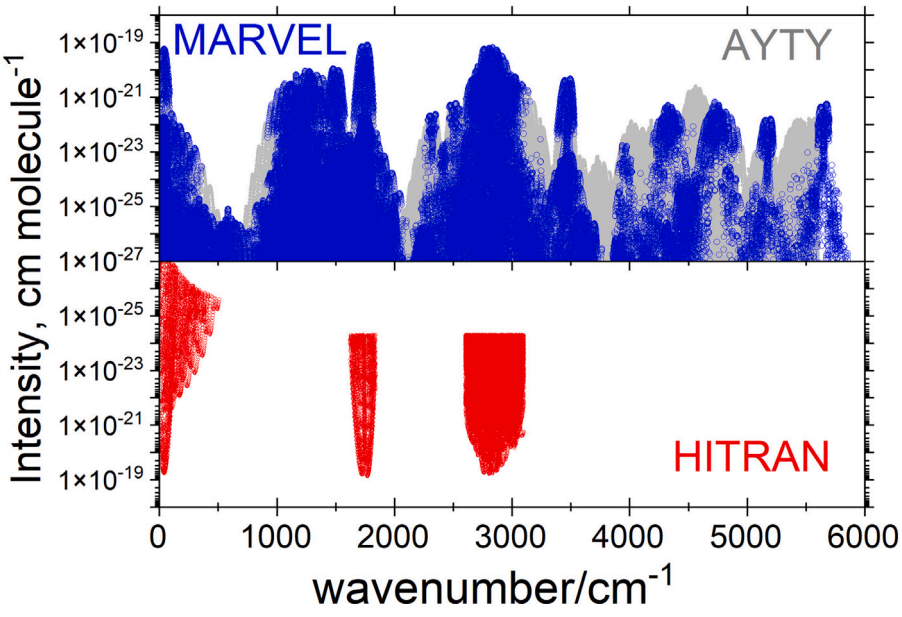

Fig. 7. Room temperature (T = 296 K) spectra of H_2CO from three different sources: lower panel, HITRAN; upper panel, MARVELized transitions [383,384] overlaid with the AYTY line list [326].

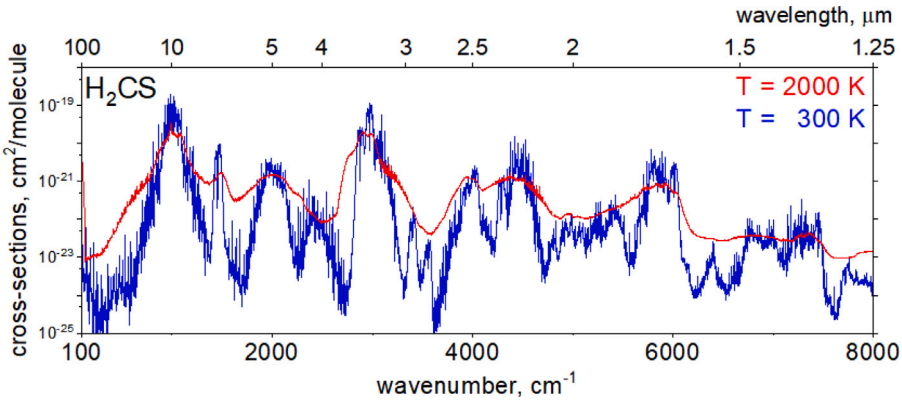

Fig. 8. Cross-sections generated using the ExoMol line list MOTY for H_2CS at T = 300 K and 2000 K.

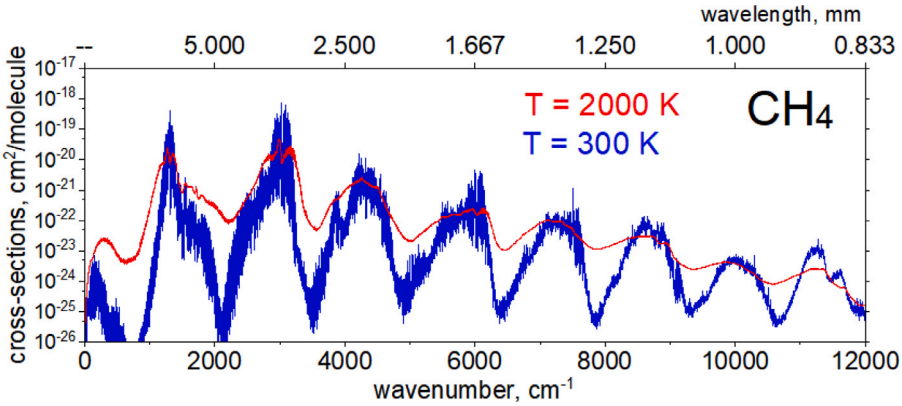

Fig. 9. Cross-sections of CH_4 generated using the ExoMol line list MM at T = 300 K and 2000 K.

indeed give accurate predictions for the transition wavenumbers, the line lists do not contain uncertainties for their individual energy levels which means that within the ExoMol data structure wavenumber uncertainties cannot be estimated. These datasets have not been marked

Table 2
Datasets recommended as part of the ExoMol project but imported from other sources.

Molecule	N_{iso}	T_{max}	N_{elec}	N_{lines}	DSName		Reference	Methodology
CH	1	5 000	4	52 201	MoLLIST		[472]	Empirical
AlF	1	5 000	1	40 490	MoLLIST		[473]	Empirical
CaF	1	5 000	6	14 817	MoLLIST		[474]	Empirical
MgF	1	5 000	3	8 136	MoLLIST		[475]	Empirical
KF	1	5 000	2	10 572	MoLLIST		[476]	Empirical
NaF	1	5 000	1	7 884	MoLLIST		[476]	Empirical
LiCl	1	5 000	4	26 260	MoLLIST		[477]	Empirical
LiF	1	5 000	2	10 621	MoLLIST		[477]	Empirical
TiH	1	5 000	3	181 080	MoLLIST		[478]	Empirical
CrH	1	5 000	2	13 824	MoLLIST		[479]	Empirical
FeH	1	5 000	2	93 040	MoLLIST		[480]	Empirical
LaO	1	8 000	2	2 066 535	BDL		[481]	Empirical
HF	2	5 000	1	7 956	Coxon-Hajig		[482,483]	Empirical
HCl	4	5 000	1	2 588	HITRAN		[484,485]	Empirical
HBr	1	5 000	1	3 039	HITRAN-HBr		[483,485]	Empirical
CO	9	9 000	1	125 496	Li2015		[486]	Empirical
CP	1	5 000	2	28 752	MoLLIST		[487]	Empirical
ScH	1	5 000	6	1 152 827	LYT		[488]	Ab initio
LiH	1	12 000	1	18 982	CLT		[489]	Ab initio
LiH^+	1	12 000	1	332	CLT		[489]	Ab initio
HeH^+	4	9 000	1	1 430	ADSJAAM		[490]	Ab initio
H_2	1	10 000	1	4 712	RACPPK		[491]	Ab initio
H_2	1	10 000	3	32 915	ARLR		[492]	Ab initio
HD	1	9 000	1	10 285	ADSJAAM		[490]	Ab initio
HD^+	1	9 000	1	10 285	ADSJAAM		[490]	Ab initio
CH_3F	1	300	1	139 188 215	OYKYT		[493]	Ab initio
AsH_3	1	300	1	3 600 000	CYT18		[494]	Ab initio
P_2H_2[a]	2	300	1	10 667 208 951	OY-Trans		[495]	Ab initio
P_2H_2[a]	2	300	1	11 020 092 365	OY-Cis		[495]	Ab initio
PF_3	1	300	1	68 000 000 000	MCYTY		[496]	Ab initio
CH_3	1	1 500	1	2 058 655 166	AYYJ		[497]	Ab initio
BeH	3	5 000	2	592 308	Darby-Lewis	✔	[405]	ExoMol
SiH_2	1	2 000	1	254 061 207	CATS		[498]	ExoMol
CN	4	10 000	3	2 285 103	Trihybrid	✔	[499]	ExoMol
ZrO	6	10 000	10	47 662 773	ZorrO	✔	[500]	ExoMol
NH	4	10 000	5	327 014	kNigHt	✔	[501]	ExoMol
HBO	2	3 000	1	142 038 890	LQL		[502]	ExoMol
N_2	1	10 000	4	7 182 000	WCCRMT		[503]	Empirical
H_2O[b]	1	300	1	109 263	CKYKKY		[504]	Empirical

N_{iso} Number of isotopologues considered;
T_{max} Maximum temperature for which the line list is complete;
N_{elec} Number of electronic states considered;
N_{lines} Number of lines: value is for the main isotope.
✔ indicates line list that provide energy levels with individual uncertainties and contain lines suitable for use in high resolution studies.
[a] There are separate line lists for cis and trans P_2H_2.
[b] An electric quadrupole (E2) line list for $H_2^{16}O$.

as suitable for high resolution studies and it is necessary to check the original (cited) reference to establish the accuracy of the transitions.

A number of the line lists presented in Table 2 are taken from Bernath's MoLLIST project [318] including the one for the CP radical [487]. We note that an alternative line list for CP has been computed by Qin et al. [505]. A new MoLLIST line list covering the B $^2\Sigma^+$ - X $^2\Sigma^+$ band system of LaO by Bernath et al. [481] has been added. Compared to the 2020 release a number of MoLLIST line lists, namely OH, AlCl, CaH and NH, have been replaced by ones generated by ExoMol.

Diatomic line lists for four molecules have also been taken from HITRAN [2], namely those for CO, HCl, HF and HBr. These line lists provide extensive compilations of rotation-vibration transitions within the electronic ground states and are appropriate for elevated temperatures. In the case of CO, a number of improvements to the treatment of the already very accurate ground state line list [506,507] and extensions to consider rovibronic transitions [508] have been undertaken. These will be used to provide updated and greatly extended line lists.

HITRAN data have also been used to create opacities for the oxygen molecule; these data do not extend to high temperature. An extensive, ExoMol high-temperature line list for O_2 should be available soon. To this end, new methodology to treat magnetic dipole and electric quadrupole transitions in diatomic molecules has been developed and implemented in Duo [509,510].

Molecular hydrogen, H_2, is one of the relatively few molecules for which the database provides more than one recommended line list. The weak, dipole-forbidden infrared spectrum of H_2 is given by the RACPPK line list [491] which includes electric quadrupole transitions, for which $\Delta J = 0, \pm 2$, and magnetic dipole transitions with $\Delta J = 0$ only. The dipole-allowed Lyman (B $^1\Sigma_u^+$ – X $^1\Sigma_g^+$) and Werner (C $^1\Pi_u$ – X $^1\Sigma_g^+$) H_2 electronic band systems are provided by the ARLR [492] line list. An infrared line list of HD is provided from high accuracy *ab initio* calculations by Amaral et al. (ADSJAAM) [490]; in this case it is also necessary to consider weak dipole-allowed transitions which arise from failure of Born–Oppenheimer approximation. *Ab initio* infrared line lists for HD^+ and HeH^+ from Amaral et al. [490] are also included. *Ab initio* line lists for LiH^+ and LiH, designed primarily for studies of the early Universe, due to Coppola et al. [489] are also included.

An electric quadrupole (E2) line list CKYKKY for $H_2^{16}O$ has been produced [504] using the POKAZATEL PES and a new *ab initio* electric quadrupole moment surface of H_2O. The line list was used to identify E2 transitions of $H_2^{16}O$ experimentally for the first time [504].

The UNSW (University of New South Wales) group of McKemmish have generated a number of ExoMol style diatomic line lists which are available and recommended in the database. All these line lists have been the subject of an associated MARVEL study and therefore provide high accuracy data and are suitable for high resolution studies. They are:

- CN: Syme and McKemmish [499] ExoMol style line list from UNSW calculated using Duo [511] hybridised with MARVEL [512] and MoLLIST [513] data.
- ZrO: Perri et al. [500] ExoMol style line list from UNSW calculated using Duo [511] hybridised with MARVEL [514] and MoLLIST [515] data.
- NH: Perri and McKemmish [501] ExoMol style line list from UNSW calculated using Duo [511] hybridised with MARVEL [516] and MoLLIST [517–519] data.

In addition Li et al. [502] have recently used ExoMol methodology to compute line lists for two isotopologues of HBO. This line list has been added to the database.

Finally the website provides partial data for two other diatomic molecules, N_2 and NiH.

Though the nitrogen molecule has a singlet ground state, at present data are only provided for transitions between excited triplet states; these transitions are prominent in nitrogen and air plasmas. The empirical dataset WCCRMT line list due to Western et al. [503] covering the 4500–15 700 cm^{-1} region is available. Recently, Jans [520] extended this work to consider the N_2 ($C\ ^3\Pi_u$ – $B\ ^3\Pi_g$) second positive system, providing the data in ExoMol format. These two datasets have been merged to form a single N_2 triplet dataset.

The website currently provides a link to a list of observed nickel monohydride (NiH) transitions recorded by Vallon et al. [521] and Harker et al. [522]. These datasets which consider the isotopologues ^{58}NiH, ^{60}NiH and ^{62}NiH as well as the effects of magnetic fields, are not presented in ExoMol format. However, Havalyova [523] has constructed a high accuracy, empirical spectroscopic model for NiH which is currently being used as the starting point for constructing an ExoMol line list for this system.

2.7. Atoms

Thus far the ExoMol database has concentrated on molecular spectra. However, atomic spectra are also important for exoplanet studies. So far the website contains data on two neutral atoms:

- Potassium: Kurucz–Allard dataset for ^{39}K [320,524]
- Sodium: Kurucz–Allard dataset for ^{23}Na [320,525]

These data are given only in the form of opacities [299]. We note that Allard et al. [526] have recently updated the opacities for broadening of K by He.

2.8. Partition functions

Partition functions are provided for all molecular line lists in two column format of temperature in K and partition function. The data are provided in 1 K steps up to the temperature maximum specified by the line list and given in the `.def` file. ExoMol follows the HITRAN convention [527] and includes the full nuclear spin degeneracy contribution in the partition function unlike many astronomy oriented compilations of partition functions [528–530] which use a reduced nuclear spin factor. Our convention makes the treatment of hyperfine resolved spectra, as done in the HyVO VO line list [366], straightforward.

It is possible to compute partition functions by direct summation of the levels provided in the `.states` file; both ExoCross [385] and PyExoCross [386] offer this service. However, we recommend using the partition functions provided in the .pf file as part of the line list, as for some molecules these represent more reliable values than those that would be obtained by direct summation [531].

Table 3
Summary of data provided by the ExoMol database.

Data type
Line lists
Absorption cross-sections
Pressure broadening coefficients
Temperature dependent super-lines (histograms)
Partition functions
Cooling functions
Specific heat - heat capacity
Temperature and pressure dependent opacities
Photo-absorption continuum cross-section[a]
Photo-dissociation cross-sections including VUV absorption[a]
Spectroscopic Models

[a] Denotes a new or updated data type, see text for details.

3. Data provided

Table 3 provides a summary of the various datasets available for each isotopologue on the ExoMol website. These data can be either downloaded manually or accessed through the API (applications program interface) described in Section 3.2 below.

The following subsections describe some of these datasets, again concentrating mainly on changes since the 2020 release.

3.1. ExoMol format

Table 4 gives an overview of the ExoMol file structure. Note that ExoCross/PyExoCross generates other file types such as `.os` for oscillator strengths but these files are not distributed via the ExoMol website/database.

The core of the ExoMol data structure is the provision of a `.states` and `.trans` file [532] which give, respectively, the energy levels with associated quantum numbers and Einstein A coefficients identified by upper and lower state indices (counting numbers) which point to the `.states` file. The format of the `.trans` file is unchanged from previous releases while there have been some minor changes to data structure of the `.states`. Tables 5 and 6 present the structure of these two files. The states and, particularly, the `.trans` files can be very large so both files are supplied compressed using `.bz2` format. For larger line lists the transitions are provided as a series of files which store data for a wavenumber region specified in the file name. Wavenumbers are only provided in the `.trans` file of smaller line lists and even in these cases it is recommended to recompute them using the energies in the `.states` file as they may not reflect improvements to the states file through various corrections.

A sample extract from a `.states` file is given in Table 7. The `.states` file gives the state ID, which should correspond to the line number, and is used by the `.trans` file to identify initial and final states. The state energy, degeneracy and total angular momentum are then specified. For most species the total angular momentum corresponds to the quantum number J but for hyperfine resolved line lists this is F where $\underline{F} = |\underline{J} + \underline{I}|$ and I is the nuclear spin. The uncertainty, introduced in the 2020 release, is now a compulsory element of recommended ExoMol line lists, although it is still not available for older line lists and most non-ExoMol ones. The uncertainty provides important information for high resolutions studies and can also help to inform future experimental priorities. The state lifetime, τ, is also now compulsory for recommended ExoMol line lists; its definition is now generalised so that τ gives the lifetime obtained by considering both radiative decay [533] and predissociation effects, see Tennyson et al. [21].

The optional fields in the `.states` file are defined in the `.def` discussed below. These fields generally comprise a set of quantum numbers which characterise the state. These always include the total symmetry of the state, either in the form of a total parity (denoted

Table 4
Specification of the ExoMol file types. (Contents in brackets are optional.)

File extension	$N_{\rm files}$	File DSname	Contents
`.all`	1	Master	Single file defining contents of the ExoMol database.
`.def`	$N_{\rm tot}$	Definition	Defines contents of other files for each isotopologue.
`.states`	$N_{\rm tot}$	States	Energy levels, quantum numbers, Uncertainties, lifetimes, (Landé g-factors).
`.trans`	[a]	Transitions	Einstein A coefficients, (wavenumber).
`.broad`	$N_{\rm mol}$	Broadening	Parameters for pressure-dependent line profiles.
`.cross`	[b]	Cross-sections	Temperature or temperature and pressure-dependent cross-sections.
`.kcoef`	[c]	k-coefficients	Temperature and pressure-dependent k-coefficients.
`.pf`	$N_{\rm tot}$	Partition function	Temperature-dependent partition function.
`.cf`	$N_{\rm tot}$	Cooling function	Temperature-dependent cooling function.
`.super`	[d]	Super-lines	Temperature dependent super-lines (histograms) on a wavenumber grid.
`.nm`	[e]	VUV cross-sections	Temperature and pressure dependent VUV cross-sections (wavelength, nm).
`.fits, .h5, .kta`	[f]	Opacities	Temperature and pressure dependent opacities for radiative-transfer applications.
`.overview`	$N_{\rm mol}$	Overview	Overview of datasets available.
`.readme`	$N_{\rm iso}$	Readme	Specifies data formats.
`.model`	$N_{\rm iso}$	Model	Model specification.

$N_{\rm files}$ total number of possible files;
$N_{\rm mol}$ Number of molecules in the database;
$N_{\rm tot}$ is the sum of $N_{\rm iso}$ for the $N_{\rm mol}$ molecules in the database;
$N_{\rm iso}$ Number of isotopologues considered for the given molecule.
[a] There are $N_{\rm tot}$ sets of `.trans` files but for molecules with large numbers of transitions the `.trans` files are subdivided into wavenumber regions.
[b] There are $N_{\rm cross}$ sets of `.cross` files for each isotopologue.
[c] There are $N_{\rm kcoef}$ sets of `.kcoef` files for each isotopoplogue.
[d] There are N_T sets of T-dependent super-lines.
[e] There are $N_{\rm VUV}$ sets of VUV cross-sections.
[f] Set of opacity files in the format native to specific radiative-transfer programs.

Table 5
Transitions file specification.

Field	Fortran format	C format	Description
i	`I12`	`%12d`	Upper state ID
f	`I12`	`%12d`	Lower state ID
A	`ES10.4`	`%10.4e`	Einstein A coefficient in s^{-1}
$\tilde{\nu}_{fi}$	`E15.6`	`%15.6e`	Transition wavenumber in cm^{-1} (optional).

Fortran format: `(I12,1x,I12,1x,ES10.4,1x,ES15.6)`.

+/−), a rotationless parity (denoted e/f) or an irreducible representation of the molecular symmetry group the molecule is associated with. The latter is more typical for polyatomic molecules with complex symmetry groups. Other quantum numbers are always approximate; for many polyatomic molecules, two or even three sets of quantum numbers are available. For those line lists denoted as being high resolution in Table 1 two extra columns have been added to the `.states` file. High resolution line lists have energy levels that have been updated either using MARVEL energies (denoted Ma) or energies from some other source with very high accuracy/low uncertainties. The penultimate column of the line list gives the original calculated energy level; of course if the state energy remains the calculated one (denoted Ca) then these two levels will be the same. The final auxiliary column gives the source of this updated energy level, see Table 8; the various means of improving on the original energy levels are discussed by McKemmish et al. [16].

3.2. API, versioning, master and def files

The ExoMol database has an application programming interface (API) which allows users to extract data computer to computer without the need to manually download datasets from the website. Details of how to use the API are given in the ExoMol2020 release [5].

It is ExoMol practice to give each line list a name, denoted <DATASET> below. Alongside the name, each line list has a version number given by the version date in YYYYMMDD format. MARVELization or other energy level updates to the `.states` file just lead to a new version of the line list. Conversely, a newly calculated line list, and hence a new `.trans` file, is always given an new name. Both old versions and old (retired) line lists are retained in the database to allow users to compare with previous results. The most recent version is stored without a version number (date); all previous versions are also retained and have the version in YYYYMMDD format added to their name.

To facilitate the use of the API and to provide complete metadata, the database contains a `.master` file, which is located at www.exomol.com/exomol.all. The `.master` file points to a `.def` for each recommended line list. Note that there are `.def` and `_def.json` files for each isotopologue for which ExoMol provides a line list. The `.master` file itself has a version number in YYYYMMDD format; this date corresponds the latest update of a `.def`. The version dates of the individual line lists are given in the `.master` file.

JSON (JavaScript Object Notation) [536] is a lightweight human-readable, data-interchange format. ExoMol database newly provides JSON format `.master` (`exomol.json`) and definition (<ISOTOPOLOGUE>__<DATASET>_`def.json`) files. In the Appendix, Listing 1 gives an extract from the current, JSON format `.master` file (`exomol.json`) with keywords defined in Table 9 and Listing 2 shows the JSON format definition file (`_def.json`) of the POKAZATEL $H_2{}^{16}O$ line list. Table 10 gives the JSON keyword structure for the `.def` file.

3.3. Cross-sections and continuum absorption

Table 11 gives the general ExoMol format for cross-sections (`.cross`) files. Cross-sections for line lists are supplied [322] to allow users to get an overall picture of the line lists contained in the database. These are provided for different temperatures but at zero pressure (i.e. there is no allowance for pressure broadening) via the ExoMol cross-section app allowing users to select the temperature, wavenumber range and the resolution (in cm^{-1}).

The extension of line lists into the UV means that molecules often have a continuum contribution to their spectrum alongside their characteristic, sharp line absorption. This temperature-dependent continuum component of the absorption is provided as a set of `.cont` files given at 100 K intervals from 100 K to the stated $T_{\rm max}$ for the given line list in same format as the `.cross` file. The continuum functions were generated neglecting effects due to pressure broadening which are unlikely to be significant for continuum absorptions. The methodology has been introduced in Tennyson et al. [21]. `.cont` files are currently available for AlH and AlD [19], and OH [372].

Table 6
Specification of the `.states` file including extra data options; the formats at the end of the table are for the compulsory section only.

Field	Fortran format	C format	Description
i	`I12`	`%12d`	State ID
$\tilde{E}$	`F12.6`	`%12.6f`	Recommended state energy in cm^{-1}
g_{tot}	`I6`	`%6d`	State degeneracy
J	`I7/F7.1`	`%7d/%7.1f`	Total angular momentum quantum number, J or F (integer/half-integer)
Unc	`F12.6`	`%12.6f`	Uncertainty in the state energy in cm^{-1}
τ	`ES12.4`	`%12.4e`	State lifetime (aggregated radiative and predissociative lifetimes) in s
(g)	`F10.6`	`%10.6f`	Landé g-factor (optional)
(QN)	See `.def` file		State quantum numbers, may be several columns (optional)
(Abbr)	`A2`	`%2s`	Abbreviation giving source of state energy, see Table 8.
($\tilde{E}_0$)	`F12.6`	`%12.6f`	Calculated state energy in cm^{-1} (optional)

Fortran format, J integer: `(I12,1x,F12.6,1x,I6,I7,1x,F12.6,1x,ES12.4,1x,F10.6)`
or J half-integer: `(I12,1x,F12.6,1x,I6,F7.1,1x,F12.6,1x,ES12.4,1x,F10.6)`.

Table 7
Extract from the state file for XAB line list for $^{24}Ca^{1}H$ [359].

i	$\tilde{E}$	g	J	unc	τ	g	+/−	e/f	State	v	Λ	Σ	Ω	Abbr	$\tilde{E}_0$
33	24 428.044063	4	0.5	0.007010	1.7190E−07	2.002233	+	e	B'(2SIGMA+)	3	0	0.5	0.5	Ma	24 428.027169
34	24 986.629171	4	0.5	2.507500	5.4398E−08	−0.000637	+	e	A(2PI)	4	1	−0.5	0.5	Ca	24 986.629171
35	25 163.713092	4	0.5	0.022010	2.0005E−07	2.002233	+	e	B'(2SIGMA+)	4	0	0.5	0.5	Ma	25 163.694359
36	25 876.111435	4	0.5	0.101011	3.1000E−07	2.002217	+	e	B'(2SIGMA+)	5	0	0.5	0.5	Ma	25 876.060619
37	26 224.114885	4	0.5	3.007500	5.8534E−08	−0.000612	+	e	A(2PI)	5	1	−0.5	0.5	Ca	26 224.114885

i: State counting number.
$\tilde{E}$: State energy in cm^{-1}.
g: State degeneracy.
J: Total angular momentum.
unc: Energy uncertainty in cm^{-1}.
τ: Lifetime in s.
g: Landé g-factor.
+/−: Total parity.
e/f: rotationless-parity.
State: state term value using `PyValem` format [534,535].
v: State vibrational quantum number.
Λ: Projection of the electronic angular momentum.
Σ: Projection of the electronic spin.
Ω: $\Omega = \Lambda + \Sigma$, projection of the total angular momentum.
Abbr: Abbreviation giving source of state energy, see Table 8.
$\tilde{E}_0$: Original (calculated) state energy in cm^{-1}.

Table 8
Source type abbreviations used to describe energy levels in hybrid (MARVELized) line lists; see McKemmish et al. [16] for further details.

Abbr	Meaning
Ca	Calculated
Ma	MARVEL
EH	Effective Hamiltonian
Mo	MOLLIST
HI	HITRAN
PS	Predicted Shift
IE	Isotopologue Extrapolation

Table 9
Keywords used in the JSON format `.master` (`exomol.json`) file.

Keywords	Meaning
ID	Always the string "`EXOMOL.master`"
version	Version number with format YYYYMMDD
num_molecules	Number of molecules in the database
num_isotopologues	Number of isotopologues in the database
num_datasets	Number of datasets in the database
num_species	Number of species in the database
molecules	List of molecules
| formula[a]	Molecule chemical formula
| | num_molecule_names	Number of molecule names listed
| | molecule_names	List of the molecule names
| | num_isotopologues	Number of isotopologues considered
| | linelist	Line list
| | | inchikey	InChIKey of isotopologue
| | | iso_slug	Iso-slug
| | | iso_formula	Formula of isotopologue
| | | dataset_name	Isotopologue dataset name
| | | version	Version number with format YYYYMMDD

[a] The keywords with * are variable.

3.4. Specific heats and cooling functions

The specific heat capacity at constant pressure (isobaric) C_p is supplied on a 1 K grid from $T = 0$ K to T_{max} in units of J mol^{-1} K^{-1}, where available. Otherwise, it can be computed from the available partition function by [537]

$$C_p(T) = R\left[\frac{Q''}{Q} - \left(\frac{Q'}{Q}\right)^2\right] + \frac{3R}{2}, \tag{2}$$

where the second term is the translational contribution, and

$$Q'(T) = T\frac{\mathrm{d}Q}{\mathrm{d}T}, \tag{3}$$

$$Q''(T) = T^2\frac{\mathrm{d}^2Q}{\mathrm{d}T^2} + 2Q', \tag{4}$$

and R is the gas constant. A complete set of specific heats was generated for the main (parent) isotopologue for each recommended ExoMol line list as part of the project to provide these data in standard (NASA) polynomial form [297].

Cooling functions can be important for astronomical studies [403,489,538,539] and can be computed from ExoMol line lists. The temperature-dependent cooling function, $W(T)$ (units erg (s sr molecule)$^{-1}$ = 10^{-7} Watts (molecule sr)$^{-1}$) is the total energy per unit solid angle emitted by a molecule:

$$W(T) = \frac{1}{4\pi Q(T)}\sum_{f,i} A_{fi} hc\tilde{\nu}_{fi} g'_f e^{-c_2\tilde{E}'_f/T}. \tag{5}$$

Table 10
Keywords use in the JSON format definition (`<ISOTOPOLOGUE>__<DATASET>_def.json`) file.

Keywords	Meaning
isotopologue	Isotopologue section
| iso_formula	Formula of isotopologue
| iso_slug	Iso-slug
| inchikey	InChIKey of isotopologue
| inchi	InChI of isotopologue
| mass_in_Da	Mass of isotopologue (sum of atom masses) in Da
| point_group	Symmetry group
atoms	Atoms section
| number_of_atoms	Number of atoms
| element	Element symbol
| | atom[a]	In format: Element symbol : Isotope number
irreducible_representations	Irreducible representation section
| label[a]	In format: Irreducible representation label : Nuclear spin degeneracy
dataset	Dataset line list files section
| name	Isotopologue dataset name
| version	Version number with format YYYYMMDD
| doi	DOI of dataset paper
| max_temperature	Maximum temperature of linelist
| num_pressure_broadeners	Number of pressure broadeners available
| nxsec_files	Number of cross-section files available
| nkcoeff_files	Number of k-coefficient files available
| dipole_available	Dipole availability (true = yes, false = no, null = undefinded)
| cooling_function_available	Cooling function availability (true = yes, false = no, null = undefinded)
| specific_heat_available	Specific heat availability (true = yes, false = no, null = undefinded)
| continuum	Photo-absorption continuum cross-sections availability (true = yes, false = no, null = undefinded)
| predis	Photo-dissociation cross-sections availability (true = yes, false = no, null = undefinded)
| states	States file part
| | number_of_states	Number of states in `.states` file
| | max_energy	Maximum energy (in cm^{-1}) in the states file
| | uncertainty_description	Uncertainty description
| | uncertainties_available	Uncertainty availability (true = yes, false = no, null = undefinded)
| | lifetime_available	Lifetime availability (true = yes, false = no, null = undefinded)
| | lande_g_available	Lande g-factor availability (true = yes, false = no, null = undefinded)
| | num_quanta	Number of quanta defined
| | states_file_fields	Columns list in the states file
| | | name	Column name in `.states` file. There are three formats:
| | |	1. Main column name; 2. Quantum case label : Quantum label; 3. Auxiliary : Auxiliary title
| | | desc	Description of column in the states file
| | | ffmt	Fortran format
| | | cfmt	C format
| transitions	Transitions file(s) part
| | number_of_transitions	Total number of transitions in `.trans` file(s)
| | number_of_transition_files	Number of `.trans` file(s)
| | max_wavenumber	Maximum wavenumber (in cm^{-1})
partition_function	Partition function file section
| max_partition_function_temperature	Maximum temperature of partition function
| partition_function_step_size	Step size of temperature
broad	Broadening files section
| default_Lorentzian_half-width	Default value of Lorentzian half-width for all lines (in cm^{-1}/bar)
| default_temperature_exponent	Default value of temperature exponent for all lines
| label[a]	A label for a particular broadener
| | filename	Filename of particular broadener
| | max_J	Maximum J for which pressure broadening parameters are provided
| | Lorentzian_half_width	Value of Lorentzian half-width for $J'' > J_{max}$
| | temperature_exponent	Value of temperature exponent for lines with $J'' > J_{max}$
| | num_quantum_number_sets	Number of defined quantum number sets
| | quantum_number_sets	Defined quantum number sets
| | | code	A code that defines this set of quantum numbers
| | | num_lines	Number of lines in the broad that contain this code
| | | num_quantum_numbers	Number of quantum numbers defined
| | | quantum_numbers	Defined quantum number(s)

[a] The keywords with * are variable.

Table 11
Specification of the `.cross` cross-section and `.cont` file format.

Field	Fortran format	C format	Description
$\tilde{\nu}_i$	`F12.6`	`%12.6f`	Central bin wavenumber, cm^{-1}
σ_i	`ES14.8`	`%14.8e`	Absorption cross-section, cm^2 $molec^{-1}$

Fortran format: `(F12.6,1x,ES14.8)`.

where Q is the partition function, A_{fi} the relevant Einstein-A coefficient, $\tilde{\nu}_{fi}$ is the transition wavenumber, g'_f is the degeneracy of the upper state and $\tilde{E}'_f$ is the energy of the upper state. Finally, c_2 is the second radiation coefficient which allows for an energy level given in terms of wavenumbers. This can be done using either ExoCross [385] or PyExoCross [386]. At present the ExoMol website provides a small number of precomputed cooling functions.

3.5. ExoMolOP: Opacities

Chubb et al. [299] computed opacity cross-sections for all molecules available from the ExoMol database plus the oxygen molecule, and atoms Na and K (using line position data from Kurucz [320] and data for the broadening of the strong doublets from [524,525]) for a grid of temperatures and pressures and broadening regime appropriate for hot Jupiters, *i.e.* broadening by H_2 and He. The data are provided in formats appropriate for direct use in exoplanetary retrieval and modelling codes ARCiS [222], which uses the well established .fits format [540], petitRADTRANS [541,542], NEMESIS [543] and Tau-REx [216]. The data format and gridding is code dependent with opacities for ARCiS, petitRADTRANS, and NEMESIS given as k-tables at a resolving power of $R = \frac{\lambda}{\Delta\lambda} = 1000$ while cross-sections are provided for Tau-REx with R = 15 000. The work of Chubb et al. has been updated for the newly created ExoMol line lists listed in Table 1. At present these opacities are typically only for the main (parent) isotopologue for each molecule (with some exceptions, for example CO is available with isotopologues mixed at terrestrial natural abundances).

The plan for the future will be to provide a broader range of opacities which (a) allow for mixtures of isotopologues and (b) using our newly derived broadening parameters (see below) to provide opacities for a variety of atmospheric compositions.

4. Collisional line broadening

The generation of opacities requires knowledge of line shape parameters, with collisional line broadening being a key process [544] in determining the frequency distribution of a line's intensity. In the course of previous works in the group, an ExoMol diet was introduced [545] which provided parameters characterising the collisional line broadening required for the Voigt profile. The reference collisional line width γ_0 (in $\mathrm{cm^{-1}\ atm^{-1}}$) and its temperature exponent n are assumed to obey the following power law:

$$\gamma(T,P) = \gamma_0(T_{\rm ref},P_{\rm ref})\left(\frac{T_{\rm ref}}{T}\right)^n \frac{P}{P_{\rm ref}}, \tag{6}$$

where $T_{\rm ref}$, $P_{\rm ref}$ are some reference temperature and pressure, which in ExoMol are chosen as 296 K and 1 atm, respectively. The ExoMol diet tabulates Lorentzian half-width, γ_0, and its temperature dependence, n, for each perturbing species, and the final half-width is calculated as a sum of contributions from all the perturbers. The ExoMol diet is organised in the form of 'recipes', tabulating the dependence of γ_0 and n on the rotational and vibrational quantum numbers.

The pressure broadening `.broad` file structures used by the ExoMol diet are illustrated in Table 12. For each radiator–perturber pair, the diet files contain one or more recipes indicated by a unique label in the first column (`a0`, `a1`, etc.). This label is followed by collisional broadening parameters, for instance $\gamma_0(T_{\rm ref},P_{\rm ref})$ and n from Eq. (6), and by a set of quantum numbers used in the recipe's parametrisation scheme. For example, J'' is used in `a0`, while `a1` additionally uses K''. Note that a file might have a varying number of columns if different recipes require it. The naming convention for all pressure broadening files is to give broadening data for the main isotopologue, however pressure broadening data are not isotope specific in the current iteration of the database. If a user wishes to include pressure broadening for minor isotopologues, then they should use the data provided for the major isotopologue.

Table 13 lists the current menu of ExoMol diets. As a new diet option, the spectroscopic index $|m|$ has been introduced to better describe the rotational dependence of collisional parameters γ_0 and n, where m is defined as $m = -J''$ for P-branch transitions, $m = J'' + 1$ for R-branch, and $m = J''$ for Q-branch (i.e. the same as done in HITRAN). The "m0" option (see Table 13) has been used to define $\gamma_{\rm L}$ for AlH as part of the recent AloHa line list [19] (labelled in the diet `.broad` file as `m0`); the "m1" recipe was introduced to describe the dependence on the lower state K'' quantum number for a symmetric top molecule $^{15}NH_3$ in addition to the dependence on $|m|$ [371].

Table 12
Examples of the .broad ExoMol diet files for the 'a0', 'a1' and 'm0' recipes.

Label	γ	n	J''/m	K''
`24Mg-16O__O2.broad`				
a0	0.043	0.500	0	
...				
`1H2-16O__H2.broad`				
a1	0.0916	0.790	0	1
a1	0.0852	0.608	1	2
a1	0.0764	0.541	2	3
a1	0.0699	0.502	3	4
a1	0.0635	0.458	4	5
...				
`27Al-1H__H2.broad`				
m0	0.1554	0.6406	1	
m0	0.1489	0.6235	2	
m0	0.1450	0.6128	3	
m0	0.1410	0.6002	4	
...				

Table 13
Parameters defined in the ExoMol broadening diets.

Diet code	Quantum numbers	Systems
`a0`	J''	General use (e.g. [545])
`a1`	J'', K''	General use (e.g. [545])
`m0`	$\|m\|$	General use (e.g. [19])
`m1`	$\|m\|$, K''	General use (e.g. [371])
`a5`	J', K'_a, K'_c, J'', K''_a, K''_c	Asymmetric tops (e.g. SO_2 [545])

The ExoMol database contains empirical broadening data for seven species: H_2O, NH_3, SO_2, CH_4, PH_3, HCN, and H_2CO broadened by H_2 and He. In addition, for most of the other ExoMol molecules, especially exotic ones, the ExoMol diet now provides theoretical line broadening parameters computed using at least one of three methods, simple semi-classical calculations, explicit semi-classical Modified Complex Robert-Bonamy (MCRB) approach and Machine Learning described below.

The MCRB semi-classical approach [546] is capable of producing broadening parameters accurate to within experimental uncertainty if an accurate interaction potential between the radiating and perturbing molecule is available. If only rough model potential data are available, fitting of the interaction potential to experimental line broadening coefficients can be used to improve the description for a range of transitions and temperatures. Calculations of vibrational contributions to broadening coefficients additionally require the knowledge of ro-vibrational state-dependent molecular quantities for the radiating molecule (dipole moment, polarisability). Broadening calculations have been done for AlH broadened by H_2, He, N_2, and AlH [19], and work on C_2H_2 broadened by H_2, He, N_2, C_2H_2, and CO_2 is currently under way [547]. In these cases, the vibrational contributions have been found to be negligible, so the respective `.broad` files only contain the dependence on the rotational quantum number J. Future work includes producing J (m)-dependent broadening parameters for a number of diatomic molecules from the ExoMol database broadened by various perturbers using model interaction potentials, where the calculations are not too demanding.

A novel Machine Learning (ML) method has been developed [548] to predict the line broadening parameters γ_0. This ML approach is suitable for the cheap mass production of pressure broadening parameters for any active neutral molecule; the ML code and associated data available on the ExoMol Zenodo area [549]. The algorithm considers the rotational dependence of the broadening but ignores any dependence on vibrational and/or electronic states.

Using this ML code, J-dependent air-broadening parameters $\gamma_{\rm air}$ have been produced for all molecules in the ExoMol database, suitable

Table 14
Availability of new air broadening data, $\gamma_{\rm air}$. The molecules with ML data were generated with [548]. Other air broadening data are taken from the HITRAN database [2].

ML data					HITRAN data	
MgH	NaH	NiH	AlH	CrH	HCl	CH_3Cl
CaH	BeH	TiH	FeH	LiH	HF	C_2H_4
ScH	NH	CH	OH	SiH	HBr	C_2H_2
SH	PH	VO	ALO	YO	CO	PH_3
MgO	TiO	SiO	CaO	NaO	NO	H_2O
LaO	ZrO	SO	PO	PN	O_2	CO_2
KCl	NaCl	LiCl	CN	C_2	CS	SO_2
H_2	CP	PS	NS	SiS	N_2	HCN
NaF	AlCl	AlF	KF	LiF	CH_4	N_2O
CaF	MgF	SiN	H_2O_2	SO_3	NH_3	H_2S
SiH_4	AsH_3	PF_3	CH_3	P_2H_2	HNO_3	OCS
H_2CS	CaOH	KOH	NaOH	SiH_2	H_2CO	
SiO_2	LiOH				CH_3F	

Table 15
New (rotationally-independent) line broadening data γ_0 in the ExoMol database generated using the semi-classical method by Buldyreva et al. [550].

Active molecules				Perturbers
AlCl	CrH	NaCl	SH	self
AlH	CS	NaF	SiH	Ar
AlO	KCl	NaH	SiH_2	CH_4
AsH_3	KF	NaOH	SiO	CO
BeH	KOH	NH	SiO_2	CO_2
C_3	LiCl	NS	SiS	H_2
CaF	LiF	PF_3	TiH	H_2O
CaH	LiH	PH	TiO	He
CaO	LiH^+	PN	VO	N_2
CaOH	MgF	PO		NH_3
CH_3	MgH	PS		NO
CP	MgO	ScH		O_2

for room temperature and pressure environments, where air is the primary source of broadening. The empirical $\gamma_0^{\rm air}$ values for training were taken from the HITRAN database [2]. These data are available on the ExoMol website, where the temperature exponent value of $n = 0.5$ is assumed. Further work using machine learning to predict γ_0 for other perturbing species is ongoing. The molecules for which J-dependent air-broadening data are available is summarised in Table 14. High quality data have simply been copied from the HITRAN database [2] while other values are machine learned predictions [548].

The need for at least approximate values of pressure-broadened rovibrational line widths for "exotic" molecular pairs relevant to exoplanetary atmospheres initiated a theoretical study [550] giving access to simple semi-classical (rotationally-independent) estimates from the knowledge of molecular masses and kinetic diameters. Being valid for neutral active molecules but also for spectroscopically active molecular ions, this method allowed the ExoMol database to be populated with estimates of pressure-broadening coefficients for perturbation by H_2, O_2, N_2, He, Ar, CO, CS, NO, CO_2, H_2O, CH_4, NH_3 and self-perturbation for 45 active molecules (main species) [551] in ExoMol, see Table 15; work is in progress on producing similar data for their most abundant isotopologues. Available on the ExoMol website are the reference-temperature (296 K) predictions issued from data considered as the most reliable/recent kinetic diameter values. Results for CH_2, FeO, PO_2, SH_3, SiC, SiH_3 and TiF are not currently available on the ExoMol website, as there are no corresponding line lists available for these molecules. Results for temperatures above 296 K are easily obtained by a simple scaling factor $\sqrt{296/T}$ but the temperature considered should not be too low as classical-path approximation has to remain valid (i.e. the kinetic energy of the relative molecular motion should be higher than the isotropic intermolecular potential depth), see the discussion by [551].

Pressure-induced line-shape parameters have also been addressed for the case of vibronic transitions connecting low-lying vibrational levels in the ground and excited (bound) electronic states [552]. In this case the collisional (pressure) broadening is still not dominated by predissociative effects. Pre-computed potential-energy surfaces for interactions of some representative molecular pairs enabled both line-width and line-shift calculations comparing favourably with available measurements from room temperature to 2800 K [552]. Further attempts at improvements are in progress, in order to establish a reliable computational scheme for providing line widths and shifts for rovibronic transitions of active molecular species listed in ExoMol.

In instances where a new set of broadening data is introduced for a system with already available data, a version number is added to the filename of the older data set in order to distinguish multiple versions of the same system. The version number is a timestamp indicating the date the dataset was created (uploaded to the data base) in the YYYYMMDD format as described in Section 3.2. The most recent or recommended version does not contain a version number. Although, at present, there is only one molecule, AlH, with broadening parameters computed by more than one method, we expect this number to grow. Apart from the experimental sources as e.g. provided by HITRAN, line broadening parameters have been provided by different computational methods such as ML [548], MCRB [546], simple semi-classical [550, 551] as well phase shift [552] approaches.

5. Predissociative line broadening

As introduced in Section 3, the definition of the lifetimes in ExoMol has been extended to include the predissociative lifetimes as part of the `.states` file provision. The practical purpose of this extension is to be able to model the predissociative broadening together with the collisional and Doppler broadening. The lifetime broadening is described by Lorentzian line shape like pressure broadening with γ_τ, the half-width in $\rm cm^{-1}$, given by

$$\gamma_\tau = \frac{\hbar}{2\tau hc}, \tag{7}$$

where τ is the half-harmonic mean of the radiative $\tau_{\rm r}$ and predissociative τ_p lifetimes via

$$\tau = \frac{\tau_{\rm r}\tau_{\rm p}}{\tau_{\rm r} + \tau_{\rm p}}. \tag{8}$$

The half-width γ_τ can be added to the pressure-broadening half-width, γ in Eq. (6), to give the total Lorentzian component of the line profile.

Predissociation due to rotational barrier effects has been studied for AlH, see Section 2.2.3. Predissociative line broadening due to spin–orbit interactions with the continuum has also been studied for OH [20], see 2.2.13, using a modified stabilisation method [18,553–555]. Predissociation lifetimes will also soon be released for SH and SD using the spectroscopic model from current linelist [341,400] with the addition of the dissociative states, $1\,^2\Sigma^-$, $1\,^4\Sigma^-$, and $1\,^4\Pi$.

6. Photodissociation and continuum absorption

The extension of the database to consider photodissociation means we define a new file type `.photo`, which provides temperature-dependent photodissociation cross-sections. The format of the photodissociation cross section has been introduced in Tennyson et al. [21] and specified in Table 16. In contrast to other data in the database, `.photo` files give results as a function of wavelength in nm. The project is only just starting to generate photodissociation cross-sections, and so far, calculated cross-sections are available for HF and HCl [556]. A major expansion of this part of the database is planned.

The previous section in the database/on the website called photoabsorption continuum cross-sections, which contained measured UV

Table 16
Specification of the wavelength-dependent `.photo` cross-section file format.

Field	Fortran format	C format	Description
λ_i	F6.2	%6.2f	Central bin length, nm
σ_i	ES14.8	%14.8e	Photodissociation cross-section, cm^2 $molec^{-1}$

Fortran format: (F6.2,1x,ES14.8).

photoabsorption cross-sections, had been moved into the photodissociation area. These data are presented in the same format as the computed photodissociation cross-sections, but the temperature, pressure and broadening parameters are determined by the experimental conditions used and generally do not form a regular grid. Measured cross-sections are available for H_2O, CO_2, SO_2, NH_3, H_2CO, C_2H_4 and CO. These cross-sections probably represent a good approximation to the photodissociation cross-section for the given species [557]. Table 4 of the ExoMol2020 release [5] gives more details on these cross sections provided which are due to Venot et al. [557] and Fateev and co-workers (private communication, 2020).

7. Post-processing

ExoMol provides post-processing capabilities through the Fortran program ExoCross (GitHub: https://github.com/ExoMol/ExoCross) [385] and the Python program PyExoCross [386] (GitHub: https://github.com/ExoMol/PyExoCross). There are example jobs for both ExoCross and PyExoCross on their GitHub pages.

ExoCross has many functions such as generating pressure and temperature dependent cross-sections, partition functions, specific heat, state-resolved radiative lifetimes, non-local thermodynamic equilibrium (non-LTE) spectra, electric dipole, electric quadrupole and magnetic dipole spectra. ExoCross can read data in both ExoMol and HITRAN [558] formats and output them in these formats as well as SPECTRA (http://spectra.iao.ru/) and Phoenix formats [559]. Should data be required in HITRAN format, it is strongly recommended that the data are downloaded to a local computer in the much more compact ExoMol format and then processed using ExoCross.

As a Python adaptation of the post-processing program ExoCross, PyExoCross supports importing and exporting line lists in the ExoMol and HITRAN formats [314] and can convert data format between ExoMol and HITRAN formats. PyExoCross provides functions for calculating partition functions, specific heats, radiative lifetimes, cooling functions, oscillator strengths, LTE and non-LTE absorption and emission stick spectra and cross-sections. Users can extract low uncertainties, high intensities and specified quantum number labels and values by using uncertainty, threshold and quantum number filters when calculating stick spectra and cross-sections. PyExoCross can also help users automatically download line lists files from the ExoMol database in batches. The user instruction manual is available on https://pyexocross.readthedocs.io/.

8. New web services

8.1. ExoMolHR

ExoMolHR (ExoMol High-Resolution) [298] is a new high-resolution molecular spectroscopic database based on the ExoMol line list database; it is available at www.exomol.com/exomolhr. The ExoMolHR database is focused on providing high accuracy line positions for high-resolution studies such as line identification or simulations of high-resolution spectra. Initially reduced line lists are constructed by scraping the ExoMol database for energy levels (and hence transitions) which are determined to high accuracy (uncertainty ≤ 0.01 cm^{-1}). After this all transitions which can be predicted at high resolution ($R > 100\,000$) are stored; these transitions provide the core of the database. For each transition, ExoMolHR provides the frequency, uncertainty, Einstein A-coefficient, intensity (at a user specified temperature), lower energy, total level degeneracy, angular momentum and quantum numbers for upper and lower states. Users can download datasets using the API directly with the intensities computed at a reference temperature $T_{ref} = 296$ K. Alternatively, they can use the interactive web interface where one can set parameters to filter the wavenumber range, extract low uncertainties and lines with strong intensities, and then store the results generated for downloading. The ExoMolHR database currently contains data for 55 isotopologues from 32 molecules, see Table 17; this number is growing quite rapidly as more MARVEL studies are completed.

8.2. LiDB

LiDB (Lifetimes Database) is a newly developed database of molecular vibrational and vibronic state radiative lifetimes [296], created to enable radiative effects to be properly captured in low-temperature plasma models. The main data output of LiDB is radiative lifetimes at vibrational and electronic state resolution. Partial lifetimes, which give information on the dominant decay channels in a molecule, are also provided. Datasets for 36 molecules are available, produced from the respective molecular line list in the ExoMol database. LiDB is freely available and hosted at www.exomol.com/lidb. Users can dynamically view molecular datasets or use a specially-designed API to perform data requests. LiDB is linked directly to the Quantemol DataBase (QDB) [560] which aims to provide comprehensive datasets for plasma modelling. LiDB will expand in the future with the addition of more molecules, important isotopologues, and neutral and singly-charged atomic species.

9. Future development

The ExoMol project will continue not only to provide high quality data on more molecules, but the type of data available will be expanded to maximise the scientific richness that can be extracted from observations possible with new and upcoming telescopes. We are also open to hosting high quality, relevant datasets (both computed and measured) obtained by other groups.

The start in computing photodissociation cross-sections and rates, as well as the treatment of rovibronic spectra signals our intention to extend the database to cover processes which occur at ultraviolet (UV) wavelengths. This will mean developing methods of performing calculations involving many electronic states for molecules larger than diatomics.

The calculations on the Renner–Teller system of CaOH [561] were performed using the variational rovibronic nuclear motion code EVEREST [448]. We are currently using EVEREST to explore the calculation of photodissociation spectra of triatomic systems using HCN as a test case [562]. The plan will be to start providing extended coverage of temperature-dependent photoabsorption cross-sections. For photodissociation we have already identified a number of studies on diatomics which provide temperature-dependent cross sections [282, 563–572] which we hope to add to the database.

The methodology for generating atomic as opposed to molecular data is actually very different and thus done by different research groups with information dispersed. However, astronomically, both species are often present together; for example, there is now a significant number of neutral and singly charged atoms that have been observed in exoplanetary atmospheres [573–575]. To support exoplanet studies, therefore, users have requested that atomic data also be provided in the same ExoMol format to facilitate more convenient analysis. We have started to address this need with the inclusion of the opacities for Na and K in a H_2/He atmosphere, see Section 2.7. Further expansions to include atomic data are being actively pursued with NIST [576,577] and/or the Kurucz database [320] as possible sources.

Table 17
Contents of the ExoMolHR database [298]; lines are extracted from the ExoMol database on the basis that they have low uncertainties.

ID	Molecule	Isotopologue	Dataset	$N_{\rm states}$	$N_{\rm files}$	$N_{\rm trans}$	$N_{\rm HRstates}$	$N_{\rm HRlines}$
1	AlCl	$^{27}Al^{35}Cl$	YNAT	65 869	1	4 722 048	41	101
2	AlCl	$^{27}Al^{37}Cl$	YNAT	67 507	1	5 748 704	41	121
3	AlH	$^{27}Al^{1}H$	AloHa	1 364	1	29 725	135	692
4	AlO	$^{26}Al^{16}O$	ATP	93 350	1	4 866 540	4 783	143 197
5	AlO	$^{27}Al^{16}O$	ATP	94 862	1	4 945 580	4 980	149 577
6	AlO	$^{27}Al^{17}O$	ATP	96 350	1	5 148 996	4 787	142 905
7	AlO	$^{27}Al^{18}O$	ATP	98 269	1	5 365 592	4 799	142 976
8	C_2	$^{12}C_2$	8states	44 189	1	6 080 920	8 376	445 682
9	C_2H_2	$^{12}C_2^1H_2$	aCeTY	5 160 803	100	4 347 381 911	8 898	473 850
10	CH_4	$^{12}C^1H_4$	MM	9 155 208	121	50 395 644 806	21 021	7 649 736
11	CN	$^{12}C^{14}N$	Trihybrid	28 004	1	2 285 103	4 833	244 808
12	CO_2	$^{12}C^{16}O_2$	UCL-4000	3 480 477	20	2 557 549 946	18 881	2 600 218
13	CaH	$^{40}Ca^{1}H$	XAB	6 825	1	293 151	1 165	12 341
14	CaOH	$^{40}Ca^{16}O^{1}H$	OYT6	3 187 522	18	23 384 729 495	1 424	12 984
15	H_2CO	$^{1}H_2^{12}C^{16}O$	AYTY	10 297 025	100	12 688 112 669	4 813	317 729
16	H_2CS	$^{1}H_2^{12}C^{32}S$	MOTY	52 292 454	8	43 561 116 660	3 625	72 218
17	H_2O	$^{1}H_2^{16}O$	POKAZATEL	810 269	412	5 745 071 340	14 395	3 520 554
18	H_2S	$^{1}H_2^{32}S$	AYT2	220 631	35	115 032 941	2 061	63 719
19	H_3O^+	$^{1}H_3^{16}O^+$	eXeL	1 173 114	100	2 089 331 073	232	1 785
20	H_3^+	$^{1}H_2^{3}H^+$	ST	33 330	1	22 164 810	109	646
21	H_3^+	$^{1}H_3^+$	MiZATeP	158 721	1	127 542 657	994	13 606
22	H_3^+	$^{2}H_2^{1}H^+$	MiZo	369 500	32	2 290 235 000	115	683
23	H_3^+	$^{2}H_3^+$	MiZo	37 410	21	36 078 183	115	225
24	LiOH	$^{6}Li^{16}O^{1}H$	OYT7	192 412	5	294 573 305	255	840
25	LiOH	$^{7}Li^{16}O^{1}H$	OYT7	203 762	5	331 274 717	240	749
26	MgH	$^{24}Mg^{1}H$	XAB	3 148	1	88 575	237	2 462
27	MgH	$^{25}Mg^{1}H$	XAB	3 156	1	88 776	548	5 850
28	MgH	$^{26}Mg^{1}H$	XAB	3 160	1	88 891	537	5 339
29	N_2O	$^{14}N_2^{16}O$	TYM	1 759 068	21	1 360 351 722	17 018	3 459 640
30	NH	$^{14}N^{1}H$	kNigHt	4 076	1	327 014	1 030	26 131
31	NH	$^{14}N^{2}H$	kNigHt	7 406	1	778 105	118	943
32	NH	$^{15}N^{1}H$	kNigHt	4 089	1	327 877	118	943
33	NH	$^{15}N^{2}H$	kNigHt	7 465	1	785 940	118	943
34	NH_3	$^{14}N^{1}H_3$	CoYuTe	5 095 730	200	16 941 637 250	4 720	412 149
35	NO	$^{14}N^{16}O$	XABC	30 811	1	4 596 666	3 044	106 711
36	OCS	$^{16}O^{12}C^{32}S$	OYT8	2 399 110	10	2 527 364 150	5 198	279 273
37	PN	$^{31}P^{14}N$	PaiN	30 327	1	1 333 445	32	44
38	SO	$^{32}S^{16}O$	SOLIS	84 114	1	7 086 100	536	2 501
39	SO_2	$^{32}S^{16}O_2$	ExoAmes	3 270 271	80	1 300 000 000	14 924	1 504 495
40	SiN	$^{28}Si^{14}N$	SiNfull	131 936	1	43 646 806	99	670
41	SiN	$^{28}Si^{15}N$	SiNfull	133 460	1	44 816 182	56	464
42	SiN	$^{29}Si^{14}N$	SiNfull	132 335	1	43 946 969	56	464
43	SiN	$^{30}Si^{14}N$	SiNfull	132 706	1	44 223 730	56	464
44	SiO	$^{28}Si^{16}O$	SiOUVenIR	174 250	1	91 395 763	911	8 729
45	TiO	$^{48}Ti^{16}O$	Toto	301 245	1	58 983 952	8 725	499 775
46	VO	$^{51}V^{16}O$	HyVO	3 410 598	90	58 904 173 243	7 043	635 722
47	YO	$^{89}Y^{16}O$	BRYTS	173 621	1	60 678 140	28	25
48	YO	$^{89}Y^{17}O$	BRYTS	182 598	1	62 448 157	28	25
49	YO	$^{89}Y^{18}O$	BRYTS	182 547	1	64 164 605	28	25
50	ZrO	$^{90}Zr^{16}O$	ZorrO	227 118	1	47 662 773	5 313	145 317
51	ZrO	$^{91}Zr^{16}O$	ZorrO	227 118	1	47 748 501	1 058	5 164
52	ZrO	$^{92}Zr^{16}O$	ZorrO	227 124	1	47 830 250	1 058	5 164
53	ZrO	$^{93}Zr^{16}O$	ZorrO	227 126	1	47 928 979	1 058	5 164
54	ZrO	$^{94}Zr^{16}O$	ZorrO	227 128	1	47 994 352	1 058	5 164
55	ZrO	$^{96}Zr^{16}O$	ZorrO	227 134	1	48 136 388	1 058	5 164

$N_{\rm states}$: Number of states in states file;
$N_{\rm files}$: Number of transitions files;
$N_{\rm trans}$: Number of transitions in transitions file(s);
$N_{\rm HRstates}$: Number of states with uncertainties ≤ 0.01 cm^{-1};
$N_{\rm HRlines}$: Number of lines in ExoMolHR dataset with $R > 100\,000$.

As discussed in Section 4 there is a real need for an extended set of broadening parameters. Clearly this is a major focus of on-going work. At present ExoMol opacities and others are largely all focused on hot Jupiter planets. An extended set of broadening parameters would allow the generation of opacities for other atmospheres such as lava planets and rocky planets. What we do have as a result of our machine learning study is a full set of air-broadening parameters. This means we are already in a position to generate a full set of opacities for a planet whose atmosphere is Earth-like, ie close to 80% N_2 and 20% O_2. The use of different methodologies to generate broadening parameters, as discussed in Section 4, means that it is possible to have more than one file containing broadening parameters for a given perturber and molecule combination. Generalisation of the ExoMol data structure to allow for this possibility will form part of an upcoming paper on the revised ExoMol broadening diet.

Currently, the ExoMol molecular opacities are generated assuming the LTE conditions, where the temperature dependent populations of the molecular states obey the Boltzmann distribution. The non-LTE processes assume a departure from LTE thus making the ExoMol opacities non-applicable for modelling, e.g., the solution of the radiative transfer equation at non-LTE conditions. Some work on using our data for non-LTE studies has already been performed [578]. However, a more general solution will require a new cross-section format capable of preserving the information on the (rotation-)vibrational state that is therefore needed to allow for the solution of the statistical equilibrium equation. This will be addressed in the near future.

Finally but importantly, a major driver in our choice of species and processes to study is requests from interested users. We are always happy to receive such requests although we do not guarantee rapid delivery of results.

10. Conclusions

Since the ExoMol2020 data release [5], 27 new molecules have been added to the database. For many others the coverage for the line lists has been extended into the ultra violet and/or the energy levels, and hence transition wavenumbers, have been made significantly more accurate. Indeed, ExoMol-style line lists have proven extremely effective in providing very high quality data for astronomers, especially when supported by MARVEL studies of available experimental data.

The period since the last release of the ExoMol database in 2020 has seen the launch of JWST, the most important space observatory in decades, and its impact on astronomy research particularly in exoplanet atmospheric characterisation has been immediate. The ExoMol line list data have proven extremely powerful for modelling JWST observations when the molecule was predicted, with no identified shortcomings in the ExoMol databases' line list modelling of known molecular spectral bands at different temperatures. Yet spectral bands of unknown molecular origin are being identified regularly. Each of these unidentified spectral bands promises to shed light on physics, chemistry, geology (or maybe even biology) that was unsuspected in planetary models for exoplanetary systems. The set of molecules for which spectral data are required is clearly larger than already available in ExoMol, yet shortlisting the set of likely molecular candidates is not straightforward [117], especially for unusual non-terrestrial exoplanets. Computationally generated approximate spectral data for a very large number of potential atmospheric molecules [117,579] is likely to be useful in helping to prioritise the molecules for which production of high-quality line lists suitable for the ExoMol database is warranted. Improved chemical models of a diverse set of atmospheres capable of predicting abundances of minor components with strong absorption would also be extremely valuable. With the planned launch of the Ariel space mission [580,581] in 2029 producing a rapid increase in the number of exoplanet transit spectra available, we expect a corresponding increase in unidentified spectral features and thus the need to produce high-quality molecular spectral data on an increasing number of molecules [310].

Yet, despite the launch of JWST, it is the ground-based observations that have generated the most substantial changes in the ExoMol database over the last four years as the high-resolution cross-correlation (HRCC) techniques has reached maturity. HRCC makes extremely high demands on the position accuracy of the strong spectral lines that are quite different from the high completeness required to model space observations. This difference has necessitated major changes in how line lists are created that had started in the 2020 ExoMol release with the introduction of MARVELized line lists but have become dominant in this 2024 release with the essential inclusion of energy level uncertainties within all line lists, major changes to line list construction methodology particularly the formalisation of the predicted shift and hybridisation approach, creation of the ExoMolHR web app, and even substantial updates to nuclear motion codes to enable modelling of hyperfine interactions.

ExoMol was originally designed to provide spectroscopic data at infrared and visible wavelengths. However, increasing demands to study the effects of ultraviolet radiation both in terms of photoabsorption and photodissociation has led to the scope of the database being extended to address these issues. Processes involving temperature-dependent photodissociation, line and continuum photoabsortion at UV wavelengths and predissociation are now being included in the database. These data are needed both to interpret observations and for chemical models of exoplanets. We are working on increasing our offering at UV wavelengths.

CRediT authorship contribution statement

Jonathan Tennyson: Writing – original draft, Validation, Supervision, Software, Resources, Project administration, Methodology, Investigation, Funding acquisition, Formal analysis, Data curation, Conceptualization. **Sergei N. Yurchenko:** Writing – review & editing, Visualization, Validation, Supervision, Software, Methodology, Investigation, Funding acquisition, Formal analysis, Data curation, Conceptualization. **Jingxin Zhang:** Writing – review & editing, Validation, Software, Methodology, Data curation. **Charles A. Bowesman:** Writing – original draft, Software, Methodology, Investigation, Formal analysis, Data curation. **Ryan P. Brady:** Software, Methodology, Formal analysis. **Jeanna Buldyreva:** Writing – review & editing, Methodology, Investigation, Formal analysis. **Katy L. Chubb:** Investigation. **Robert R. Gamache:** Methodology, Investigation. **Maire N. Gorman:** Writing – review & editing, Investigation. **Elizabeth R. Guest:** Writing – review & editing, Methodology, Investigation. **Christian Hill:** Methodology, Data curation. **Kyriaki Kefala:** Investigation. **A.E. Lynas-Gray:** Writing – review & editing, Investigation. **Thomas M. Mellor:** Methodology, Investigation. **Laura K. McKemmish:** Writing – review & editing, Methodology, Investigation. **Georgi B. Mitev:** Writing – review & editing, Software, Methodology, Investigation. **Irina I. Mizus:** Investigation. **Alec Owens:** Supervision, Investigation. **Zhijian Peng:** Data curation. **Armando N. Perri:** Writing – review & editing, Methodology, Investigation. **Marco Pezzella:** Software, Methodology, Investigation, Formal analysis. **Oleg L. Polyansky:** Supervision, Investigation. **Qianwei Qu:** Writing – review & editing, Software, Methodology, Investigation. **Mikhail Semenov:** Writing – review & editing, Investigation. **Oleksiy Smola:** Investigation. **Andrei Solokov:** Writing – review & editing, Methodology, Investigation. **Wilfrid Somogyi:** Investigation. **Apoorva Upadhyay:** Investigation. **Samuel O.M. Wright:** Investigation, Conceptualization. **Nikolai F. Zobov:** Investigation.

Declaration of competing interest

The authors declare no competing financial interests

Data availability

The data discussed in this paper can be accessed at www.exomol.com. Programs associated with the ExoMol project including ExoCross and PyExoCross are available from https://github.com/ExoMol/.

Acknowledgements

This work was supported by the European Research Council (ERC) under the European Union's Horizon 2020 research and innovation programme through Advance Grant numbers 267219 and 883830, and STFC Projects No. ST/I001050/1, ST/M001334/1 and ST/R000476/1, State Project IAP RAS No. FFUF-2024-0016

Appendix. Sample JSON files

Listing 1: JSON format master file `exomol.json`.


```
{
    "ID": "EXOMOL.master",
    "version": 20240603,
    "num_molecules": 91,
    "num_isotopologues": 224,
    "num_datasets": 106,
    "num_species": 269,
    "molecules": {
        "H2O": {
            "num_molecule_names": 11,
            "molecule_names": [
                "Water",
                "Oxidane",
                "Hydrogen oxide",
                "Dihydrogen monoxide",
                "Hydrogen monoxide",
                "Dihydrogen oxide",
                "Hydrogen hydroxide",
                "Hydric acid",
                "Hydrohydroxic acid",
                "Hydroxic acid",
                "Hydrol"
            ],
            "num_isotopologues": 7,
            "linelist": [
                {
                    "inchikey": "XLYOFNOQVPJJNP-UHFFFAOYSA-N",
                    "iso_slug": "1H2-16O",
                    "iso_formula": "(1H)2(16O)",
                    "dataset_name": "POKAZATEL",
                    "version": 20180501
                },
                {
                    "inchikey": "XLYOFNOQVPJJNP-OUBTZVSYSA-N",
                    "iso_slug": "1H2-17O",
                    "iso_formula": "(1H)2(17O)",
                    "dataset_name": "HotWat78",
                    "version": 20161222
                },
                {
                    "inchikey": "XLYOFNOQVPJJNP-NJFSPNSNSA-N",
                    "iso_slug": "1H2-18O",
                    "iso_formula": "(1H)2(18O)",
                    "dataset_name": "HotWat78",
                    "version": 20161222
                },
                {
                    "inchikey": "XLYOFNOQVPJJNP-DYCDLGHISA-N",
                    "iso_slug": "1H-2H-16O",
                    "iso_formula": "(1H)(2H)(16O)",
                    "dataset_name": "VTT",
                    "version": 20160726
                },
                {
                    "inchikey": "XLYOFNOQVPJJNP-DYCDLGHISA-N",
                    "iso_slug": "1H-2H-16O",
                    "iso_formula": "(1H)(2H)(16O)",
                    "dataset_name": "Hewitt",
                    "version": 20161222
                },
                {
                    "inchikey": "XLYOFNOQVPJJNP-DYCDLGHISA-N",
                    "iso_slug": "1H-2H-16O",
                    "iso_formula": "(1H)(2H)(16O)",
                    "dataset_name": "TDB",
                    "version": 20240603
                },
                {
                    "inchikey": "XLYOFNOQVPJJNP-ZSJDYOACSA-N",
                    "iso_slug": "2H2-16O",
                    "iso_formula": "(2H)2(16O)",
                    "dataset_name": "Hewitt",
                    "version": 20161222
                }
            ]
        }
    }
}
```


Listing 2: JSON format definition (`.json`) file of $^{1}H_{2}^{16}O$ POKAZATEL dataset.


```
{
    "isotopologue": {
        "iso_formula" : "(1H)2(16O)",
        "iso_slug" : "1H2-16O",
        "inchikey" : "XLYOFNOQVPJJNP-UHFFFAOYSA-N",
        "inchi": "1S/H2O/h1H2",
        "mass_in_Da": 18.010565,
        "point_group": "C2v"
    },
    "atoms": {
        "number_of_atoms": 3,
        "element": {
            "H": 1,
            "O": 16
        }
    },
    "nuclear_spin_degeneracy": {
        "A1": 1,
        "A2": 1,
        "B1": 3,
        "B2": 3
    },
    "dataset": {
        "name" : "POKAZATEL",
        "version" : 20230621,
        "doi": "10.1093/mnras/sty1877",
        "max_temperature": 6000.0,
        "num_pressure_broadeners": 4,
        "nxsec_files": 0,
        "nkcoeff_files": 0,
        "dipole_available": false,
        "cooling_function_available": false,
        "specific_heat_available": true,
        "continuum": null,
        "predis": null,
        "states": {
            "number_of_states": 810269,
            "max_energy": 41200.00,
            "uncertainties_available": true,
            "lifetime_available": false,
            "lande_g_available": false,
            "num_quanta": 6,
            "states_file_fields": [
                {
                    "name" : "ID",
                    "desc" : "Unique integer identifier for the energy level",
                    "ffmt" : "I12",
                    "cfmt" : "%12d"
                },
                {
                    "name" : "E",
                    "desc" : "State energy in cm-1",
                    "ffmt" : "F12.6",
                    "cfmt" : "%12.6f"
                },
                {
                    "name" : "gtot",
                    "desc" : "Total energy level degeneracy",
                    "ffmt" : "I6",
                    "cfmt" : "%6d"
                },
                {
                    "name" : "J",
                    "desc" : "Total rotational quantum number, excluding nuclear spin
    ",
                    "ffmt" : "I7",
                    "cfmt" : "%7d"
                },
                {
                    "name" : "unc",
                    "desc" : "Energy uncertainty in cm-1",
                    "ffmt" : "F12.6",
                    "cfmt" : "%12.6f"
                },
                {
                    "name" : "nltcs:Ka",
                    "ffmt" : "I2",
                    "cfmt" : "%2d",
                    "desc" : "Ka rotational quantum number"
                },
                {
                    "name" : "nltcs:Kc",
                    "ffmt" : "I2",
                    "cfmt" : "%2d",
                    "desc" : "Kc rotational quantum number"
                },
                {
                    "name" : "nltcs:v1",
                    "ffmt" : "I2",
                    "cfmt" : "%2d",
                    "desc" : "v1 symmetric stretch quantum number(3)"
                },
                {
                    "name" : "nltcs:v2",
                    "ffmt" : "I2",
                    "cfmt" : "%2d",
                    "desc" : "v2 bend quantum number"
                },
                {
                    "name" : "nltcs:v3",
                    "ffmt" : "I2",
                    "cfmt" : "%2d",
                    "desc" : "v3 asymmetrics stretch quantum number"
                },
                {
                    "name" : "nltcs:Grve",
                    "ffmt" : "A3",
                    "cfmt" : "%3s",
                    "desc" : "Rovibrational symmetry label"
                },
                {
```

```
                    "name" : "Auxiliary:Ecal",
                    "desc" : "Energy in cm-1 from variational spectroscopic model",
                    "ffmt" : "F12.6",
                    "cfmt" : "%12.6f"
                },
                {
                    "name" : "Auxiliary:SourceType",
                    "ffmt" : "A2",
                    "cfmt" : "%2s",
                    "desc" : "Indicates if the value is from MARVEL (Ma) or
    calculated (Ca)"
                }
            ]
        },
        "transitions": {
            "number_of_transitions": 5745071340,
            "number_of_transition_files": 412,
            "max_wavenumber": 41200.00
        }
    },
    "partition_function": {
        "max_partition_function_temperature": 10000.0,
        "partition_function_step_size": 1.0
    },
    "broad": {
        "default_Lorentzian_half-width": 0.07,
        "default_temperature_exponent": 0.5,
        "H2": {
            "filename": "1H2-16O__H2.broad",
            "max_J": 50,
            "Lorentzian_half_width": 0.0209,
            "temperature_exponent": 0.027,
            "quantum_number_sets": [
                {
                    "code" : "a3",
                    "num_lines" : 23731,
                    "quantum_numbers" : [
                        "J" ,
                        "Ka\" ,
                        "Ka"
                    ]
                },
                {
                    "code" : "a1",
                    "num_lines" : 100,
                    "quantum_numbers" : [
                        "J"
                    ]
                },
                {
                    "code" : "a0",
                    "num_lines" : 51,
                    "quantum_numbers" : []
                }
            ]
        },
        "He": {
            "filename": "1H2-16O__He.broad",
            "max_J": 50,
            "Lorentzian_half_width": 0.0042,
            "temperature_exponent": 0.02,
            "quantum_number_sets": [
                {
                    "code" : "b1",
                    "num_lines" : 253,
                    "quantum_numbers" : [
                        "J" ,
                        "Ka\" ,
                        "Ka" ,
                        "Kc\" ,
                        "Kc" ,
                        "v1\" ,
                        "v2\" ,
                        "v3\" ,
                        "v1" ,
                        "v2" ,
                        "v3"
                    ]
                },
                {
                    "code" : "a3",
                    "num_lines" : 23731,
                    "quantum_numbers" : [
                        "J" ,
                        "Ka\" ,
                        "Ka"
                    ]
                },
                {
                    "code" : "a1",
                    "num_lines" : 100,
                    "quantum_numbers" : [
                        "J"
                    ]
                },
                {
                    "code" : "a0",
                    "num_lines" : 51,
                    "quantum_numbers" : []
                }
            ]
        }
    }
}
```


References

[1] Tennyson J, Yurchenko SN. ExoMol: molecular line lists for exoplanet and other atmospheres. Mon Not R Astron Soc 2012;425:21–33. http://dx.doi.org/10.1111/j.1365-2966.2012.21440.x.

[2] Gordon IE, Rothman LS, Hargreaves RJ, Hashemi R, Karlovets EV, Skinner FM, Conway EK, Hill C, Kochanov RV, Tan Y, Wcisło P, Finenko AA, Nelson K, Bernath PF, Birk M, Boudon V, Campargue A, Chance KV, Coustenis A, Drouin BJ, Flaud J, Gamache RR, Hodges JT, Jacquemart D, Mlawer EJ, Nikitin AV, Perevalov VI, Rotger M, Tennyson J, Toon GC, Tran H, Tyuterev VG, Adkins EM, Baker A, Barbe A, Canè E, Császár AG, Dudaryonok A, Egorov O, Fleisher AJ, Fleurbaey H, Foltynowicz A, Furtenbacher T, Harrison JJ, Hartmann J, Horneman V, Huang X, Karman T, Karns J, Kassi S, Kleiner I, Kofman V, Kwabia-Tchana F, Lavrentieva NN, Lee TJ, Long DA, Lukashevskaya AA, Lyulin OM, Makhnev VY, Matt W, Massie ST, Melosso M, Mikhailenko SN, Mondelain D, Müller HSP, Naumenko OV, Perrin A, Polyansky OL, Raddaoui E, Raston PL, Reed ZD, Rey M, Richard C, Tóbiás R, Sadiek I, Schwenke DW, Starikova E, Sung K, Tamassia F, Tashkun SA, Vander Auwera J, Vasilenko IA, Vigasin AA, Villanueva GL, Vispoel B, Wagner G, Yachmenev A, Yurchenko SN. The HITRAN2020 molecular spectroscopic database. J Quant Spectrosc Radiat Transfer 2022;277:107949. http://dx.doi.org/10.1016/j.jqsrt.2021.107949.

[3] Tennyson J, Lodi L, McKemmish LK, Yurchenko SN. The ab initio calculation of spectra of open shell diatomic molecules. J Phys B 2016;49:102001. http://dx.doi.org/10.1088/0953-4075/49/10/102001.

[4] Tennyson J, Yurchenko SN, Al-Refaie AF, Barton EJ, Chubb KL, Coles PA, Diamantopoulou S, Gorman MN, Hill C, Lam AZ, Lodi L, McKemmish LK, Na Y, Owens A, Polyansky OL, Rivlin T, Sousa-Silva C, Underwood DS, Yachmenev A, Zak E. The ExoMol database: molecular line lists for exoplanet and other hot atmospheres. J Mol Spectrosc 2016;327:73–94. http://dx.doi.org/10.1016/j.jms.2016.05.002.

[5] Tennyson J, Yurchenko SN, Al-Refaie AF, Clark VHJ, Chubb KL, Conway EK, Dewan A, Gorman MN, Hill C, Lynas-Gray AE, Mellor T, McKemmish LK, Owens A, Polyansky OL, Semenov M, Somogyi W, Tinetti G, Upadhyay A, Waldmann I, Wang Y, Wright S, Yurchenko OP. The 2020 release of the ExoMol database: Molecular line lists for exoplanet and other hot atmospheres. J Quant Spectrosc Radiat Transfer 2020;255:107228. http://dx.doi.org/10.1016/j.jqsrt.2020.107228.

[6] Tennyson J, Yurchenko SN. ExoMol at 10. Astron Geophys 2021;62:6.16–21. http://dx.doi.org/10.1093/astrogeo/atab102.

[7] Yurchenko SN, Tennyson J, Bailey J, Hollis MDJ, Tinetti G. Spectrum of hot methane in astronomical objects using a comprehensive computed line list. Proc Natl Acad Sci 2014;111:9379–83. http://dx.doi.org/10.1073/pnas.1324219111.

[8] Snellen IAG. A new method for probing the atmospheres of transiting exoplanets. Mon Not R Astron Soc 2004;353:L1–6. http://dx.doi.org/10.1111/j.1365-2966.2004.08169.x.

[9] Snellen I. High-dispersion spectroscopy of extrasolar planets: from CO in hot jupiters to O_2 in exo-earths. Philos Trans R Soc Lond Ser A 2014;372:20130075. http://dx.doi.org/10.1098/rsta.2013.0075.

[10] Brogi M, Birkby J. High-resolution spectroscopy. In: ExoFrontiers. IOP Publishing; 2021, p. 2514–3433. http://dx.doi.org/10.1088/2514-3433/abfa8fch8, pp. 8–1 to 8–10.

[11] Hoeijmakers HJ, de Kok RJ, Snellen IAG, Brogi M, Birkby JL, Schwarz H. A search for TiO in the optical high-resolution transmission spectrum of HD 209458b: Hindrance due to inaccuracies in the line database. Astron Astrophys 2015;575:A20. http://dx.doi.org/10.1051/0004-6361/201424794.

[12] de Regt S, Kesseli AY, Snellen IAG, Merritt SR, Chubb KL. A quantitative assessment of the VO line list: Inaccuracies hamper high-resolution VO detections in exoplanet atmospheres. Astron Astrophys 2022;661:A109. http://dx.doi.org/10.1051/0004-6361/202142683.

[13] Yurchenko SN, Tennyson J, Brogi M. High-resolution spectroscopy of exoplanets: data challenges and prospects. Nat Rev Phys 2024. (submitted for publication).

[14] Tennyson J. The ExoMol project: Molecular opacity calculations at university college London. In: C. Mendoza J Colgan, editor. Workshop on astrophysical opacities. Astron. soc. Pac. conf. ser., vol. 515, Astronomical Society of the Pacific; 2018, p. 137–44.

[15] Furtenbacher T, Császár AG, Tennyson J. MARVEL: measured active rotational-vibrational energy levels. J Mol Spectrosc 2007;245:115–25. http://dx.doi.org/10.1016/j.jms.2007.07.005.

[16] McKemmish LK, Bowesman CA, Kefala K, Perri AN, Syme AM, Yurchenko SN, Tennyson J. A hybrid approach to generating diatomic line lists for high resolution studies of exoplanets and other hot astronomical objects: Updates to ExoMol MgO, VO and TiO line lists. RAS Tech Instrum 2024. (submitted for publication).

[17] Pezzella M, Yurchenko SN, Tennyson J. A method for calculating temperature-dependent photodissociaiton cross-sections and rates. Phys Chem Chem Phys 2021;23:16390–400. http://dx.doi.org/10.1039/D1CP02162A.

[18] Mitev GB, Brady RP, Smola O, Tennyson J, Yurchenko SN. Calculation of spin–orbit induced predissociation lifetimes in rovibronic states of diatomic molecules. Phys Chem Chem Phys 2024. (in preparation).

[19] Yurchenko SN, Szajna W, Hakalla R, Semenov M, Sokolov A, Tennyson J, Pavlenko Y, Schmidt MR. ExoMol line lists – LIV. Empirical line lists for AlH and AlD and emission spectroscopy of AlD in $A\,^1\Pi$ ($v = 0, 1, 2$). Mon Not R Astron Soc 2024;527:9736–56. http://dx.doi.org/10.1093/mnras/stad3802.

[20] Mitev GB, Yurchenko SN, Tennyson J. Predissociation dynamics of the hydroxyl radical (OH) based on a five-state spectroscopic model. J Chem Phys 2024;160:144110. http://dx.doi.org/10.1063/5.0198241.

[21] Tennyson J, Pezzella M, Zhang J, Yurchenko SN. Data structures for photoadsorption within the ExoMol project. RAS Tech Instrum 2023;2:231–7. http://dx.doi.org/10.1093/rasti/rzad014.

[22] Hood CE, Fortney JJ, Line MR, Martin EC, Morley CV, Birkby JL, Rustamkulov Z, Lupu RE, Freedman RS. Prospects for characterizing the haziest sub-Neptune exoplanets with high-resolution spectroscopy. Astron J 2020;160:198. http://dx.doi.org/10.3847/1538-3881/abb46b.

[23] Piette AAA, Madhusudhan N. On the temperature profiles and emission spectra of mini-Neptune atmospheres. Astrophys J 2020;904:154. http://dx.doi.org/10.3847/1538-4357/abbfb1.

[24] Tsai S-M, Innes H, Lichtenberg T, Taylor J, Malik M, Chubb K, Pierrehumbert R. Inferring shallow surfaces on sub-Neptune exoplanets with JWST. Astrophys J Lett 2021;922:L27. http://dx.doi.org/10.3847/2041-8213/ac399a.

[25] Blain D, Charnay B, Bézard B. 1D atmospheric study of the temperate sub-Neptune K2-18b. Astron Astrophys 2021;646:A15. http://dx.doi.org/10.1051/0004-6361/202039072.

[26] Charnay B, Blain D, Bezard B, Leconte J, Turbet M, Falco A. Formation and dynamics of water clouds on temperate sub-Neptunes: the example of K2-18b. Astron Astrophys 2021;646:A171. http://dx.doi.org/10.1051/0004-6361/202039525.

[27] Gasman D, Min M, Chubb KL. Investigating the detectability of hydrocarbons in exoplanet atmospheres with JWST. Astron Astrophys 2022;659:A114. http://dx.doi.org/10.1051/0004-6361/202141468.

[28] Batalha NE, Wolfgang A, Teske J, Alam MK, Alderson L, Batalha NM, López-Morales M, Wakeford HR. Importance of sample selection in exoplanet-atmosphere population studies. Astron J 2022;165:14. http://dx.doi.org/10.3847/1538-3881/ac9f45.

[29] Zamyatina M, Hébrard E, Drummond B, Mayne NJ, Manners J, Christie DA, Tremblin P, Sing DK, Kohary K. Observability of signatures of transport-induced chemistry in clear atmospheres of hot gas giant exoplanets. Mon Not R Astron Soc 2022;519:3129–53. http://dx.doi.org/10.1093/mnras/stac3432.

[30] Constantinou S, Madhusudhan N. Characterizing atmospheres of cloudy temperate mini-Neptunes with JWST. Mon Not R Astron Soc 2022;514:2073–91. http://dx.doi.org/10.1093/mnras/stac1277.

[31] Guzmán-Mesa A, Kitzmann D, Mordasini C, Heng K. Chemical diversity of the atmospheres and interiors of sub-Neptunes: a case study of GJ 436b. Mon Not R Astron Soc 2022;513:4015–36. http://dx.doi.org/10.1093/mnras/stac1066.

[32] Lowson N, Zhou G, Huang CX, Wright DJ, Edwards B, Nabbie E, Venner A, Quinn SN, Collins KA, Gillen E, Battley M, Triaud A, Hellier C, Seager S, Winn JN, Jenkins JM, Wohler B, Shporer A, Schwarz RP, Murgas F, Pallé E, Anderson DR, West RG, Wittenmyer RA, Bowler BP, Horner J, Kane SR, Kielkopf J, Plavchan P, Zhang H, Fairnington T, Okumura J, Mengel MW, Addison BC. Two mini-Neptunes transiting the adolescent K-star HIP 113103 confirmed with TESS and CHEOPS. Mon Not R Astron Soc 2023;527:1146–62. http://dx.doi.org/10.1093/mnras/stad2756.

[33] Gao P, Piette AAA, Steinrueck ME, Nixon MC, Zhang M, Kempton EM-R, Bean JL, Rauscher E, Parmentier V, Batalha NE, Savel AB, Arnold KE, Roman MT, Malsky I, Taylor J. The hazy and metal-rich atmosphere of GJ 1214 b constrained by near- and mid-infrared transmission spectroscopy. Astrophys J 2023;951:96. http://dx.doi.org/10.3847/1538-4357/acd16f.

[34] Kempton EMR, Zhang M, Bean JL, Steinrueck ME, Piette AAA, Parmentier V, Malsky I, Roman MT, Rauscher E, Gao P, Bell TJ, Xue Q, Taylor J, Savel AB, Arnold KE, Nixon MC, Stevenson KB, Mansfield M, Kendrew S, Zieba S, Ducrot E, Dyrek A, Lagage P-O, Stassun KG, Henry GW, Barman T, Lupu R, Malik M, Kataria T, Ih J, Fu G, Welbanks L, McGill P. A reflective, metal-rich atmosphere for GJ 1214b from its JWST phase curve. Nature 2023;620:67–71. http://dx.doi.org/10.1038/s41586-023-06159-5.

[35] Mikal-Evans T, Madhusudhan N, Dittmann J, Günther MN, Welbanks L, Eylen VV, Crossfield IJM, Daylan T, Kreidberg L. Hubble Space Telescope transmission spectroscopy for the temperate sub-Neptune TOI-270 d: A possible hydrogen-rich atmosphere containing water vapor. Astron J 2023;165:84. http://dx.doi.org/10.3847/1538-3881/aca90b.

[36] Holmberg, Måns, Madhusudhan, Nikku. Possible hycean conditions in the sub-Neptune TOI-270 d. Astron Astrophys 2024;683:L2. http://dx.doi.org/10.1051/0004-6361/202348238.

[37] Dash S, Brogi M, Gandhi S, Lafarga M, Meech A, Bello-Arufe A, Wheatley PJ. Constraints on atmospheric water abundance and cloud deck pressure in the warm Neptune GJ 3470b via CARMENES transmission spectroscopy. Mon Not R Astron Soc 2024;530:3100. http://dx.doi.org/10.1093/mnras/stae997.

[38] Guzmán-Mesa A, Kitzmann D, Fisher C, Burgasser AJ, Hoeijmakers HJ, Márquez-Neila P, Grimm SL, Mandell AM, Sznitman R, Heng K. Information content of JWST NIRSpec transmission spectra of warm Neptunes. Astron J 2020;160:15. http://dx.doi.org/10.3847/1538-3881/ab9176.

[39] Guilluy G, Gressier A, Wright S, Santerne A, Jaziri AY, Edwards B, Changeat Q, Modirrousta-Galian D, Skaf N, Al-Refaie A, Baeyens R, Bieger MF, Blain D, Kiefer F, Morvan M, Mugnai LV, Pluriel W, Poveda M, Zingales T, Whiteford N, Yip KH, Charnay B, Leconte J, Drossart P, Sozzetti A, Marcq E, Tsiaras A, Venot O, Waldmann I, Beaulieu J-P. ARES IV: Probing the atmospheres of the two warm small planets HD 106315c and HD 3167c with the HST/WFC3 camera. Astron J 2020;161:19. http://dx.doi.org/10.3847/1538-3881/abc3c8.

[40] A-thano N, Awiphan S, Jiang I-G, Kerins E, Priyadarshi A, McDonald I, Joshi YC, Chulikorn T, Hayes JJC, Charles S, Huang C-K, Rattanamala R, Yeh L-C, Dhillon VS. Revisiting the transit timing and atmosphere characterization of the Neptune-mass planet HAT-P-26 b. Astron J 2023;166:223. http://dx.doi.org/10.3847/1538-3881/acfeea.

[41] Edwards B, Changeat Q, Tsiaras A, Allan A, Behr P, Hagey SR, Himes MD, Ma S, Stassun KG, Thomas L, Thompson A, Boley A, Booth L, Bouwman J, France K, Lowson N, Meech A, Phillips CL, Vidotto AA, Yip KH, Bieger M, Gressier A, Janin E, Jiang I-G, Leonardi P, Sarkar S, Skaf N, Taylor J, Yang M, Ward-Thompson D. Characterizing a world within the hot-Neptune desert: Transit observations of LTT 9779b with the Hubble Space Telescope/WFC3. Astron J 2023;166:158. http://dx.doi.org/10.3847/1538-3881/acea77.

[42] Radica M, Coulombe L-P, Taylor J, Albert L, Allart R, Benneke B, Cowan NB, Dang L, Lafrenière D, Thorngren D, Artigau Étienne, Doyon R, Flagg L, Johnstone D, Pelletier S, Roy P-A. Muted features in the JWST NIRISS transmission spectrum of hot Neptune LTT 9779b. Astrophys J Lett 2024;962:L20. http://dx.doi.org/10.3847/2041-8213/ad20e4.

[43] Madhusudhan N, Piette AAA, Constantinou S. Habitability and biosignatures of hycean worlds. Astrophys J 2021;918:1. http://dx.doi.org/10.3847/1538-4357/abfd9c.

[44] Madhusudhan N, Sarkar S, Constantinou S, Holmberg M, Piette AAA, Moses JI. Carbon-bearing molecules in a possible hycean atmosphere. Astrophys J Lett 2023;956:L13. http://dx.doi.org/10.3847/2041-8213/acf577.

[45] Kempton EM-R, Lessard M, Malik M, Rogers LA, Futrowsky KE, Ih J, Marounina N, Munoz-Romero CE. Where are the water worlds?: Self-consistent models of water-rich exoplanet atmospheres. Astrophys J 2023;953:57. http://dx.doi.org/10.3847/1538-4357/ace10d.

[46] Spake JJ, Sing DK, Wakeford HR, Nikolov N, Mikal-Evans T, Deming D, Barstow JK, Anderson DR, Carter AL, Gillon M, Goyal JM, Hebrard G, Hellier C, Kataria T, Lam KWF, Triaud AHMJ, Wheatley PJ. Abundance measurements of H_2O and carbon-bearing species in the atmosphere of WASP-127b confirm its supersolar metallicity. Mon Not R Astron Soc 2020;500:4042–64. http://dx.doi.org/10.1093/mnras/staa3116.

[47] Anisman LO, Edwards B, Changeat Q, Venot O, Al-Refaie AF, Tsiaras A, Tinetti G. WASP-117b: An eccentric hot Saturn as a future complex chemistry laboratory. Astron J 2020;160:233. http://dx.doi.org/10.3847/1538-3881/abb9b0.

[48] Changeat Q, Edwards B, Al-Refaie AF, Morvan M, Tsiaras A, Waldmann IP, Tinetti G. KELT-11 b: Abundances of water and constraints on carbon-bearing molecules from the Hubble transmission spectrum. Astron J 2020;160:260. http://dx.doi.org/10.3847/1538-3881/abbe12.

[49] Colón KD, Kreidberg L, Welbanks L, Line MR, Madhusudhan N, Beatty T, Tamburo P, Stevenson KB, Mandell A, Rodriguez JE, Barclay T, Lopez ED, Stassun KG, Angerhausen D, Fortney JJ, James DJ, Pepper J, Ahlers JP, Plavchan P, Awiphan S, Kotnik C, McLeod KK, Murawski G, Chotani H, LeBrun D, Matzko W, Rea D, Vidaurri M, Webster S, Williams JK, Cox LS, Tan N, Gilbert EA. An unusual transmission spectrum for the sub-Saturn KELT-11b suggestive of a subsolar water abundance. Astron J 2020;160:280. http://dx.doi.org/10.3847/1538-3881/abc1e9.

[50] Maimone MC, Brogi M, Chiavassa A, van den Ancker ME, Manara CF, Leconte J, Gandhi S, Pluriel W. Detecting H_2O with CRIRES+: WASP-20b. Astron Astrophys 2022;667:A106. http://dx.doi.org/10.1051/0004-6361/202244383.

[51] Ahrer E-M, Alderson L, Batalha NM, Batalha NE, Bean JL, Beatty TG, Bell TJ, Benneke B, Berta-Thompson ZK, Carter AL, Crossfield IJM, Espinoza N, Feinstein AD, Fortney JJ, Gibson NP, Goyal JM, Kempton EM-R, Kirk J, Kreidberg L, Lopez-Morales M, Line MR, Lothringer JD, Moran SE, Mukherjee S, Ohno K, Parmentier V, Piaulet C, Rustamkulov Z, Schlawin E, Sing DK, Stevenson KB, Wakeford HR, Allen NH, Birkmann SM, Brande J, Crouzet N, Cubillos PE, Damiano M, Desert J-M, Gao P, Harrington J, Hu R, Kendrew S, Knutson HA, Lagage P-O, Leconte J, Lendl M, MacDonald RJ, May EM, Miguel Y, Molaverdikhani K, Moses J, Murray ICA, Nehring M, Nikolov NK, de la Roche DJMPD, Radica M, Roy P-A, Stassun KG, Taylor J, Waalkes WC, Wachiraphan P, Welbanks L, Wheatley PJ, Aggarwal K, Alam MK, Banerjee A, Barstow JK, Blecic J, Casewell SL, Changeat Q, Chubb KL, Colon KD, Coulombe L-P, Daylan T, De Val-Borro M, Decin L, Dos Santos LA, Flagg L, France K, Fu G, Munoz AG, Gizis JE, Glidden A, Grant D, Heng K, Henning T, Hong Y-C, Inglis J, Iro N, Kataria T, Komacek TD, Krick JE, Lee EKH, Lewis NK, Lillo-Box J, Lustig-Yaeger J, Mancini L, Mandell AM, Mansfield M, Marley MS, Mikal-Evans T, Morello G, Nixon MC, Ceballos KO, Piette AAA, Powell D, Rackham B, Ramos-Rosado VL, Rauscher E, Redfield S, Rogers LK, Roman MT, Roudier GM, Scarsdale N, Shkolnik EL, Southworth J, Spake JJ, Steinrueck ME, Tan X, Teske JK, Tremblin P, Tsai S-M, Tucker GS, Turner JD, Valenti JA, Venot O, Waldmann IP, Wallack NL, Zhang X, Zieba S. Identification of carbon dioxide in an exoplanet atmosphere. Nature 2023;614:649–52. http://dx.doi.org/10.1038/s41586-022-05269-w.

[52] Nikolov NK, Sing DK, Spake JJ, Smalley B, Goyal JM, Mikal-Evans T, Wakeford HR, Rustamkulov Z, Deming D, Fortney JJ, Carter A, Gibson NP, Mayne NJ. Solar-to-supersolar sodium and oxygen absolute abundances for a 'hot Saturn' orbiting a metal-rich star. Mon Not R Astron Soc 2022;515:3037–58. http://dx.doi.org/10.1093/mnras/stac1530.

[53] Tsai S-M, Lee EKH, Powell D, Gao P, Zhang X, Moses J, Hébrard E, Venot O, Parmentier V, Jordan S, Hu R, Alam MK, Alderson L, Batalha NM, Bean JL, Benneke B, Bierson CJ, Brady RP, Carone L, Carter AL, Chubb KL, Inglis J, Leconte J, Line M, López-Morales M, Miguel Y, Molaverdikhani K, Rustamkulov Z, Sing DK, Stevenson KB, Wakeford HR, Yang J, Aggarwal K, Baeyens R, Barat S, de Val-Borro M, Daylan T, Fortney JJ, France K, Goyal JM, Grant D, Kirk J, Kreidberg L, Louca A, Moran SE, Mukherjee S, Nasedkin E, Ohno K, Rackham BV, Redfield S, Taylor J, Tremblin P, Visscher C, Wallack NL, Welbanks L, Youngblood A, Ahrer E-M, Batalha NE, Behr P, Berta-Thompson ZK, Blecic J, Casewell SL, Crossfield IJM, Crouzet N, Cubillos PE, Decin L, Désert J-M, Feinstein AD, Gibson NP, Harrington J, Heng K, Henning T, Kempton EM-R, Krick J, Lagage P-O, Lendl M, Lothringer JD, Mansfield M, Mayne NJ, Mikal-Evans T, Palle E, Schlawin E, Shorttle O, Wheatley PJ, Yurchenko SN. Photochemically produced SO_2 in the atmosphere of WASP-39b. Nature 2023;617:483–7. http://dx.doi.org/10.1038/s41586-023-05902-2.

[54] Samra D, Helling C, Chubb KL, Min M, Carone L, Schneider AD. Clouds form on the hot Saturn JWST ERO target WASP-96b. Astron Astrophys 2023;669:17. http://dx.doi.org/10.1051/0004-6361/202244939.

[55] Radica M, Welbanks L, Espinoza N, Taylor J, Coulombe L-P, Feinstein AD, Goyal J, Scarsdale N, Albert L, Baghel P, Bean JL, Blecic J, Lafreni'ere D, MacDonald RJ, Zamyatina M, Allart R, Artigau E, Batalha NE, Cook NJ, Cowan NB, Dang L, Doyon R, Fournier-Tondreau M, Johnstone D, Line MR, Moran SE, Mukherjee S, Pelletier S, Roy P-A, Talens GJ, Filippazzo J, Pontoppidan K, Volk K. Awesome SOSS: transmission spectroscopy of WASP-96b with NIRISS/SOSS. Mon Not R Astron Soc 2023;524:835–56. http://dx.doi.org/10.1093/mnras/stad1762.

[56] Alderson L, Wakeford HR, Alam MK, Batalha NE, Lothringer JD, Redai JA, Barat S, Brande J, Damiano M, Daylan T, Espinoza N, Flagg L, Goyal JM, Grant D, Hu R, Inglis J, Lee EKH, Mikal-Evans T, Ramos-Rosado L, Roy P-A, Wallack NL, Batalha NM, Bean JL, Benneke B, Berta-Thompson ZK, Carter AL, Changeat Q, Colon KD, Crossfield IJM, Desert J-M, Foreman-Mackey D, Gibson NP, Kreidberg L, Line MR, Lopez-Morales M, Molaverdikhani K, Moran SE, Morello G, Moses JI, Mukherjee S, Schlawin E, Sing DK, Stevenson KB, Taylor J, Aggarwal K, Ahrer E-M, Allen NH, Barstow JK, Bell TJ, Blecic J, Casewell SL, Chubb KL, Crouzet N, Cubillos PE, Decin L, Feinstein AD, Fortney JJ, Harrington J, Heng K, Iro N, Kempton EMR, Kirk J, Knutson HA, Krick J, Leconte J, Lendl M, MacDonald RJ, Mancini L, Mansfield M, May EM, Mayne NJ, Miguel Y, Nikolov NK, Ohno K, Palle E, Parmentier V, de la Roche DJMPD, Piaulet C, Powell D, Rackham BV, Redfield S, Rogers LK, Rustamkulov Z, Tan X, Tremblin P, Tsai S-M, Turner JD, de Val-Borro M, Venot O, Welbanks L, Wheatley PJ, Zhang X. Early release science of the exoplanet WASP-39b with JWST NIRSpec G395H. Nature 2023;614:664–9. http://dx.doi.org/10.1038/s41586-022-05591-3.

[57] Fournier-Tondreau M, MacDonald RJ, Radica M, Lafrenière D, Welbanks L, Piaulet C, Coulombe L-P, Allart R, Morel K, Artigau E, Albert L, Lim O, Doyon R, Benneke B, Rowe JF, Darveau-Bernier A, Cowan NB, Lewis NK, Cook NJ, Flagg L, Genest F, Pelletier S, Johnstone D, Dang L, Kaltenegger L, Taylor J, Turner JD. Near-infrared transmission spectroscopy of HAT-P-18 b with NIRISS: Disentangling planetary and stellar features in the era of JWST. Mon Not R Astron Soc 2023;528:3354–77. http://dx.doi.org/10.1093/mnras/stad3813.

[58] Taylor J, Radica M, Welbanks L, MacDonald RJ, Blecic J, Zamyatina M, Roth A, Bean JL, Parmentier V, Coulombe L-P, Feinstein AD, Espinoza N, Benneke B, Lafreni'ere D, Doyon R, Ahrer E-M. Awesome SOSS: atmospheric characterization of WASP-96b using the JWST early release observations. Mon Not R Astron Soc 2023;524:817–34. http://dx.doi.org/10.1093/mnras/stad1547.

[59] Boucher A, Lafreniére D, Pelletier S, Darveau-Bernier A, Radica M, Allart R, Artigau e, Cook NJ, Debras F, Doyon R, Gaidos E, Benneke B, Cadieux C, Carmona A, Cloutier R, Cortés-Zuleta P, Cowan NB, Delfosse X, Donati J-F, Fouqué P, Forveille T, Grankin K, Hébrard G, Martins JHC, Martioli E, Masson A, Vinatier S. CO or no CO? Narrowing the CO abundance constraint and recovering the H_2O detection in the atmosphere of WASP-127 b using SPIRou. Mon Not R Astron Soc 2023;522:5062–83. http://dx.doi.org/10.1093/mnras/stad1247.

[60] Whiteford N, Glasse A, Chubb KL, Kitzmann D, Ray S, Phillips MW, Biller BA, Palmer PI, Rice K, Waldmann IP, Changeat Q, Skaf N, Wang J, Edwards B, Al-Refaie A. Retrieval study of cool, directly imaged exoplanet 51 Eri b. Mon Not R Astron Soc 2023;525:1375–400. http://dx.doi.org/10.1093/mnras/stad670.

[61] Xu S, Diamond-Lowe H, MacDonald RJ, Vanderburg A, Blouin S, Dufour P, Gao P, Kreidberg L, Leggett SK, Mann AW, Morley CV, Stephens AW, O'Connor CE, Thao PC, Lewis NK. Gemini/GMOS transmission spectroscopy of the grazing planet candidate WD 1856+534 b. Astron J 2021;162:296. http://dx.doi.org/10.3847/1538-3881/ac2d26.

[62] Guilluy G, Giacobbe P, Carleo I, Cubillos PE, Sozzetti A, Bonomo AS, Brogi M, Gandhi S, Fossati L, Nascimbeni V, Turrini D, Schisano E, Borsa F, Lanza AF, Mancini L, Maggio A, Malavolta L, Micela G, Pino L, Rainer M, Bignamini A, Claudi R, Cosentino R, Covino E, Desidera S, Fiorenzano A, Harutyunyan A, Lorenzi V, Knapic C, Molinari E, Pacetti E, Pagano I, Pedani M, Piotto G, Poretti E. The GAPS programme at TNG XXXVIII. Five molecules in the atmosphere of the warm giant planet WASP-69b detected at high spectral resolution. Astron Astrophys 2022;665:A104. http://dx.doi.org/10.1051/0004-6361/202243854.

[63] Zhang Z, Mollière P, Hawkins K, Manea C, Fortney JJ, Morley CV, Skemer A, Marley MS, Bowler BP, Carter AL, Franson K, Maas ZG, Sneden C. Elemental abundances of planets and brown dwarfs imaged around stars (ELPIS). I. Potential metal enrichment of the exoplanet AF lep b and a novel retrieval approach for cloudy self-luminous atmospheres. Astron J 2023;166:198. http://dx.doi.org/10.3847/1538-3881/acf768.

[64] Carleo I, Giacobbe P, Guilluy G, Cubillos PE, Bonomo AS, Sozzetti A, Brogi M, Gandhi S, Fossati L, Turrini D, Biazzo K, Borsa F, Lanza AF, Malavolta L, Maggio A, Mancini L, Micela G, Pino L, Poretti E, Rainer M, Scandariato G, Schisano E, Andreuzzi G, Bignamini A, Cosentino R, Fiorenzano A, Harutyunyan A, Molinari E, Pedani M, Redfield S, Stoev H. The GAPS programme at TNG XXXIX. Multiple molecular species in the atmosphere of the warm giant planet WASP-80 b unveiled at high resolution with GIANO-B. Astron Astrophys 2022;164:101. http://dx.doi.org/10.3847/1538-3881/ac80bf.

[65] Bell TJ, Welbanks L, Schlawin E, Line MR, Fortney JJ, Greene TP, Ohno K, Parmentier V, Rauscher E, Beatty TG, Mukherjee S, Wiser LS, Boyer ML, Rieke MJ, Stansberry JA. Methane throughout the atmosphere of the warm exoplanet WASP-80b. Nature 2023;623:709–12. http://dx.doi.org/10.1038/s41586-023-06687-0.

[66] Kanodia S, Mahadevan S, Libby-Roberts J, Stefansson G, Canas CI, Piette AAA, Boss A, Teske J, Chambers J, Zeimann G, Monson A, Robertson P, Ninan JP, Lin ASJ, Bender CF, Cochran WD, Diddams SA, Gupta AF, Halverson S, Hawley S, Kobulnicky HA, Metcalf AJ, Parker BA, Powers L, Ramsey LW, Roy A, Schwab C, Swaby TN, Terrien RC, Wisniewski J. TOI-5205b: A short-period Jovian planet transiting a mid-M dwarf. Astron J 2023;165:120. http://dx.doi.org/10.3847/1538-3881/acabce.

[67] Zhang M, Chachan Y, Kempton EM-R, Knutson HA, Chang WH. PLATON II: New capabilities and a comprehensive retrieval on HD 189733b transit and eclipse data. Astrophys J 2020;899:27. http://dx.doi.org/10.3847/1538-4357/aba1e6.

[68] Piette AAA, Madhusudhan N, McKemmish LK, Gandhi S, Masseron T, Welbanks L. Assessing spectra and thermal inversions due to TiO in hot jupiter atmospheres. Mon Not R Astron Soc 2020;496:3870–86. http://dx.doi.org/10.1093/mnras/staa1592.

[69] Yip KH, Changeat Q, Edwards B, Morvan M, Chubb KL, Tsiaras A, Waldmann IP, Tinetti G. On the compatibility of ground-based and space-based data: WASP-96b, an example. Astron J 2020;161:4.

[70] Lendl M, Csizmadia S, Deline A, Fossati L, Kitzmann D, Heng K, Hoyer S, Salmon S, Benz W, Broeg C, Ehrenreich D, Fortier A, Queloz D, Bonfanti A, Brandeker A, Collier Cameron A, Delrez L, Garcia Muñoz A, Hooton MJ, Maxted PFL, Morris BM, Van Grootel V, Wilson TG, Alibert Y, Alonso R, Asquier J, Bandy T, Bárczy T, Barrado D, Barros SCC, Baumjohann W, Beck M, Beck T, Bekkelien A, Bergomi M, Billot N, Biondi F, Bonfils X, Bourrier V, Busch MD, Cabrera J, Cessa V, Charnoz S, Chazelas B, Corral Van Damme C, Davies MB, Deleuil M, Demangeon ODS, Demory BO, Erikson A, Farinato J, Fridlund M, Futyan D, Gandolfi D, Gillon M, Guterman P, Hasiba J, Hernandez E, Isaak KG, Kiss L, Kuntzer T, Lecavelier des Etangs A, Lüftinger T, Laskar J, Lovis C, Magrin D, Malvasio L, Marafatto L, Michaelis H, Munari M, Nascimbeni V, Olofsson G, Ottacher H, Ottensamer R, Pagano I, Pallé E, Peter G, Piazza D, Piotto G, Pollacco D, Ratti F, Rauer H, Ragazzoni R, Rando N, Ribas I, Rieder M, Rohlfs R, Safa F, Santos NC, Scandariato G, Ségransan D, Simon AE, Singh V, Smith AMS, Sordet M, Sousa SG, Steller M, Szabó GM, Thomas N, Tschentscher M, Udry S, Viotto V, Walter I, Walton NA, Wildi F, Wolter D. The hot dayside and asymmetric transit of WASP-189 b seen by CHEOPS. Astron Astrophys 2020;643:A94. http://dx.doi.org/10.1051/0004-6361/202038677.

[71] Lacy BI, Burrows A. JWST transit spectra. I. Exploring potential biases and opportunities in retrievals of tidally locked hot jupiters with clouds and hazes. Astrophys J 2020;905:131. http://dx.doi.org/10.3847/1538-4357/abc01c.

[72] Chen G, Casasayas-Barris N, Palle E, Welbanks L, Madhusudhan N, Luque R, Murgas F. Detection of Na in WASP-21b's lower and upper atmosphere. Astron Astrophys 2020;642:A54. http://dx.doi.org/10.1051/0004-6361/202038661.

[73] Wilcomb KK, Konopacky QM, Barman TS, Theissen CA, Ruffio J-B, Brock L, Macintosh B, Marois C. Moderate-resolution K-band spectroscopy of substellar companion κ andromedae b. Astron J 2020;160:207. http://dx.doi.org/10.3847/1538-3881/abb9b1.

[74] Giacobbe P, Brogi M, Gandhi S, Cubillos PE, Bonomo AS, Sozzetti A, Fossati L, Guilluy G, Carleo I, Rainer M, Harutyunyan A, Borsa F, Pino L, Nascimbeni V, Benatti S, Biazzo K, Bignamini A, Chubb KL, Claudi R, Cosentino R, Covino E, Damasso M, Desidera S, Fiorenzano AFM, Ghedina A, Lanza AF, Leto G, Maggio A, Malavolta L, Maldonado J, Micela G, Molinari E, Pagano I, Pedani M, Piotto G, Poretti E, Scandariato G, Yurchenko SN, Fantinel D, Galli A, Lodi M, Sanna N, Tozzi A. Five carbon- and nitrogen-bearing species in a hot giant planet's atmosphere. Nature 2021;592:205–8. http://dx.doi.org/10.1038/s41586-021-03381-x.

[75] Casasayas-Barris N, Palle E, Stangret M, Bourrier V, Tabernero HM, Yan F, Borsa F, Allart R, Zapatero Osorio MR, Lovis C, Sousa SG, Chen G, Oshagh M, Santos NC, Pepe F, Rebolo R, Molaro P, Cristiani S, Adibekyan V, Alibert Y, Prieto CAllende, Bouchy F, Demangeon ODS, Marcantonio PDi, D´Odorico V, Ehrenreich D, Figueira P, Santos RGénova, González Hernández JI, Lavie B, Lillo-Box J, Curto GLo, Martins CJAP, Mehner A, Micela G, Nunes NJ, Poretti E, Sozzetti A, Mascareño ASuárez, Udry S. The atmosphere of HD 209458b seen with ESPRESSO - no detectable planetary absorptions at high resolution. Astron Astrophys 2021;647:A26. http://dx.doi.org/10.1051/0004-6361/202039539.

[76] Serindag DB, Snellen IAG, Mollière P. Measuring titanium isotope ratios in exoplanet atmospheres. Astron Astrophys 2021;655:A69. http://dx.doi.org/10.1051/0004-6361/202141941.

[77] Sheppard KB, Welbanks L, Mandell AM, Madhusudhan N, Nikolov N, Deming D, Henry GW, Williamson MH, Sing DK, López-Morales M, Ih J, Sanz-Forcada J, Lavvas P, Ballester GE, Evans TM, Muñoz AG, dos Santos LA. The hubble PanCET program: A metal-rich atmosphere for the inflated hot jupiter HAT-p-41b. Astrophys J 2021;161:51. http://dx.doi.org/10.3847/1538-3881/abc8f4.

[78] Braam M, van der Tak FFS, Chubb KL, Min M. Evidence for chromium hydride in the atmosphere of hot jupiter WASP-31b. Astron Astrophys 2021;646:A17. http://dx.doi.org/10.1051/0004-6361/202039509.

[79] Changeat Q, Al-Refaie AF, Edwards B, Waldmann IP, Tinetti G. An exploration of model degeneracies with a unified phase curve retrieval analysis: The light and dark sides of WASP-43 b. Astrophys J 2021;913:73. http://dx.doi.org/10.3847/1538-4357/abf2bb.

[80] Rathcke AD, MacDonald RJ, Barstow JK, Goyal JM, Lopez-Morales M, ao M. Mendonça J, Sanz-Forcada J, Henry GW, Sing DK, Alam MK, Lewis NK, Chubb KL, Taylor J, Nikolov N, Buchhave LA. HST PanCET program: A complete near-UV to infrared transmission spectrum for the hot jupiter WASP-79b. Astron J 2021;162:138. http://dx.doi.org/10.3847/1538-3881/ac0e99.

[81] Ishizuka M, Kawahara H, Nugroho SK, Kawashima Y, Hirano T, Tamura M. Neutral metals in the atmosphere of HD 149026b. Astron J 2021;161:153. http://dx.doi.org/10.3847/1538-3881/abdb25.

[82] Cubillos PE, Keating D, Cowan NB, Vos JM, Burningham B, Ygouf M, Karalidi T, Zhou Y, Gonzales EC. Longitudinally resolved spectral retrieval (ReSpect) of WASP-43b. Astrophys J 2021;915:45. http://dx.doi.org/10.3847/1538-4357/abfe14.

[83] Lee EKH, Parmentier V, Hammond M, Grimm SL, Kitzmann D, Tan X, Tsai S-M, Pierrehumbert RT. Simulating gas giant exoplanet atmospheres with exo-FMS: comparing semigrey, picket fence, and correlated-k radiative-transfer schemes. Mon Not R Astron Soc 2021;506:2695–711. http://dx.doi.org/10.1093/mnras/stab1851.

[84] Baeyens R, Decin L, Carone L, Venot O, Agúndez M, Molli'ere P. Grid of pseudo-2D chemistry models for tidally locked exoplanets - I. The role of vertical and horizontal mixing. Mon Not R Astron Soc 2021;505:5603–53. http://dx.doi.org/10.1093/mnras/stab1310.

[85] Ruffio J-B, Konopacky QM, Barman T, Macintosh B, Hoch KKW, Rosa RJD, Wang JJ, Czekala I, Marois C. Deep exploration of the planets HR 8799 b, c, and d with moderate-resolution spectroscopy. Astron J 2021;162:290. http://dx.doi.org/10.3847/1538-3881/ac273a.

[86] Sedaghati E, MacDonald RJ, Casasayas-Barris N, Hoeijmakers HJ, Boffin HMJ, Rodler F, Brahm R, Jones M, Sánchez-López A, Carleo I, Figueira P, Mehner A, López-Puertas M. A spectral survey of WASP-19b with ESPRESSO. Mon Not R Astron Soc 2021;505:435–58. http://dx.doi.org/10.1093/mnras/stab1164.

[87] Line MR, Brogi M, Bean JL, Gandhi S, Zalesky J, Parmentier V, Smith P, Mace GN, Mansfield M, Kempton EM-R, Fortney JJ, Shkolnik E, Patience J, Rauscher E, Desert J-M, Wardenier JP. A solar C/O and sub-solar metallicity in a hot jupiter atmosphere. Nature 2021;598:580. http://dx.doi.org/10.1038/s41586-021-03912-6.

[88] Wang JJ, Ruffio J-B, Morris E, Delorme J-R, Jovanovic N, Pezzato J, Echeverri D, Finnerty L, Hood C, Zanazzi JJ, Bryan ML, Bond CZ, Cetre S, Martin EC, Mawet D, Skemer A, Baker A, Xuan JW, Wallace JK, Wang J, Bartos R, Blake GA, Boden A, Buzard C, Calvin B, Chun M, Doppmann G, Dupuy TJ, Duchêne G, Feng YK, Fitzgerald MP, Fortney J, Freedman RS, Knutson H, Konopacky Q, Lilley S, Liu MC, Lopez R, Lupu R, Marley MS, Meshkat T, Miles B, Millar-Blanchaer M, Ragland S, Roy A, Ruane G, Sappey B, Schofield T, Weiss L, Wetherell E, Wizinowich P, Ygouf M. Detection and bulk properties of the HR 8799 planets with high-resolution spectroscopy. Astron J 2021;162:148. http://dx.doi.org/10.3847/1538-3881/ac1349.

[89] Welbanks L, Madhusudhan N. On atmospheric retrievals of exoplanets with inhomogeneous terminators. Astrophys J 2022;933:79. http://dx.doi.org/10.3847/1538-4357/ac6df1.

[90] Chubb KL, Min M. Exoplanet atmosphere retrievals in 3D using phase curve data with ARCiS: Application to WASP-43b. Astron Astrophys 2022;665:A2. http://dx.doi.org/10.1051/0004-6361/202142800.

[91] Saba A, Tsiaras A, Morvan M, Thompson A, Changeat Q, Edwards B, Jolly A, Waldmann I, Tinetti G. The transmission spectrum of WASP-17 b from the optical to the near-infrared wavelengths: Combining STIS, WFC3, and IRAC data sets. Astron J 2022;164:2. http://dx.doi.org/10.3847/1538-3881/ac6c01.

[92] Changeat Q, Edwards B, Al-Refaie AF, Tsiaras A, Skinner JW, Cho JYK, Yip KH, Anisman L, Ikoma M, Bieger MF, Venot O, Shibata S, Waldmann IP, Tinetti G. Five key exoplanet questions answered via the analysis of 25 hot-jupiter atmospheres in eclipse. Astrophys J Suppl Ser 2022;260:3. http://dx.doi.org/10.3847/1538-4365/ac5cc2.

[93] Schneider AD, Carone L, Decin L, Jørgensen UG, Mollière P, Baeyens R, Kiefer S, Helling C. Exploring the deep atmospheres of HD 209458b and WASP-43b using a non-gray general circulation model. Astron Astrophys 2022;664:A56. http://dx.doi.org/10.1051/0004-6361/202142728.

[94] Schneider AD, Carone L, Decin L, Jørgensen UG, Helling C. No evidence for radius inflation in hot jupiters from vertical advection of heat. Astron Astrophys 2022;666:L11. http://dx.doi.org/10.1051/0004-6361/202244797.

[95] Al-Refaie AF, Changeat Q, Venot O, Waldmann IP, Tinetti G. A comparison of chemical models of exoplanet atmospheres enabled by TauREx 3.1. Astrophys J 2022;932:123. http://dx.doi.org/10.3847/1538-4357/ac6dcd.

[96] Kasper D, Bean JL, Line MR, Seifahrt A, Brady MT, Lothringer J, Pino L, Fu G, Pelletier S, Stürmer J, Benneke B, Brogi M, Désert J-M. Unifying high- and low-resolution observations to constrain the dayside atmosphere of KELT-20b/MASCARA-2b. Astron J 2022;165:7. http://dx.doi.org/10.3847/1538-3881/ac9f40.

[97] Webb RK, Gandhi S, Brogi M, Birkby JL, de Mooij E, Snellen I, Zhang Y. Water observed in the atmosphere of τ Boötis Ab with CARMENES/CAHA. Mon Not R Astron Soc 2022;514:4160–72. http://dx.doi.org/10.1093/mnras/stac1512.

[98] Deitrick R, Heng K, Schroffenegger U, Kitzmann D, Grimm SL, Malik M, a. M. Mendonça J, Morris BM. The THOR + HELIOS general circulation model: multiwavelength radiative transfer with accurate scattering by clouds/hazes. Mon Not R Astron Soc 2022;512:3759–87. http://dx.doi.org/10.1093/mnras/stac680.

[99] Blažek M, Kabáth P, Piette AAA, Madhusudhan N, Skarka M, Šubjak J, Anderson DR, Boffin HMJ, Cáceres CC, Gibson NP, Hoyer S, Ivanov VD, Rojo PM. Constraints on TESS albedos for five hot jupiters. Mon Not R Astron Soc 2022;513:3444–57. http://dx.doi.org/10.1093/mnras/stac992.

[100] Pluriel W, Leconte J, Parmentier V, Zingales T, Falco A, Selsis F, Borde P. Toward a multidimensional analysis of transmission spectroscopy II. Day-night-induced biases in retrievals from hot to ultrahot jupiters. Astron Astrophys 2022;658:A42. http://dx.doi.org/10.1051/0004-6361/202141943.

[101] Nixon MC, Madhusudhan N. Aura-3D: A three-dimensional atmospheric retrieval framework for exoplanet transmission spectra. Astrophys J 2022;935:73. http://dx.doi.org/10.3847/1538-4357/ac7c09.

[102] Spyratos P, Nikolov NK, Constantinou S, Southworth J, Madhusudhan N, Sedaghati E, Ehrenreich D, Mancini L. A precise blue-optical transmission spectrum from the ground: evidence for haze in the atmosphere of WASP-74b. Mon Not R Astron Soc 2023;521:2163–80. http://dx.doi.org/10.1093/mnras/stad637.

[103] Bazinet L, Pelletier S, Benneke B, Salinas R, Mace GN. A subsolar metallicity on the ultra-short-period planet HIP 65Ab. Astron J 2024;167:206. http://dx.doi.org/10.3847/1538-3881/ad3071.

[104] Rathcke AD, Buchhave LA, a. M. Mendonça J, Sing DK, López-Morales M, Alam MK, Henry GW, Nikolov NK, García Muñoz A, Mikal-Evans T, Wakeford HR, Dos Santos LA, Rajpaul VM. HST PanCET programme: a flat optical transmission spectrum for the hot jupiter WASP-101b. Mon Not R Astron Soc 2023;522:582–94. http://dx.doi.org/10.1093/mnras/stad1010.

[105] Wang F, Changeat Q, Tinetti G, Turrini D, Wright SOM. Constraining the atmospheric elements in hot jupiters with ariel. Mon Not R Astron Soc 2023;523:4365–80. http://dx.doi.org/10.1093/mnras/stad1721.

[106] Cubillos PE, Fossati L, Koskinen T, Huang C, Sreejith AG, France K, Wilson Cauley P, Haswell CA. The hubble/STIS near-ultraviolet transmission spectrum of HD 189733 b. Astron Astrophys 2023;671:A170. http://dx.doi.org/10.1051/0004-6361/202245064.

[107] Bello-Arufe A, Knutson HA, Mendonca JM, Zhang MM, Cabot SHC, Rathcke AD, Ulla A, Vissapragada S, Buchhave LA. Transmission spectroscopy of the lowest-density gas giant: Metals and a potential extended outflow in HAT-p-67b. Astron J 2023;166:69. http://dx.doi.org/10.3847/1538-3881/acd935.

[108] Chubb KL, Stam DM, Helling C, Samra D, Carone L. Modelling reflected polarized light from close-in giant exoplanet WASP-96b using PolHEx (polarization of hot exoplanets). Mon Not R Astron Soc 2023;527:4955–82. http://dx.doi.org/10.1093/mnras/stad3413.

[109] Rustamkulov Z, Sing DK, Mukherjee S, May EM, Kirk J, Schlawin E, Line MR, Piaulet C, Carter AL, Batalha NE, Goyal JM, López-Morales M, Lothringer JD, MacDonald RJ, Moran SE, Stevenson KB, Wakeford HR, Espinoza N, Bean JL, Batalha NM, Benneke B, Berta-Thompson ZK, Crossfield IJM, Gao P, Kreidberg L, Powell DK, Cubillos PE, Gibson NP, Leconte J, Molaverdikhani K, Nikolov NK, Parmentier V, Roy P, Taylor J, Turner JD, Wheatley PJ, Aggarwal K, Ahrer E, Alam MK, Alderson L, Allen NH, Banerjee A, Barat S, Barrado D, Barstow JK, Bell TJ, Blecic J, Brande J, Casewell S, Changeat Q, Chubb KL, Crouzet N, Daylan T, Decin L, Désert J, Mikal-Evans T, Feinstein AD, Flagg L, Fortney JJ, Harrington J, Heng K, Hong Y, Hu R, Iro N, Kataria T, Kempton EM-R, Krick J, Lendl M, Lillo-Box J, Louca A, Lustig-Yaeger J, Mancini L, Mansfield M, Mayne NJ, Miguel Y, Morello G, Ohno K, Palle E, Petit dit de la Roche DJM, Rackham BV, Radica M, Ramos-Rosado L, Redfield S,

Rogers LK, Shkolnik EL, Southworth J, Teske J, Tremblin P, Tucker GS, Venot O, Waalkes WC, Welbanks L, Zhang X, Zieba S. Early release science of the exoplanet WASP-39b with JWST NIRSpec PRISM. Nature 2023;614:659–63. http://dx.doi.org/10.1038/s41586-022-05677-y.

[110] Louca AJ, Miguel Y, Kubyshkina D. Metallicity and spectral evolution of WASP 39b: The limited role of hydrodynamic escape. Astrophys J Lett 2023;956:L19. http://dx.doi.org/10.3847/2041-8213/acfaec.

[111] Banerjee A, Barstow JK, Haswell CA, Lewis SR. Effect of centrifugal force on transmission spectroscopy of exoplanet atmospheres. Mon Not R Astron Soc 2023;523:L64–8. http://dx.doi.org/10.1093/mnrasl/slad058.

[112] Crossfield IJM. Volatile-to-sulfur ratios can recover a gas giant's accretion history. Astrophys J Lett 2023;952:L18. http://dx.doi.org/10.3847/2041-8213/ace35f.

[113] Constantinou S, Madhusudhan N, Gandhi S. Early insights for atmospheric retrievals of exoplanets using JWST transit spectroscopy. Astrophys J Lett 2023;943:L10. http://dx.doi.org/10.3847/2041-8213/acaead.

[114] Feinstein AD, Radica M, Welbanks L, Murray CA, Ohno K, Coulombe L-P, Espinoza N, Bean JL, Teske JK, Benneke B, Line MR, Rustamkulov Z, Saba A, Tsiaras A, Barstow JK, Fortney JJ, Gao P, Knutson HA, MacDonald RJ, Mikal-Evans T, Rackham BV, Taylor J, Parmentier V, Batalha NM, Berta-Thompson ZK, Carter AL, Changeat Q, dos Santos LA, Gibson NP, Goyal JM, Kreidberg L, López-Morales M, Lothringer JD, Miguel Y, Molaverdikhani K, Moran SE, Morello G, Mukherjee S, Sing DK, Stevenson KB, Wakeford HR, Ahrer E-M, Alam MK, Alderson L, Allen NH, Batalha NE, Bell TJ, Blecic J, Brande J, Caceres C, Casewell SL, Chubb KL, Crossfield IJM, Crouzet N, Cubillos PE, Decin L, Désert J-M, Harrington J, Heng K, Henning T, Iro N, Kempton EM-R, Kendrew S, Kirk J, Krick J, Lagage P-O, Lendl M, Mancini L, Mansfield M, May EM, Mayne NJ, Nikolov NK, Palle E, Petit dit de la Roche DJM, Piaulet C, Powell D, Redfield S, Rogers LK, Roman MT, Roy P-A, Nixon MC, Schlawin E, Tan X, Tremblin P, Turner JD, Venot O, Waalkes WC, Wheatley PJ, Zhang X. Early release science of the exoplanet WASP-39b with JWST NIRISS. Nature 2023;614:670–5. http://dx.doi.org/10.1038/s41586-022-05674-1.

[115] Grant D, Lewis NK, Wakeford HR, Batalha NE, Glidden A, Goyal J, Mullens E, MacDonald RJ, May EM, Seager S, Stevenson KB, Valenti JA, Visscher C, Alderson L, Allen NH, nas CIC, Colón K, Clampin M, Espinoza N, Gressier A, Huang J, Lin Z, Long D, Louie DR, na Guerrero MP, Ranjan S, Sotzen KS, Valentine D, Anderson J, Balmer WO, Bellini A, Hoch KKW, Kammerer J, Libralato M, Mountain CM, Perrin MD, Pueyo L, Rickman E, Rebollido I, Sohn ST, van der Marel RP, Watkins LL. JWST-TST DREAMS: Quartz clouds in the atmosphere of WASP-17b. Astrophys J Lett 2023;956:L32. http://dx.doi.org/10.3847/2041-8213/acfc3b.

[116] Gandhi S, de Regt S, Snellen I, Zhang Y, Rugers B, van Leur N, Bosschaart Q. JWST measurements of ^{13}C, ^{18}O, and ^{17}O in the atmosphere of super-jupiter VHS 1256 b. Astrophys J Lett 2023;957:L36. http://dx.doi.org/10.3847/2041-8213/ad07e2.

[117] Zapata Trujillo JC, Pettyjohn MM, McKemmish LK. High-throughput quantum chemistry: empowering the search for molecular candidates behind unknown spectral signatures in exoplanetary atmospheres. Mon Not R Astron Soc 2023;524:361–76. http://dx.doi.org/10.1093/mnras/stad1717.

[118] Welbanks L, McGill P, Line M, Madhusudhan N. On the application of Bayesian leave-one-out cross-validation to exoplanet atmospheric analysis. Astron J 2023;165:112. http://dx.doi.org/10.3847/1538-3881/acab67.

[119] Taylor J, Parmentier V. Another look at the dayside spectra of WASP-43b and HD 209458b: Are there scattering clouds? Mon Not R Astron Soc 2023;526:2133–40. http://dx.doi.org/10.1093/mnras/stad2287.

[120] Chen Y-X, Burrows A, Sur A, Arevalo RT. Jupiter atmospheric models and outer boundary conditions for giant planet evolutionary calculations. Astrophys J 2023;957:36. http://dx.doi.org/10.3847/1538-4357/acf456.

[121] Hayoz J, Cugno G, Quanz SP, Patapis P, Alei E, Bonse MJ, Dannert FA, Garvin EO, Gebhard TD, Konrad BS, Sartori LF. Incorporating medium-resolution spectroscopy of close-in directly imaged exoplanets into atmospheric retrievals via cross-correlation. Astron Astrophys 2023;678:22. http://dx.doi.org/10.1051/0004-6361/202245752.

[122] Yang J, Irwin PGJ, Barstow JK. Testing 2D temperature models in Bayesian retrievals of atmospheric properties from hot jupiter phase curves. Mon Not R Astron Soc 2023;525:5146–67. http://dx.doi.org/10.1093/mnras/stad2555.

[123] Cheverall CJ, Madhusudhan N, Holmberg M. Robustness measures for molecular detections using high-resolution transmission spectroscopy of exoplanets. Mon Not R Astron Soc 2023;522:661–77. http://dx.doi.org/10.1093/mnras/stad648.

[124] Ahrer E-M, Stevenson KB, Mansfield M, Moran SE, Brande J, Morello G, Murray CA, Nikolov NK, de la Roche DJMPD, Schlawin E, Wheatley PJ, Zieba S, Batalha NE, Damiano M, Goyal JM, Lendl M, Lothringer JD, Mukherjee S, Ohno K, Batalha NM, Battley MP, Bean JL, Beatty TG, Benneke B, Berta-Thompson ZK, Carter AL, Cubillos PE, Daylan T, Espinoza N, Gao P, Gibson NP, Gill S, Harrington J, Hu R, Kreidberg L, Lewis NK, Line MR, Lopez-Morales M, Parmentier V, Powell DK, Sing DK, Tsai S-M, Wakeford HR, Welbanks L, Alam MK, Alderson L, Allen NH, Anderson DR, Barstow JK, Bayliss D, Bell TJ, Blecic J, Bryant EM, Burleigh MR, Carone L, Casewell SL, Changeat Q, Chubb KL, Crossfield IJM, Crouzet N, Decin L, Desert J-M, Feinstein AD, Flagg L, Fortney JJ, Gizis JE, Heng K, Iro N, Kempton EMR, Kendrew S, Kirk J, Knutson HA, Komacek TD, Lagage P-O, Leconte J, Lustig-Yaeger J, MacDonald RJ, Mancini L, May EM, Mayne NJ, Miguel Y, Mikal-Evans T, Molaverdikhani K, Palle E, Piaulet C, Rackham BV, Redfield S, Rogers LK, Roy P-A, Rustamkulov Z, Shkolnik EL, Sotzen KS, Taylor J, Tremblin P, Tucker GS, Turner JD, de Val-Borro M, Venot O, Zhang X. Early release science of the exoplanet WASP-39b with JWST NIRCam. Nature 2023;614:653–8. http://dx.doi.org/10.1038/s41586-022-05590-4.

[125] Lesjak F, Nortmann L, Yan F, Cont D, Reiners A, Piskunov N, Hatzes A, Boldt-Christmas L, Czesla S, Heiter U, Kochukhov O, Lavail A, Nagel E, Rains AD, Rengel M, Rodler F, Seemann U, Shulyak D. Retrieval of the dayside atmosphere of WASP-43b with CRIRES$^+$. Astron Astrophys 2023;678:A23. http://dx.doi.org/10.1051/0004-6361/202347151.

[126] Edwards B, Changeat Q. Measuring tracers of planet formation in the atmosphere of WASP-77A b: Substellar O/H and C/H ratios, with a stellar C/O ratio and a potentially superstellar Ti/H ratio. Astrophys J Lett 2024;962. http://dx.doi.org/10.3847/2041-8213/ad2000.

[127] Smith PCB, Line MR, Bean JL, Brogi M, August P, Welbanks L, Desert J-M, Lunine J, Sanchez J, Mansfield M, Pino L, Rauscher E, Kempton E, Zalesky J, Fowler M. A combined ground-based and JWST atmospheric retrieval analysis: Both IGRINS and NIRSpec agree that the atmosphere of WASP-77A b is metal-poor. Astron J 2024;167:110. http://dx.doi.org/10.3847/1538-3881/ad17bf.

[128] Schneider AD, Mollière P, Louppe G, Carone L, Jørgensen UG, Decin L, Helling C. Harnessing machine learning for accurate treatment of overlapping opacity species in general circulation models. Astron Astrophys 2024;682:A79. http://dx.doi.org/10.1051/0004-6361/202348221.

[129] Bell TJ, Crouzet N, Cubillos PE, Kreidberg L, Piette AAA, Roman MT, Barstow JK, Blecic J, Carone L, Coulombe L-P, Ducrot E, Hammond M, Mendonça Jão M, Moses JI, Parmentier V, Stevenson KB, Teinturier L, Zhang M, Batalha NM, Bean JL, Benneke B, Charnay B, Chubb KL, Demory B-O, Gao P, Lee EKH, López-Morales M, Morello G, Rauscher E, Sing DK, Tan X, Venot O, Wakeford HR, Aggarwal K, Ahrer E-M, Alam MK, Baeyens R, Barrado D, Caceres C, Carter AL, Casewell SL, Challener RC, Crossfield IJM, Decin L, Désert J-M, Dobbs-Dixon I, Dyrek A, Espinoza N, Feinstein AD, Gibson NP, Harrington J, Helling C, Hu R, Iro N, Kempton EMR, Kendrew S, Komacek TD, Krick J, Lagage P-O, Leconte J, Lendl M, Lewis NT, Lothringer JD, Malsky I, Mancini L, Mansfield M, Mayne NJ, Mikal-Evans T, Molaverdikhani K, Nikolov NK, Nixon MC, Palle E, dit de la Roche DJMP, Piaulet C, Powell D, Rackham BV, Schneider AD, Steinrueck ME, Taylor J, Welbanks L, Yurchenko SN, Zhang X, Zieba S. Nightside clouds and disequilibrium chemistry on the hot Jupiter WASP-43b. Nature 2024. http://dx.doi.org/10.1038/s41550-024-02230-x.

[130] Powell D, Feinstein AD, Lee EKH, Zhang M, Tsai S-M, Taylor J, Kirk J, Bell T, Barstow JK, Gao P, Bean JL, Blecic J, Chubb KL, Crossfield IJM, Jordan S, Kitzmann D, Moran SE, Morello G, Moses JI, Welbanks L, Yang J, Zhang X, Ahrer E-M, Bello-Arufe A, Brande J, Casewell SL, Crouzet N, Cubillos PE, Demory B-O, Dyrek A, Flagg L, Hu R, Inglis J, Jones KD, Kreidberg L, López-Morales M, Lagage P-O, Meier Valdés EA, Miguel Y, Parmentier V, Piette AAA, Rackham BV, Radica M, Redfield S, Stevenson KB, Wakeford HR, Aggarwal K, Alam MK, Batalha NM, Batalha NE, Benneke B, Berta-Thompson ZK, Brady RP, Caceres C, Carter AL, Désert J-M, Harrington J, Iro N, Line MR, Lothringer JD, MacDonald RJ, Mancini L, Molaverdikhani K, Mukherjee S, Nixon MC, Oza AV, Palle E, Rustamkulov Z, Sing DK, Steinrueck ME, Venot O, Wheatley PJ, Yurchenko SN. Sulphur dioxide in the mid-infrared transmission spectrum of WASP-39b. Nature 2024;626:979–83. http://dx.doi.org/10.1038/s41586-024-07040-9.

[131] Yip KH, Changeat Q, Al-Refaie A, Waldmann IP. To sample or not to sample: Retrieving exoplanetary spectra with variational inference and normalizing flows. Astrophys J 2024;961:30. http://dx.doi.org/10.3847/1538-4357/ad063f.

[132] Landman R, Stolker T, Snellen IAG, Costes J, de Regt S, Zhang Y, Gandhi S, Molliere P, Kesseli A, Vigan A, Sanchez-Lopez A. β Pictoris b through the eyes of the upgraded crires plus atmospheric composition, spin rotation, and radial velocity. Astron Astrophys 2024;682:A48. http://dx.doi.org/10.1051/0004-6361/202347846.

[133] Wilson J, Gibson NP, Nikolov N, Constantinou S, Madhusudhan N, Goyal J, Barstow JK, Carter AL, de Mooij EJW, Drummond B, Mikal-Evans T, Helling C, Mayne NJ, Sing DK. Ground-based transmission spectroscopy with FORS2: A featureless optical transmission spectrum and detection of H_2O for the ultra-hot jupiter WASP-103b. Mon Not R Astron Soc 2020;497:5155–70. http://dx.doi.org/10.1093/mnras/staa2307.

[134] Gandhi S, Jermyn AS. Coupled day-night models of exoplanetary atmospheres. Mon Not R Astron Soc 2020;499:4984–5003. http://dx.doi.org/10.1093/mnras/staa3143.

[135] Tabernero HM, Zapatero Osorio MR, Allart R, Borsa F, Casasayas-Barris N, Demangeon O, Ehrenreich D, Lillo-Box J, Lovis C, Palle E, Sousa SG, Rebolo R, Santos NC, Pepe F, Cristiani S, Adibekyan V, Allende Prieto C, Alibert Y, Barros SCC, Bouchy F, Bourrier V, D'Odorico V, Dumusque X, Faria JP, Figueira P, Genova Santos R, Gonzalez Hernandez J, Hojjatpanah IS, Lo Curto G, Lavie B, Martins CJAP, Martins JHC, Mehner A, Micela G, Molaro P, Nunes NJ, Poretti E, Seidel J, Sozzetti VA, Suarez Mascareno A, Udry S, Aliverti M,

Affolter M, Alves D, Amate M, Avila G, Bandy T, Benz W, Bianco A, Broeg C, Cabral A, Conconi P, Coelho J, Cumani C, Deiries S, Dekker H, Delabre B, Fragoso A, Genoni M, Genolet L, Hughes I, Knudstrup J, Kerber F, Landoni M, Lizon JL, Maire C, Manescau A, Di Marcantonio P, Megevand D, Monteiro M, Moschetti M, Mueller E, Modigliani A, Oggioni L, Oliveira A, Pariani G, Pasquini L, Rasilla JL, Redaelli E, Riva M, Santana-Tschudi S, Santin P, Santos P, Segovia A, Sosnowska D, Spano P, Tenegi F, Iwert O, Zanutta A, Zerbi F. ESPRESSO high-resolution transmission spectroscopy of WASP-76 b. Astron Astrophys 2024;646. http://dx.doi.org/10.1051/0004-6361/202039511.

[136] May EM, Komacek TD, Stevenson KB, Kempton EM-R, Bean JL, Malik M, Ih J, Mansfield M, Savel AB, Deming D, Desert J-M, Feng YK, Fortney JJ, Kataria T, Lewis N, Morley C, Rauscher E, Showman A. Spitzer phase-curve observations and circulation models of the inflated ultrahot jupiter WASP-76b. Astron J 2021;162:158. http://dx.doi.org/10.3847/1538-3881/ac0e30.

[137] Gharib-Nezhad E, Iyer AR, Line MR, Freedman RS, Marley MS, Batalha NE. EXOPLINES: Molecular absorption cross-section database for brown dwarf and giant exoplanet atmospheres. Astrophys J Suppl Ser 2021;254:34. http://dx.doi.org/10.3847/1538-4365/abf504.

[138] Stangret M, Pallé E, Casasayas-Barris N, Oshagh M, Bello-Arufe A, Luque R, Nascimbeni V, Yan F, Orell-Miquel J, Sicilia D, Malavolta L, Addison BC, Buchhave LA, Bonomo AS, Borsa F, Cabot SHC, Cecconi M, Fischer DA, Harutyunyan A, Mendonça JM, Nowak G, Parviainen H, Sozzetti A, Tronsgaard R. The obliquity and atmosphere of the ultra-hot jupiter TOI-1431b (MASCARA-5b): A misaligned orbit and no signs of atomic or molecular absorptions. Astron Astrophys 654. http://dx.doi.org/10.1051/0004-6361/202040100.

[139] Kasper D, Bean JL, Line MR, Seifahrt A, Stürmer J, Pino L, Désert J-M, Brogi M. Confirmation of iron emission lines and nondetection of TiO on the dayside of KELT-9b with MAROON-x. Astrophys J Lett 2021;921:L18. http://dx.doi.org/10.3847/2041-8213/ac30e1.

[140] Roth A, Drummond B, Hebrard E, Tremblin P, Goyal J, Mayne N. Pseudo-2D modelling of heat redistribution through H_2 thermal dissociation/recombination: consequences for ultra-hot jupiters. Mon Not R Astron Soc 2021;505:4515–30. http://dx.doi.org/10.1093/mnras/stab1256.

[141] Serindag DB, Nugroho SK, Mollière P, de Mooij EJW, Gibson NP, Snellen IAG. Is TiO emission present in the ultra-hot jupiter WASP-33b? A reassessment using the improved ExoMol TOTO line list. Astron Astrophys 2021;645:A90. http://dx.doi.org/10.1051/0004-6361/202039135.

[142] Kirk J, Rackham BV, MacDonald RJ, López-Morales M, Espinoza N, Lendl M, Wilson J, Osip DJ, Wheatley PJ, Skillen I, Apai D, Bixel A, Gibson NP, Jordán A, Lewis NK, Louden T, McGruder CD, Nikolov N, Rodler F, Weaver IC. ACCESS and LRG-BEASTS: A precise new optical transmission spectrum of the ultrahot jupiter WASP-103b. Astron J 2021;162:34. http://dx.doi.org/10.3847/1538-3881/abfcd2.

[143] Changeat Q, Edwards B. The hubble WFC3 emission spectrum of the extremely hot jupiter KELT-9b. Astrophys J Lett 2021;907:L22. http://dx.doi.org/10.3847/2041-8213/abd84f.

[144] Lee EKH, Prinoth B, Kitzmann D, Tsai S-M, Hoeijmakers J, Borsato NW, Heng K. The mantis network II: examining the 3D high-resolution observable properties of the UHJs WASP-121b and WASP-189b through GCM modelling. Mon Not R Astron Soc 2022;517:240–56. http://dx.doi.org/10.1093/mnras/stac2246.

[145] Prinoth B, Hoeijmakers HJ, Kitzmann D, Sandvik E, Seidel J, Lendl VM, Borsato NW, Thorsbro B, Anderson DR, Barrado D, Kravchenko K, Allart R, Bourrier V, Cegla HM, Ehrenreich D, Fisher C, Lovis C, Guzman-Mesa A, Grimm S, Hooton M, Morris BM, Oreshenko M, Pino L, Heng K. Titanium oxide and chemical inhomogeneity in the atmosphere of the exoplanet WASP-189b. Nat Astron 2022;6:449–57. http://dx.doi.org/10.1038/s41550-021-01581-z.

[146] Mikal-Evans T, Sing DK, Barstow JK, Kataria T, Goyal J, Lewis N, Taylor J, Mayne NJ, Daylan T, Wakeford HR, Marley MS, Spake JJ. Diurnal variations in the stratosphere of the ultrahot giant exoplanet WASP-121b. Nat Astron 2022;6:471–9. http://dx.doi.org/10.1038/s41550-021-01592-w.

[147] Savel AB, Kempton EM-R, Malik M, Komacek TD, Bean JL, May EM, Stevenson KB, Mansfield M, Rauscher E. No umbrella needed: Confronting the hypothesis of iron rain on WASP-76b with post-processed general circulation models. Astron J 2022;926:85. http://dx.doi.org/10.3847/1538-4357/ac423f.

[148] Bello-Arufe A, Cabot SHC, Mendonca JM, Buchhave LA, Rathcke AD. Mining the ultrahot skies of HAT-p-70b: Detection of a profusion of neutral and ionized species. Astron J 2022;163:96. http://dx.doi.org/10.3847/1538-3881/ac402e.

[149] Changeat Q. On spectroscopic phase-curve retrievals: H_2 dissociation and thermal inversion in the atmosphere of the ultrahot jupiter WASP-103b. Astron J 2022;163:106. http://dx.doi.org/10.3847/1538-3881/ac4475.

[150] Holmberg M, Madhusudhan N. A first look at CRIRES+: Performance assessment and exoplanet spectroscopy. Astron J 2022;164:79. http://dx.doi.org/10.3847/1538-3881/ac77eb.

[151] Finnerty L, Schofield T, Sappey B, Xuan JW, Ruffio J-B, Wang JJ, Delorme J-R, Blake GA, Buzard C, Fitzgerald MP, Baker A, Bartos R, Bond CZ, Calvin B, Cetre S, Doppmann G, Echeverri D, Jovanovic N, Liberman J, López RA, Martin EC, Mawet D, Morris E, Pezzato J, Phillips CL, Ragland S, Skemer A, Venenciano T, Wallace JK, Wallack NL, Wang J, Wizinowich P. Keck planet imager and characterizer emission spectroscopy of WASP-33b. Astron J 2023;166:31. http://dx.doi.org/10.3847/1538-3881/acda91.

[152] Yang Y, Chen G, Wang S, Yan F. High-resolution transmission spectroscopy of ultrahot jupiter WASP-33b with NEID. Astron J 2023;167:36. http://dx.doi.org/10.3847/1538-3881/ad10a3.

[153] Lowson N, Zhou G, Wright DJJ, Huang CXX, Mendonca JM, Cabot SHC, Pudmenzky C, Wittenmyer RAA, Latham DWW, Bieryla A, Esquerdo GAA, Berlind P, Calkins MLL. Multiepoch detections of the extended atmosphere and transmission spectra of KELT-9b with a 1.5 m telescope. Astron J 2023;165:101. http://dx.doi.org/10.3847/1538-3881/acacf3.

[154] Wardenier JP, Parmentier V, Line MR, Lee EKH. Modelling the effect of 3D temperature and chemistry on the cross-correlation signal of transiting ultra-hot jupiters: a study of five chemical species on WASP-76b. Mon Not R Astron Soc 2023;525:4942–61. http://dx.doi.org/10.1093/mnras/stad2586.

[155] Coulombe L-P, Benneke B, Challener R, Piette AAA, Wiser LS, Mansfield M, MacDonald RJ, Beltz H, Feinstein AD, Radica M, Savel AB, Dos Santos LA, Bean JL, Parmentier V, Wong I, Rauscher E, Komacek TD, Kempton EMR, Tan X, Hammond M, Lewis NT, Line MR, Lee EKH, Shivkumar H, Crossfield IJM, Nixon MC, Rackham BV, Wakeford HR, Welbanks L, Zhang X, Batalha NM, Berta-Thompson ZK, Changeat Q, Desert J-M, Espinoza N, Goyal JM, Harrington J, Knutson HA, Kreidberg L, Lopez-Morales M, Shporer A, Sing DK, Stevenson KB, Aggarwal K, Ahrer E-M, Alam MK, Bell TJ, Blecic J, Caceres C, Carter AL, Casewell SL, Crouzet N, Cubillos PE, Decin L, Fortney JJ, Gibson NP, Heng K, Henning T, Iro N, Kendrew S, Lagage P-O, Leconte J, Lendl M, Lothringer JD, Mancini L, Mikal-Evans T, Molaverdikhani K, Nikolov NK, Ohno K, Palle E, Piaulet C, Redfield S, Roy P-A, Tsai S-M, Venot O, Wheatley PJ. A broadband thermal emission spectrum of the ultra-hot jupiter WASP-18b. Nature 2023;620:292–8. http://dx.doi.org/10.1038/s41586-023-06230-1.

[156] Johnson MC, Wang J, Asnodkar AP, Bonomo AS, Gaudi BS, Henning T, Ilyin I, Keles E, Malavolta L, Mallonn M, Molaverdikhani K, Nascimbeni V, Patience J, Poppenhaeger K, Scandariato G, Schlawin E, Shkolnik E, Sicilia D, Sozzetti A, Strassmeier KG, Veillet C, Yan F. The PEPSI exoplanet transit survey (PETS). II. A deep search for thermal inversion agents in KELT-20b/MASCARA-2 b with emission and transmission spectroscopy. Astron J 165. http://dx.doi.org/10.3847/1538-3881/acb7e2.

[157] Petz S, Johnson MC, Asnodkar AP, Wang J, Gaudi BS, Henning T, Keles E, Molaverdikhani K, Poppenhaeger K, Scandariato G, Shkolnik EK, Sicilia D, Strassmeier KG, Yan F. The PEPSI exoplanet transit survey (PETS) - IV. Assessing the atmospheric chemistry of KELT-20b. Mon Not R Astron Soc 2023;527:7079–92. http://dx.doi.org/10.1093/mnras/stad3481.

[158] Kitzmann D, Hoeijmakers HJ, Grimm SL, Borsato NW, Lueber A, Prinoth B. The Mantis network I. A standard grid of templates and masks for cross-correlation analyses of ultra-hot jupiter transmission spectra. Astron Astrophys 2023;669:A113. http://dx.doi.org/10.1051/0004-6361/202142969.

[159] Pelletier S, Benneke B, Ali-Dib M, Prinoth B, Kasper D, Seifahrt A, Bean JL, Debras F, Klein B, Bazinet L, Hoeijmakers HJ, Kesseli AY, Lim O, Carmona A, Pino L, Casasayas-Barris N, Hood T, Stürmer J. Vanadium oxide and a sharp onset of cold-trapping on a giant exoplanet. Nature 2023;619:491–4. http://dx.doi.org/10.1038/s41586-023-06134-0.

[160] Shi Y, Wang W, Zhao G, Zhai M, Chen G, Jiang Z, Ouyang Q, Henning T, Zhao J, Crouzet N, van Boekel R, Esteves L. Thermal emission from the hot jupiter WASP-103 b in J and Ks bands. Mon Not R Astron Soc 2023;522:1491–503. http://dx.doi.org/10.1093/mnras/stad891.

[161] Ridden-Harper A, de Mooij E, Jayawardhana R, Gibson N, Karjalainen R, Karjalainen M. High-resolution emission spectroscopy of the ultrahot jupiter KELT-9b: Little variation in day- and nightside emission line contrasts. Astron J 2023;165:211. http://dx.doi.org/10.3847/1538-3881/acc654.

[162] Gandhi S, Kesseli A, Zhang Y, Louca A, Snellen I, Brogi M, Miguel Y, Casasayas-Barris N, Pelletier S, Landman R, Maguire C, Gibson NP. Retrieval survey of metals in six ultrahot jupiters: Trends in chemistry, rain-out, ionization, and atmospheric dynamics. Astron J 2023;165:242. http://dx.doi.org/10.3847/1538-3881/accd65.

[163] Brogi M, Emeka-Okafor V, Line MR, Gandhi S, Pino L, Kempton EM-R, Rauscher E, Parmentier V, Bean JL, Mace GN, Cowan NB, Shkolnik E, Wardenier JP, Mansfield M, Welbanks L, Smith P, Fortney JJ, Birkby JL, Zalesky JA, Dang L, Patience J, Désert J-M. The roasting marshmallows program with IGRINS on gemini south I: Composition and climate of the ultrahot jupiter WASP-18 b. Astron J 2023;165:91. http://dx.doi.org/10.3847/1538-3881/acaf5c.

[164] Prinoth B, Hoeijmakers HJ, Pelletier S, Kitzmann D, Morris BM, Seifahrt A, Kasper D, Korhonen HH, Burheim M, Bean JL, Benneke B, Borsato NW, Brady M, Grimm SL, Luque R, Stuermer J, Thorsbro B. Time-resolved transmission spectroscopy of the ultra-hot jupiter WASP-189 b. Astron Astrophys 2023;678:A182. http://dx.doi.org/10.1051/0004-6361/202347262.

[165] van Sluijs L, Birkby JL, Lothringer J, Lee EKH, Crossfield IJM, Parmentier V, Brogi M, Kulesa C, McCarthy D, Charbonneau D. Carbon monoxide emission lines reveal an inverted atmosphere in the ultra hot jupiter WASP-33 b consistent with an eastward hot spot. Mon Not R Astron Soc 2023;522:2145–70. http://dx.doi.org/10.1093/mnras/stad1103.

[166] Changeat Q, Skinner JW, Cho JY-K, Nättilä J, Waldmann IP, Al-Refaie AF, Dyrek A, Edwards B, Mikal-Evans T, Joshua M, Morello G, Skaf N, Tsiaras A, Venot O, Yip KH. Is the atmosphere of the ultra-hot jupiter WASP-121 b

variable? Astrophys J Suppl Ser 2024;270:34. http://dx.doi.org/10.3847/1538-4365/ad1191.

[167] Finnerty L, Xuan JW, Xin Y, Liberman J, Schofield T, Fitzgerald MP, Agrawal S, Baker A, Bartos R, Blake GA, Calvin B, Cetre S, Delorme J-R, Doppmann G, Echeverri D, Hsu C-C, Jovanovic N, López RA, Martin EC, Mawet D, Morris E, Pezzato J, Ruffio J-B, Sappey B, Skemer A, Venenciano T, Wallace JK, Wallack NL, Wang JJ, Wang J. Atmospheric metallicity and C/O of HD 189733 b from high-resolution spectroscopy. Astron J 2024;167:43. http://dx.doi.org/10.3847/1538-3881/ad1180.

[168] Maguire C, Gibson NP, Nugroho SK, Fortune M, Ramkumar S, Gandhi S, de Mooij E. High resolution atmospheric retrievals of WASP-76b transmission spectroscopy with ESPRESSO: monitoring limb asymmetries across multiple transits. Astron Astrophys 2024;687:A49. http://dx.doi.org/10.1051/0004-6361/202449449.

[169] Edwards B, Changeat Q, Mori M, Anisman LO, Morvan M, Yip KH, Tsiaras A, Al-Refaie A, Waldmann I, Tinetti G. Hubble WFC3 spectroscopy of the habitable-zone super-earth LHS 1140 b. Astron J 2020;161:44. http://dx.doi.org/10.3847/1538-3881/abc6a5.

[170] Piette AAA, Madhusudhan N, Mandell AM. Hydro: atmospheric retrieval of rocky exoplanets in thermal emission. Mon Not R Astron Soc 2021;511:2565–84. http://dx.doi.org/10.1093/mnras/stab3612.

[171] Mugnai LV, Modirrousta-Galian D, Edwards B, Changeat Q, Bouwman J, Morello G, Al-Refaie A, Baeyens R, Bieger MF, Blain D, Gressier A, Guilluy G, Jaziri Y, Kiefer F, Morvan M, Pluriel W, Poveda M, Skaf N, Whiteford N, Wright S, Yip KH, Zingales T, Charnay B, Drossart P, Leconte J, Venot O, Waldmann I, Beaulieu J-P. ARES. V. No evidence for molecular absorption in the HST WFC3 spectrum of GJ 1132 b. Astron J 2021;161:284. http://dx.doi.org/10.3847/1538-3881/abf3c3.

[172] Gressier A, Mori M, Changeat Q, Edwards B, Beaulieu JP, Marcq E, Charnay B. Near-infrared transmission spectrum of TRAPPIST-1h using *Hubble* WFC3 G141 observations. Astron Astrophys 2022;658:A133. http://dx.doi.org/10.1051/0004-6361/202142140.

[173] Alei E, Konrad BS, Angerhausen D, Grenfell JL, Molliere P, Quanz SP, Rugheimer S, Wunderlich F, Collaboration L. Large interferometer for exoplanets (LIFE) V. Diagnostic potential of a mid-infrared space interferometer for studying earth analogs. Astron Astrophys 2022;665:A106. http://dx.doi.org/10.1051/0004-6361/202243760.

[174] Bower DJ, Hakim K, Sossi PA, Sanan P. Retention of water in terrestrial magma oceans and carbon-rich early atmospheres. Planet Sci J 2022;3:93. http://dx.doi.org/10.3847/PSJ/ac5fb1.

[175] Claringbold AB, Rimmer PB, Rugheimer S, Shorttle O. Prebiosignature molecules can be detected in temperate exoplanet atmospheres with JWST. Astron J 166. http://dx.doi.org/10.3847/1538-3881/acdacc.

[176] Diamond-Lowe H, ao M. Mendonça J, Charbonneau D, Buchhave LA. Ground-based optical transmission spectroscopy of the nearby terrestrial exoplanet LTT 1445Ab. Astron J 2023;165:169. http://dx.doi.org/10.3847/1538-3881/acbf39.

[177] Zhou L, Ma B, Wang Y-H, Zhu Y-N. Hubble WFC3 spectroscopy of the terrestrial planets L 98-59 c and d: No evidence for a clear hydrogen dominated primary atmosphere. Res Astron Astrophys 2023;23:025011. http://dx.doi.org/10.1088/1674-4527/acaceb.

[178] Phillips CL, Wang J, Edwards B, Martínez RR, Asnodkar AP, Gaudi BS. Exploring the potential of twinkle to unveil the nature of LTT 1445 Ab. Mon Not R Astron Soc 2023;526:2251–64. http://dx.doi.org/10.1093/mnras/stad2822.

[179] Moran SE, Stevenson KB, Sing DK, MacDonald RJ, Kirk J, Lustig-Yaeger J, Peacock S, Mayorga LC, Bennett KA, López-Morales M, May EM, Rustamkulov Z, Valenti JA, Redai JIA, Alam MK, Batalha NE, Fu G, Gonzalez-Quiles J, Highland AN, Kruse E, Lothringer JD, Ceballos KNO, Sotzen KS, Wakeford HR. High tide or riptide on the cosmic shoreline? A water-rich atmosphere or stellar contamination for the warm super-earth GJ 486b from JWST observations. Astrophys J Lett 2023;948:L11. http://dx.doi.org/10.3847/2041-8213/accb9c.

[180] Zhou L, Ma B, Wang Y, Zhu Y. Hubble WFC3 spectroscopy of the rocky planet L 98-59 b: No evidence for a cloud-free primordial atmosphere. Astron J 2022;164:203. http://dx.doi.org/10.3847/1538-3881/ac8fe9.

[181] Zilinskas M, van Buchem CPA, Miguel Y, Louca A, Lupu R, Zieba S, van Westrenen W. Observability of evaporating lava worlds star. Astron Astrophys 2022;661:A126. http://dx.doi.org/10.1051/0004-6361/202142984.

[182] Whittaker EA, Malik M, Ih J, Kempton EM-R, Mansfield M, Bean JL, Kite ES, Koll DDB, Cronin TW, Hu R. The detectability of rocky planet surface and atmosphere composition with the JWST: The case of LHS 3844b. Astron J 2022;164:258. http://dx.doi.org/10.3847/1538-3881/ac9ab3.

[183] Crossfield IJM, Malik M, Hill ML, Kane SR, Foley B, Polanski AS, Coria D, Brande J, Zhang Y, Wienke K, Kreidberg L, Cowan NB, Dragomir D, Gorjian V, Mikal-Evans T, Benneke B, Christiansen JL, Deming D, Morales FY. GJ 1252b: A hot terrestrial super-earth with no atmosphere. Astrophys J Lett 2022;937:L17. http://dx.doi.org/10.3847/2041-8213/ac886b.

[184] Zieba S, Zilinskas M, Kreidberg L, Nguyen TG, Miguel Y, Cowan NB, Pierrehumbert R, Carone L, Dang L, Hammond M, Louden T, Lupu R, Malavolta L, Stevenson KB. K2 and *Spitzer* phase curves of the rocky ultra-short-period planet K2-141b hint at a tenuous rock vapor atmosphere. Astron Astrophys 2022;664:A79. http://dx.doi.org/10.1051/0004-6361/202142912.

[185] Janssen LJ, Woitke P, Herbort O, Min M, Chubb KL, Helling C, Carone L. The sulfur species in hot rocky exoplanet atmospheres. Astron Nachr 2023;344:e20230075. http://dx.doi.org/10.1002/asna.20230075.

[186] Piette AAA, Gao P, Brugman K, Shahar A, Lichtenberg T, Miozzi F, Driscoll P. Rocky planet or water world? Observability of low-density lava world atmospheres. Astrophys J 2023;954:29. http://dx.doi.org/10.3847/1538-4357/acdef2.

[187] Heng K. The transient outgassed atmosphere of 55 Cancri e. Astrophys J Lett 2023;956:L20. http://dx.doi.org/10.3847/2041-8213/acfe05.

[188] Ridden-Harper A, Nugroho SK, Flagg L, Jayawardhana R, Turner JD, de Mooij E, MacDonald R, Deibert E, Tamura M, Kotani T, Hirano T, Kuzuhara M, Omiya M, Kusakabe N. High-resolution transmission spectroscopy of the terrestrial exoplanet GJ 486b. Astron J 2023;165:170. http://dx.doi.org/10.3847/1538-3881/acbd39.

[189] Zilinskas M, Miguel Y, van Buchem CPA, Snellen IAG. Observability of silicates in volatile atmospheres of super-earths and sub-Neptunes exploring the edge of the evaporation desert. Astron Astrophys 2023;671. http://dx.doi.org/10.1051/0004-6361/202245521.

[190] Booth RA, Owen JE, Schulik M. Dust formation in the outflows of catastrophically evaporating planets. Mon Not R Astron Soc 2023;518:1761–75. http://dx.doi.org/10.1093/mnras/stac3121.

[191] Seligman DZ, Feinstein AD, Lai D, Welbanks L, Taylor AG, Becker J, Adams FC, Morgan M, Bergner JB. Potential melting of extrasolar planets by tidal dissipation. Astrophys J 2024;961:22. http://dx.doi.org/10.3847/1538-4357/ad0b82.

[192] Greaves JS, Rimmer PB, Richards AMS, Petkowski JJ, Bains W, Ranjan S, Seager S, Clements DL, Silva CS, Fraser HJ. Low levels of sulphur dioxide contamination of Venusian phosphine spectra. Mon Not R Astron Soc 2022;514:2994–3001. http://dx.doi.org/10.1093/mnras/stac1438.

[193] Dias JA, Machado P, Ribeiro J. From atmospheric evolution to the search of species of astrobiological interest in the solar system-case studies using the planetary spectrum generator. Atmosphere 2022;13:461. http://dx.doi.org/10.3390/atmos13030461.

[194] Koga R, Suzuki T, Tsuchiya F, Sakanoi T, Hirahara Y. ALMA observation of SO_2 gas originating from Io's volcanic plume and lava areas. Astrophys J 2021;907:L6. http://dx.doi.org/10.3847/2041-8213/abd39f.

[195] Cambianica P, Cremonese G, Munaretto G, Capria MT, Fulle M, Boschin W, Di Fabrizio L, Harutyunyan A. A high-spectral-resolution catalog of emission lines in the visible spectrum of comet C/2020 F3 (NEOWISE). Astron Astrophys 2021;656:A160. http://dx.doi.org/10.1051/0004-6361/202140309.

[196] Lacy BI, Burrows A. JWST transit spectra. II. Constraining aerosol species, particle-size distributions, temperature, and metallicity for cloudy exoplanets. Astrophys J 2020;904:25. http://dx.doi.org/10.3847/1538-4357/abbc6c.

[197] Welbanks L, Madhusudhan N. Aurora: A generalized retrieval framework for exoplanetary transmission spectra. Astrophys J 2021;114. http://dx.doi.org/10.3847/1538-4357/abee94.

[198] Lavvas P, Arfaux A. Impact of photochemical hazes and gases on exoplanet atmospheric thermal structure. Mon Not R Astron Soc 2021;502:5643–57. http://dx.doi.org/10.1093/mnras/stab456.

[199] Mukherjee S, Batalha NE, Marley MS. Cloud parameterizations and their effect on retrievals of exoplanet reflection spectroscopy. Astrophys J 2021;910:158. http://dx.doi.org/10.3847/1538-4357/abe53b.

[200] Lefèvre M, Tan X, Lee EKH, Pierrehumbert RT. Cloud-convection feedback in brown dwarf atmospheres. Astrophys J 2022;929:153. http://dx.doi.org/10.3847/1538-4357/ac5e2d.

[201] Jiang C, Chen G, Palle E, Murgas F, Parviainen H, Ma Y. Featureless transmission spectra of 12 giant exoplanets observed by GTC/OSIRIS. Astron Astrophys 675. http://dx.doi.org/10.1051/0004-6361/202346091.

[202] Lacy B, Burrows A. Self-consistent models of Y dwarf atmospheres with water clouds and disequilibrium chemistry. Astrophys J 2023;950:8. http://dx.doi.org/10.3847/1538-4357/acc8cb.

[203] Ma S, Ito Y, Al-Refaie AF, Changeat Q, Edwards B, Tinetti G. YunMa: Enabling spectral retrievals of exoplanetary clouds. Astrophys J 2023;957:104. http://dx.doi.org/10.3847/1538-4357/acf8ca.

[204] Baeyens R, Konings T, Venot O, Carone L, Decin L. Grid of pseudo-2D chemistry models for tidally locked exoplanets - II. The role of photochemistry. Mon Not R Astron Soc 2022;512:4877–92. http://dx.doi.org/10.1093/mnras/stac809.

[205] Edwards B, Stotesbury I. Terminus: A versatile simulator for space-based telescopes. Astron J 2021;161:266. http://dx.doi.org/10.3847/1538-3881/abdf4d.

[206] Mugnai LV, Al-Refaie A, Bocchieri A, Changeat Q, Pascale E, Tinetti G. Alfnoor: Assessing the information content of Ariel's low-resolution spectra with planetary population studies. Astron J 2021;162:288. http://dx.doi.org/10.3847/1538-3881/ac2e92.

[207] Charnay B, Mendonca JM, Kreidberg L, Cowan NB, Taylor J, Bell TJ, Demangeon O, Edwards B, Haswell CA, Morello G, Mugnai LV, Pascale E, Tinetti G, Tremblin P, Zellem RT. A survey of exoplanet phase curves with Ariel. Exp Astron 2022;53:417–46. http://dx.doi.org/10.1007/s10686-021-09715-x.

[208] Guilluy G, Sozzetti A, Giacobbe P, Bonomo AS, Micela G. On the synergy between ariel and ground-based high-resolution spectroscopy. Exp Astron 2022;53:655–77. http://dx.doi.org/10.1007/s10686-021-09824-7.

[209] Edwards B, Tinetti G. The Ariel target list: The impact of TESS and the potential for characterizing multiple planets within a system. Astron J 2022;164:15. http://dx.doi.org/10.3847/1538-3881/ac6bf9.

[210] Barstow JK, Changeat Q, Chubb KL, Cubillos PE, Edwards B, MacDonald RJ, Min M, Waldmann IP. A retrieval challenge exercise for the ariel mission. Exp Astron 2022;53:447–71. http://dx.doi.org/10.1007/s10686-021-09821-w.

[211] Edwards B, Changeat Q, Tsiaras A, Yip KH, Al-Refaie AF, Anisman L, Bieger MF, Gressier A, Shibata S, Skaf N, Bouwman J, Cho JY-K, Ikoma M, Venot O, Waldmann I, Lagage P-O, Tinetti G. Exploring the ability of hubble space telescope WFC3 G141 to uncover trends in populations of exoplanet atmospheres through a homogeneous transmission survey of 70 gaseous planets. Astrophys J Suppl Ser 269. http://dx.doi.org/10.3847/1538-4365/ac9f1a.

[212] Bocchieri A, Mugnai LV, Pascale E, Changeat Q, Tinetti G. Detecting molecules in ariel low resolution transmission spectra. Exp Astron 2023;56:605–44. http://dx.doi.org/10.1007/s10686-023-09911-x.

[213] Changeat Q, Ito Y, Al-Refaie AF, Yip KH, Lueftinger T. Toward atmospheric retrievals of panchromatic light curves: Explor-ing generalized inversion techniques for transiting exoplanets with JWST and ariel. Astron J 2024;167:195. http://dx.doi.org/10.3847/1538-3881/ad3032.

[214] MacDonald Ryan J, Lewis Nikole K. Trident: A rapid 3D radiative-transfer model for exoplanet transmission spectra. Astrophys J 2022;929:20. http://dx.doi.org/10.3847/1538-4357/ac47fe.

[215] Waldmann IP, Rocchetto M, Tinetti G, Barton EJ, Yurchenko SN, Tennyson J. τ-REx II: Retrieval of emission spectra. Astrophys J 2015;813:13.

[216] Al-Refaie AF, Changeat Q, Waldmann IP, Tinetti G. TauREx 3: A fast, dynamic, and extendable framework for retrievals. Astrophys J 2021;917:37. http://dx.doi.org/10.3847/1538-4357/ac0252.

[217] Harrington J, Himes MD, Cubillos PE, Blecic J, Rojo PM, Challener RC, Lust NB, Bowman MO, Blumenthal SD, Dobbs-Dixon I, Foster ASD, Foster AJ, Green MR, Loredo TJ, McIntyre KJ, Stemm MM, Wright DC. An open-source Bayesian atmospheric radiative transfer (BART) code. I. Design, tests, and application to exoplanet HD 189733b. Planet Sci J 2022;3:80. http://dx.doi.org/10.3847/PSJ/ac3513.

[218] Cubillos PE, Harrington J, Blecic J, Himes MD, Rojo PM, Loredo TJ, Lust NB, Challener RC, Foster AJ, Stemm MM, Foster ASD, Blumenthal SD. An open-source Bayesian atmospheric radiative transfer (BART) code. II. The transit radiative transfer module and retrieval of HAT-P-11b. Planet Sci J 2022;3:81. http://dx.doi.org/10.3847/PSJ/ac348b.

[219] Lee EKH, Wardenier JP, Prinoth B, Parmentier V, Grimm SL, Baeyens R, Carone L, Christie D, Deitrick R, Kitzmann D, Mayne N, Roman M, Thorsbro B. 3D radiative transfer for exoplanet atmospheres. gCMCRT: A GPU-accelerated MCRT code. Astrophys J 2022;929:180. http://dx.doi.org/10.3847/1538-4357/ac61d6.

[220] Cubillos PE, Blecic J. The *pyratbay* framework for exoplanet atmospheric modelling: a population study of hubble/WFC3 transmission spectra. Mon Not R Astron Soc 2021;505:2675–702. http://dx.doi.org/10.1093/mnras/stab1405.

[221] Villanueva GL, Fauchez TJ, Kofman V, Alei E, Lee EKH, Janin E, Himes MD, Leconte J, Leung M, Faggi S, Mak MT, Sergeev DE, Kozakis T, Manners J, Mayne N, Schwieterman EW, Howe AR, Batalha N. Modeling atmospheric lines by the exoplanet community (MALBEC) version 1.0: A CUISINES radiative transfer intercomparison project. Planet Space Sci 2024;5:64. http://dx.doi.org/10.3847/PSJ/ad2681.

[222] Min M, Ormel CW, Chubb K, Helling C, Kawashima Y. The ARCiS framework for exoplanet atmospheres - modelling philosophy and retrieval. Astron Astrophys 2020;642:A28. http://dx.doi.org/10.1051/0004-6361/201937377.

[223] Mugnai LV, Modirrousta-Galian D. RAPOC: The rosseland and Planck opacity converter a user-friendly and fast opacity program for python. Exp Astron 2023;55:521–39. http://dx.doi.org/10.1007/s10686-022-09869-2.

[224] Wheeler AJ, Casey AR, Abruzzo MW. Korg: Fitting, model atmosphere interpolation, and brackett lines. Astron J 2024;167:83. http://dx.doi.org/10.3847/1538-3881/ad19cc.

[225] Zhan Z, Seager S, Petkowski JJ, Sousa-Silva C, Ranjan S, Huang J, Bains W. Assessment of isoprene as a possible biosignature gas in exoplanets with anoxic atmospheres. Astrobiology 2021;21:765–92. http://dx.doi.org/10.1089/ast.2019.2146.

[226] Ishikawa HT, Aoki W, Kotani T, Kuzuhara M, Omiya M, Reiners A, Zechmeister M. Elemental abundances of M dwarfs based on high-resolution near-infrared spectra: Verification by binary systems. Publ Astron Soc Japan 2020;72:102. http://dx.doi.org/10.1093/pasj/psaa101.

[227] Contursi G, de Laverny P, Recio-Blanco A, Palicio PA. GSP-spec line list for the parametrisation of *Gaia*-RVS stellar spectra. Astron Astrophys 654. http://dx.doi.org/10.1051/0004-6361/202140912.

[228] Marfil E, Tabernero HM, Montes D, Caballero JA, Lazaro FJ, Gonzalez Hernandez J, Nagel IE, Passegger VM, Schweitzer A, Ribas I, Reiners A, Quirrenbach A, Amado PJ, Cifuentes C, Cortes-Contreras M, Dreizler S, Duque-Arribas C, Galadi-Enriquez D, Henning T, Jeffers S, Kaminski VA, Kuerster M, Lafarga M, Lopez-Gallifa A, Morales JC, Shan Y, Zechmeister M. The CARMENES search for exoplanets around M dwarfs stellar atmospheric parameters of target stars with STEPARSYN. Astron Astrophys 656. http://dx.doi.org/10.1051/0004-6361/202141980.

[229] Lyubchyk YP, Pavlenko Y, Lyubchyk VOK, Jones HRA. Bands of NaH lines in spectra of late type stars. Kinemat Phys Celest 2022;38:159–65. http://dx.doi.org/10.3103/S0884591322030059.

[230] Jones HRA, Pavlenko Y, Lyubchik Y, Bessell M, Allard N, Pinfield DJ. A blue depression in the optical spectra of M dwarfs. Mon Not R Astron Soc 2023;523:1297–309. http://dx.doi.org/10.1093/mnras/stad1391.

[231] Cristofari PI, Donati J-F, Folsom CP, Masseron T, Fouqué P, Moutou C, Artigau E, Carmona A, Petit P, Delfosse X, Martioli E, the SLS consortium. Constraining atmospheric parameters and surface magnetic fields with ZeeTurbo: an application to SPIRou spectra. Mon Not R Astron Soc 2023;522:1342–57. http://dx.doi.org/10.1093/mnras/stad865.

[232] Xuan JW, Wang J, Finnerty L, Horstman K, Grimm S, Peck AE, Nielsen E, Knutson HA, Mawet D, Isaacson H, Howard AW, Liu MC, Walker S, Phillips MW, Blake GA, Ruffio J-B, Zhang Y, Inglis J, Wallack NL, Sanghi A, Gonzales EJ, Dai F, Baker A, Bartos R, Bond CZ, Bryan ML, Calvin B, Cetre S, Delorme J-R, Doppmann G, Echeverri D, Fitzgerald MP, Jovanovic N, Liberman J, Lopez RA, Martin EC, Morris E, Pezzato J, Ruane G, Sappey B, Schofield T, Skemer A, Venenciano T, Wallace JK, Wang J, Wizinowich P, Xin Y, Agrawal S, Do CR, Hsu C-C, Phillips CL. Validation of elemental and isotopic abundances in late-m spectral types with the benchmark HIP 55507 AB system. Astrophys J 962. http://dx.doi.org/10.3847/1538-4357/ad1243.

[233] Pavlenko YV, Evans A, Banerjee DPK, Geballe TR, Munari U, Gehrz RD, Woodward CE, Starrfield S. Isotopic ratios in the red giant component of the recurrent nova T coronae borealis. Mon Not R Astron Soc 2020;498:4853–63. http://dx.doi.org/10.1093/mnras/staa2658.

[234] Gasman D, Argyriou I, Sloan GC, Aringer B, Alvarez-Marquez J, Fox O, Glasse A, Glauser A, Jones OC, Justtanont K, Kavanagh PJ, Klaassen P, Labiano A, Larson K, Law DR, Mueller M, Nayak O, Noriega-Crespo A, Patapis P, Royer P, Vandenbussche B. JWST MIRI/MRS in-flight absolute flux calibration and tailored fringe correction for unresolved sources. Astron Astrophys 673. http://dx.doi.org/10.1051/0004-6361/202245633.

[235] Hayes CR, Venn KA, Waller F, Jensen J, Mcconnachie AW, Pazder J, Sestito F, Anthony A, Baker G, Bassett J, Bento J, Berg T, Burley G, Brzeski J, Case S, Chapin E, Chin T, Chisholm E, Churilov V, Densmore A, Diaz R, Dunn J, Edgar M, Farrell T, Firpo V, Fitzsimmons J, Font-Serra J, Fuentes J, Ganton C, Gomez-Jimenez M, Hardy T, Henderson D, Hill A, Hoff B, Ireland M, Kalari V, Kelly N, Klauser U, Kondrat Y, Labrie K, Lambert S, Luvaul L, Lawrence J, Lothrop J, Macdonald GS, Mali S, Margheim S, Mcdermid R, Mcgregor H, Miller B, Miranda F, Muller R, Nielsen J, Norbury R, Oberdorf O, Pai N, Perez G, Prado P, Price I, Quiroz C, Reshetov V, Robertson G, Ruiz-Carmona R, Salinas R, Sebo KM, Sheinis A, Shetrone M, Shortridge K, Silversides K, Silva K, Simpson C, Smith G, Szeto K, Tims J, Toro E, Urrutia C, Venkatesan S, Waller L, Wevers I, Wierzbicki R, White M, Young P, Zhelem R. GHOST commissioning science results: Identifying a new chemically peculiar star in reticulum II. Astrophys J 955. http://dx.doi.org/10.3847/1538-4357/acebc0.

[236] Brandt TD, Dupuy TJ, Bowler BP, Gagliuffi DCB, Faherty J, Brandt GM, Michalik D. A dynamical mass of 70 $\pm$5 M_{Jup} for gliese 229b, the first T dwarf. Astron J 2020;160:196. http://dx.doi.org/10.3847/1538-3881/abb45e.

[237] Piette AAA, Madhusudhan N. Considerations for atmospheric retrieval of high-precision brown dwarf spectra. Mon Not R Astron Soc 2020;497:5136–54. http://dx.doi.org/10.1093/mnras/staa2289.

[238] Meisner AM, Schneider AC, Burgasser AJ, Marocco F, Line MR, Faherty JK, Kirkpatrick JD, Caselden D, Kuchner MJ, Gelino CR, Gagne J, Theissen C, Gerasimov R, Aganze C, Hsu C-c, Wisniewski JP, Casewell SL, Bardalez Gagliuffi DC, Logsdon SE, Eisenhardt PRM, Allers K, Debes JH, Allen MB, Stevnbak Andersen N, Goodman S, Gramaize L, Martin DW, Sainio A, Cushing MC, The Backyard Worlds Planet 9 Collaboration. New candidate extreme T subdwarfs from the backyard worlds: Planet 9 citizen science project. Astrophys J 915. http://dx.doi.org/10.3847/1538-4357/ac013c.

[239] von Essen C, Mallonn M, Piette A, Cowan NB, Madhusudhan N, Agol E, Antoci V, Poppenhaeger K, Stassun KG, Khalafinejad S, Tautvaisiene G. TESS unveils the optical phase curve of KELT-1b - thermal emission and ellipsoidal variation from the brown dwarf companion along with the stellar activity. Astron Astrophys 2021;648:A71. http://dx.doi.org/10.1051/0004-6361/202038524.

[240] Mukherjee S, Fortney JJ, Jensen-Clem R, Tan X, Marley MS, Batalha NE. Modeling polarization signals from cloudy brown dwarfs luhman 16 A and B in three dimensions. Astron J 2021;923:113. http://dx.doi.org/10.3847/1538-4357/ac2d92.

[241] Marley MS, Saumon D, Visscher C, Lupu R, Freedman R, Morley C, Fortney JJ, Seay C, Smith AJRW, Teal DJ, Wang R. The sonora brown dwarf atmosphere and evolution models. I. Model description and application to cloudless atmospheres in rainout chemical equilibrium. Astrophys J 2021;920:85. http://dx.doi.org/10.3847/1538-4357/ac141d.

[242] Cushing MC, Schneider AC, Kirkpatrick JD, Morley CV, Marley MS, Gelino CR, Mace GN, Wright EL, Eisenhardt PR, Skrutskie MF, Marsh KA. An improved near-infrared spectrum of the archetype Y dwarf WISEP J182831.08+265037.8. Astrophys J 2021;920:20. http://dx.doi.org/10.3847/1538-4357/ac12cb.

[243] Lueber A, Kitzmann D, Bowler BP, Burgasser AJ, Heng K. Retrieval study of brown dwarfs across the L-T sequence. Astrophys J 2022;930:136. http://dx.doi.org/10.3847/1538-4357/ac63b9.

[244] Tannock ME, Metchev S, Hood CE, Mace GN, Fortney JJ, Morley CV, Jaffe DT, Lupu R. A 1.46-2.48 μm spectroscopic atlas of a T6 dwarf (1060 K) atmosphere with IGRINS: First detections of H_2S and H_2, and verification of H_2O, CH_4, and NH_3 line lists. Mon Not R Astron Soc 2022;514. http://dx.doi.org/10.1093/mnras/stac1412.

[245] Xuan JW, Wang J, Ruffio J-B, Knutson H, Mawet D, Molli'ere P, Kolecki J, Vigan A, Mukherjee S, Wallack N, Wang J, Baker A, Bartos R, Blake GA, Bond CZ, Bryan M, Calvin B, Cetre S, Chun M, Delorme J-R, Doppmann G, Echeverri D, Finnerty L, Fitzgerald MP, Horstman K, Inglis J, Jovanovic N, López R, Martin EC, Morris E, Pezzato J, Ragland S, Ren B, Ruane G, Sappey B, Schofield T, Skemer A, Venenciano T, Wallace JK, Wizinowich P. A clear view of a cloudy brown dwarf companion from high-resolution spectroscopy. Astrophys J 2022;937:54. http://dx.doi.org/10.3847/1538-4357/ac8673.

[246] Rowland MJ, Morley CV, Line MR. Toward robust atmospheric retrieval on cloudy L dwarfs: the impact of thermal and abundance profile assumptions. Astrophys J 2023;947:6. http://dx.doi.org/10.3847/1538-4357/acbb07.

[247] Barrado D, Mollière P, Patapis P, Min M, Tremblin P, Ardevol Martinez F, Whiteford N, Vasist M, Argyriou I, Samland M, Lagage P-O, Decin L, Waters R, Henning T, Morales-Calderón M, Guedel M, Vandenbussche B, Absil O, Baudoz P, Boccaletti A, Bouwman J, Cossou C, Coulais A, Crouzet N, Gastaud R, Glasse A, Glauser AM, Kamp I, Kendrew S, Krause O, Lahuis F, Mueller M, Olofsson G, Pye J, Rouan D, Royer P, Scheithauer S, Waldmann I, Colina L, van Dishoeck EF, Ray T, Östlin G, Wright G. $^{15}NH_3$ in the atmosphere of a cool brown dwarf. Nature 2023;624:263–6. http://dx.doi.org/10.1038/s41586-023-06813-y.

[248] Mukherjee S, Batalha NE, Fortney JJ, Marley MS. PICASO 3.0: A one-dimensional climate model for giant planets and brown dwarfs. Astrophys J 2023;942:71. http://dx.doi.org/10.3847/1538-4357/ac9f48.

[249] Hood CE, Fortney JJ, Line MR, Faherty JK. Brown dwarf retrievals on FIRE!: Atmospheric constraints and lessons learned from high signal-to-noise medium-resolution spectroscopy of a T9 dwarf. Astrophys J 2023;953:170. http://dx.doi.org/10.3847/1538-4357/ace32e.

[250] Franson K, Bowler BP, Bonavita M, Brandt TD, Chen M, Samland M, Zhang Z, Lueber A, Heng K, Kitzmann D, Wolf T, Jones BA, Tran QH, Gagliuffi DCB, Biller B, Chilcote J, Crepp JR, Dupuy TJ, Faherty J, Fontanive C, Groff TD, Gratton R, Guyon O, Jensen-Clem R, Jovanovic N, Kasdin NJ, Lozi J, Magnier EA, Mužić K, Sanghi A, Theissen CA. Astrometric accelerations as dynamical beacons: Discovery and characterization of HIP 21152 B, the first T-dwarf companion in the hyades. Astron J 2023;165:39. http://dx.doi.org/10.3847/1538-3881/aca408.

[251] Lee EKH, Tan X, Tsai S-M. Dynamically coupled kinetic chemistry in brown dwarf atmospheres - I. Performing global scale kinetic modelling. Mon Not R Astron Soc 2023;523:4477–91. http://dx.doi.org/10.1093/mnras/stad1715.

[252] Mukherjee S, Fortney JJ, Morley CV, Batalha NE, Marley MS, Karalidi T, Visscher C, Lupu R, Freedman R, Gharib-Nezhad E. The sonora substellar atmosphere models. IV. Elf owl: Atmospheric mixing and chemical disequilibrium with varying metallicity and C/O ratios. Astrophys J 2024;963:73. http://dx.doi.org/10.3847/1538-4357/ad18c2.

[253] Burgasser AJ, Bezanson R, Labbe I, Brammer G, Cutler SE, Furtak LJ, Greene JE, Gerasimov R, Leja J, Pan R, Price SH, Wang B, Weaver JR, Whitaker KE, Fujimoto S, Kokorev V, Dayal P, Nanayakkara T, Williams CC, Marchesini D, Zitrin A, van Dokkum P. UNCOVER: JWST spectroscopy of three cold brown dwarfs at kiloparsec-scale distances. Astrophys J 2024;962:177. http://dx.doi.org/10.3847/1538-4357/ad206f.

[254] Lew BWP, Roellig T, Batalha NE, Line M, Greene T, Murkherjee S, Freedman R, Meyer M, Beichman C, de Oliveira CA, De Furio M, Johnstone D, Greenbaum AZ, Marley M, Fortney JJ, Young ET, Leisenring J, Boyer M, Hodapp K, Misselt K, Stansberry J, Rieke M. High-precision atmospheric characterization of a Y dwarf with JWST nirspec G395h spectroscopy: Isotopologue, C/O ratio, metallicity, and the abundances of six molecular species. Astron J 2024;167:237. http://dx.doi.org/10.3847/1538-3881/ad3425.

[255] Guo Z, Lucas PW, Kurtev R, Borissova J, Contreras Peña C, Yurchenko SN, Smith LC, Minniti D, Saito RK, Bayo A, Catelan M, Alonso-García J, Caratti o Garatti A, Morris C, Froebrich D, Tennyson J, Maucó K, Aguayo A, Miller N, Muthu HDS. Spectroscopic confirmation of high-amplitude eruptive YSOs and dipping giants from the VVV survey. Mon Not R Astron Soc 2024;528:1769–88. http://dx.doi.org/10.1093/mnras/stad3700.

[256] Danilovich T, Gottlieb CA, Decin L, Richards AMS, Lee KLK, Kaminski T, Patel NA, Young KH, Menten KM. Rotational spectra of vibrationally excited AlO and TiO in oxygen-rich stars. Astron J 2020;904:110. http://dx.doi.org/10.3847/1538-4357/abc079.

[257] Coenegrachts A, Danilovich T, De Ceuster F, Decin L. The unusual 3D distribution of NaCl around the asymptotic giant branch star IK tau. Astron Astrophys 678. http://dx.doi.org/10.1051/0004-6361/202346116.

[258] Sandin C, Mattsson L, Chubb KL, Ergon M, Weilbacher PM. Three-component modelling of O-rich AGB star winds I. Effects of drift using forsterite. Astron Astrophys 677. http://dx.doi.org/10.1051/0004-6361/202345841.

[259] Pastorelli G, Marigo P, Girardi L, Aringer B, Chen Y, Rubele S, Trabucchi M, Bladh S, Boyer ML, Bressan A, Dalcanton JJ, Groenewegen MAT, Lebzelter T, Mowlavi N, Chubb KL, Cioni M-RL, de Grijs R, Ivanov VD, Nanni A, van Loon JT, Zaggia S. Constraining the thermally pulsing asymptotic giant branch phase with resolved stellar populations in the large magellanic cloud. Mon Not R Astron Soc 2020;498:3283–301. http://dx.doi.org/10.1093/mnras/staa2565.

[260] Eriksson K, Hofner S, Aringer B. Synthetic photometry for carbon-rich giants V. Effects of grain-size-dependent dust opacities. Astron Astrophys 673. http://dx.doi.org/10.1051/0004-6361/202245206.

[261] Karambelkar V, Kasliwal MM, Tisserand P, Clayton GC, Crawford CL, Anand SG, Geballe TR, Montiel E. R coronae borealis and dustless hydrogen-deficient carbon stars likely have different oxygen isotope ratios. Astron Astrophys 667. http://dx.doi.org/10.1051/0004-6361/202142918.

[262] García-Hernández DA, Kameswara Rao N, Lambert DL, Eriksson K, Reddy ABS, Masseron T. The carbon star DY persei may be a cool R coronae borealis variable. Astrophys J 2023;948:15. http://dx.doi.org/10.3847/1538-4357/acc574.

[263] Mobeen MZ, Kaminski T, Matter A, Wittkowski M, Paladini C. The mid-infrared environment of the stellar merger remnant V838 monocerotis. Astron Astrophys 2021;655:A100. http://dx.doi.org/10.1051/0004-6361/202142297.

[264] Steinmetz T, Kaminski T, Schmidt M, Kiljan A. A bipolar structure and shocks surrounding the stellar-merger remnant V1309 scorpii. Astron Astrophys 682. http://dx.doi.org/10.1051/0004-6361/202347818.

[265] Liljegren S, Jerkstrand A, Barklem PS, Nyman G, Brady R, Yurchenko SN. The molecular chemistry of type ibc supernovae and diagnostic potential with the james webb space telescope. Astron Astrophys 2023;674:A184. http://dx.doi.org/10.1051/0004-6361/202243491.

[266] Nickerson S, Rangwala N, Colgan SWJ, DeWitt C, Huang X, Acharyya K, Drozdovskaya M, Fortenberry RC, Herbst E, Lee TJ. The first mid-infrared detection of HNC in the interstellar medium: Probing the extreme environment toward the orion hot core. Astrophys J 2021;907:51. http://dx.doi.org/10.3847/1538-4357/abca36.

[267] Nickerson S, Rangwala N, Colgan SWJ, DeWitt C, Monzon JSS, Huang X, Acharyya K, Drozdovskaya MNN, Fortenberry RCC, Herbst E, Lee TJ. The mid-infrared molecular inventory toward orion IRc2. Astrophys J 2023;945:26. http://dx.doi.org/10.3847/1538-4357/aca6e8.

[268] Bowen KP, Hillenbrand P-M, Lievin J, Savin DW, Urbain X. Dynamics of the isotope exchange reaction of D with H_3^+, H_2D^+, and D_2H^+. J Chem Phys 2021;154:084307. http://dx.doi.org/10.1063/5.0038434.

[269] LoCurto AC, Welch MA, Sippel TR, Michael JB. High-speed visible supercontinuum laser absorption spectroscopy of metal oxides. Opt Lett 2021;46:3288–91. http://dx.doi.org/10.1364/OL.428456.

[270] Daniel KA, Murzyn CM, Allen DJ, Lynch KP, Downing CR, Wagner JL. Coaxial laser absorption and optical emission spectroscopy of high-pressure aluminum monoxide. Opt Lett 2022;47:2350–3. http://dx.doi.org/10.1364/OL.456342.

[271] Murzyn CM, Allen DJ, Baca AN, Ching ML, Marinis RT. Tunable infrared laser absorption spectroscopy of aluminum monoxide $A\ ^2\Pi_i$ - $X\ ^2\Sigma^+$. J Quant Spectrosc Radiat Transfer 2022;279:108029. http://dx.doi.org/10.1016/j.jqsrt.2021.108029.

[272] Gilvey JJ, Ruesch MD, Daniel KA, Downing CR, Lynch KP, Wagner JL, Goldenstein CS. Quantum-cascade-laser-absorption-spectroscopy diagnostic for temperature, pressure, and NO $X^2\Pi_{1/2}$ at 500 kHz in shock-heated air at elevated pressures. Appl Opt 2023;62:A12–24. http://dx.doi.org/10.1364/AO.464623.

[273] Abraham A, Lynch P, Glumac N. On using ab initio calibration to fit temperature from AlO B-X emission. Proc Combust Inst 2023;39:1249–57. http://dx.doi.org/10.1016/j.proci.2022.09.050.

[274] Riedel J, Hufgard J, You Y. LIBS at high duty-cycles: effect of repetition rate and temporal width on the excitation laser pulses. Front Phys 2023;11:1241533. http://dx.doi.org/10.3389/fphy.2023.1241533.

[275] Bobrovnikov SM, Gorlov EV, Zharkov VI. Efficiency of laser excitation of PO photofragments of organophosphates. Atmos Ocean Opt 2022;35:329–40. http://dx.doi.org/10.1134/S1024856022040017.

[276] Bobrovnikov SM, Gorlov EV, Zharkov VI. Laser-induced fluorescence of PO-photofragments of dimethyl methylphosphonate. Appl Opt 2022;61:6322–9. http://dx.doi.org/10.1364/AO.456005.

[277] Merten J, Nicholas E, Ethridge S, Bariola H, Chestnut S, Anders A, Brees J, Foster M. Following laser-induced plasma stoichiometry with atomic absorption spectroscopy. Spectrochim Acta A 2023;200:106600. http://dx.doi.org/10.1016/j.sab.2022.106600.

[278] Pawelec E, Borodin D, Brezinsek S, Dittmar T, Douai D, Mazur D, Meigs A, Shaw A, Thomas B, Contributors J, Exploitation ET. Internal energy distributions of BeH, BeD, and BeT molecules created during chemically assisted physical sputtering in JET tokamak plasma. Phys Plasmas 2024;31:042516. http://dx.doi.org/10.1063/5.0199084.

[279] Yekta M, Zanjanchi MA, Roohi H. Adsorption of HCN, HNC and CH_3CN toxic gases on the M-doped (M = Cr, Fe, Ni and Zn) GaNNS: A DFT-D study. Colloids Surf A 2024;684:133120. http://dx.doi.org/10.1016/j.colsurfa.2023.133120.

[280] Ruesch MD, McDonald AJ, Mathews GC, Son SF, Goldenstein CS. Characterization of the influence of aluminum particle size on the temperature of composite-propellant flames using CO absorption and AlO emission spectroscopy. Proc Combust Inst 2021;38:4365–72. http://dx.doi.org/10.1016/j.proci.2020.06.163.

[281] Fateev A. From optimising waste incineration to internal combustion engines and defence applications. Johnson Matthey Technol Rev 2023;67:25–35. http://dx.doi.org/10.1595/205651323x16643556587827.

[282] Qin Z, Bai T, Liu L. Rovibrationally resolved photodissociation of AlH via excited electronic states. Astrophys J 2021;917:87. http://dx.doi.org/10.3847/1538-4357/ac06d1.

[283] da Silva RS, Ballester MY, Ventura LR, Fellows CE. Theoretical study of the spin–orbit coupling in the $X^2\Pi$ state of NO. Chem Phys Lett 2021;780:138896. http://dx.doi.org/10.1016/j.cplett.2021.138896.

[284] Zammit MC, Leiding JA, Colgan J, Even W, Fontes CJ, Timmermans E. A comprehensive study of the radiative properties of NO – a first step toward a complete air opacity. J Phys B 55. http://dx.doi.org/10.1088/1361-6455/ac8213.

[285] Charmet AP, Stoppa P, De Lorenzi A, Melosso M, Achilli A, Dore L, Puzzarini C, Cane E, Tamassia F. Computational, rotational and ro-vibrational experimental investigation of monodeuterated chloromethane. J Quant Spectrosc Radiat Transfer 2023;305:108624. http://dx.doi.org/10.1016/j.jqsrt.2023.108624.

[286] Bai T, Qin Z, Liu L. Ultraviolet spectroscopy of AlO from first principle. J Quant Spectrosc Radiat Transfer 2023;302:108587. http://dx.doi.org/10.1016/j.jqsrt.2023.108587.

[287] Velasco AM, Lavín C. Absorption line oscillator strengths for the $C^2\Pi(0)$-$A^2\Sigma^+(0)$ band of nitric oxide. Astrophys J 2023;954:144. http://dx.doi.org/10.3847/1538-4357/acebcb.

[288] Ulenikov ON, Gromova OV, Bekhtereva ES, Raspopova NI, Sklyarova EA, Sydow C, Berezkin K, Maul C, Bauerecker S. Line strengths, widths and shifts analysis of the $2\nu_2$, $\nu_2 + \nu_4$ and $2\nu_4$ bands in $^{28}SiH_4$, $^{29}SiH_4$ and $^{30}SiH_4$. J Quant Spectrosc Radiat Transfer 270. http://dx.doi.org/10.1016/j.jqsrt.2021.107683.

[289] Shapko D, Dohnal P, Roucka S, Uvarova L, Kassayova M, Plasil R, Glosik J. Cavity ring-down spectroscopy study of neon assisted recombination of H_3^+ ions with electrons. J Mol Spectrosc 2021;378:111450. http://dx.doi.org/10.1016/j.jms.2021.111450.

[290] Znotins A, Grussie F, Wolf A, Urbain X, Kreckel H. An approach for multi-color action spectroscopy of highly excited states of H_3^+. J Mol Spectrosc 2021;378:111476. http://dx.doi.org/10.1016/j.jms.2021.111476.

[291] Foltynowicz A, Rutkowski L, Silander I, Johansson AC, de Oliveira VS, Axner O, Sobon G, Martynkien T, Mergo P, Lehmann KK. Measurement and assignment of double-resonance transitions to the 8900–9100-cm^{-1} levels of methane. Phys Rev A 103. http://dx.doi.org/10.1103/PhysRevA.103.022810.

[292] Lavín C, Velasco AM. Transition energies and line oscillator strengths of the $C^2\Pi(0)$-$X^2\Pi(0–6)$ absorption bands of nitric oxide. A theoretical study. Astrophys J 2022;941:29. http://dx.doi.org/10.3847/1538-4357/ac9e56.

[293] Perrin A, Manceron L, Armante R, Kwabia-Tchana F, Roy P, Toon G. First investigation of the ν_1, ν_1-ν_9, $\nu_1+\nu_9$, and $\nu_1+\nu_7$ absorption bands of nitric acid ($H^{14}N^{16}O_3$) at 3551.766 cm^{-1}, 3092.708 cm^{-1}, 4006.974 cm^{-1}, and 4127.782 cm^{-1}, respectively. J Mol Spectrosc 2023;392:111741. http://dx.doi.org/10.1016/j.jms.2023.111741.

[294] Perrin A, Manceron L, Armante R, Kwabia-Tchana F, Roy P, Toon G. Part 2: Validation for line lists generated for nitric acid ($H^{14}N^{16}O_3$) for the ν_1 band and its first two associated hot bands ($\nu_1+\nu_9$-ν_9, $\nu_1+\nu_7$-ν_7) in the 2.8 μm region, the ν_1-ν_9, $\nu_1+\nu_9$ and $\nu_1+\nu_7$ bands at 3.2 μm, 2.5 μm and 2.4 μm, respectively. J Mol Spectrosc 2023;392:111740. http://dx.doi.org/10.1016/j.jms.2023.111740.

[295] Vasilenko IA, Naumenko OV, Horneman V-M. Expert list of absorption lines of the $^{32}S^{16}O_2$ molecule in the 0–4200 cm^{-1} spectral region. Atmos Ocean Opt 2023;36:199–206. http://dx.doi.org/10.1134/S102485602303020X.

[296] Owens A, He T, Hanicinec M, Hill C, Mohr S, Tennyson J. LiDB: Database of molecular vibronic state radiative lifetimes for plasma processes. Plasma Sources Sci Technol 2023;32:085015. http://dx.doi.org/10.1088/1361-6595/aceeb0.

[297] Wang R, Balciunaite U, Chen J, Yuan C, Owens A, Tennyson J. NASA polynomial representation of molecular specific heats. J Quant Spectrosc Radiat Transfer 2023;306:108617. http://dx.doi.org/10.1016/j.jqsrt.2023.108617.

[298] Zhang J, Hill C, Tennyson J, Yurchenko SN. ExoMolHR: A relational database of empirical high-resolution molecular spectra. Astrophys J Suppl Ser 2024. (in preparation).

[299] Chubb KL, Rocchetto M, Yurchenko SN, Min M, Waldmann I, Barstow JK, Molliere P, Al-Refaie AF, Phillips M, Tennyson J. The ExoMolOP database: Cross-sections and K-tables for molecules of interest in high-temperature exoplanet atmospheres. Astron Astrophys 2021;646:A21. http://dx.doi.org/10.1051/0004-6361/202038350.

[300] Freedman RS, Lustig-Yaeger J, Fortney JJ, Lupu RE, Marley MS, Lodders K. Gaseous mean opacities for giant planet and ultracool dwarf atmospheres over a range of metallicities and temperatures. Astrophys J Suppl Ser 2014;214:25. http://dx.doi.org/10.1088/0067-0049/214/2/25.

[301] Amundsen DS, Mayne NJ, Baraffe I, Manners J, Tremblin P, Drummond B, Smith C, Acreman DM, Homeier D. The uk met office global circulation model with a sophisticated radiation scheme applied to the hot jupiter hd 209458b. Astron Astrophys 2016;595:A36. http://dx.doi.org/10.1051/0004-6361/201629183.

[302] Min M. Random sampling technique for ultra-fast computations of molecular opacities for exoplanet atmospheres. Astron Astrophys 2017;607:A9. http://dx.doi.org/10.1051/0004-6361/201731612.

[303] Goyal JM, Mayne N, Sing DK, Drummond B, Tremblin P, Amundsen DS, Evans T, Carter AL, Spake J, Baraffe I, Nikolov N, Manners J, Chabrier G, Hebrard E. A library of atmo forward model transmission spectra for hot jupiter exoplanets. Mon Not R Astron Soc 2018;474:5158–85. http://dx.doi.org/10.1093/mnras/stx3015.

[304] Villanueva GL, Smith MD, Protopapa S, Faggi S, Mandell AM. Planetary spectrum generator: An accurate online radiative transfer suite for atmospheres, comets, small bodies and exoplanets. J Quant Spectrosc Radiat Transfer 2018;217:86–104. http://dx.doi.org/10.1016/j.jqsrt.2018.05.023.

[305] Gandhi S, Brogi M, Yurchenko SN, Tennyson J, Coles PA, Webb RK, Birkby JL, Guilluy G, Madhusudhan N. Molecular cross-sections for high resolution spectroscopy of super earths, warm Neptunes and hot jupiters. Mon Not R Astron Soc 2020;495:224–37. http://dx.doi.org/10.1093/mnras/staa981.

[306] Grimm SL, Malik M, Kitzmann D, Guzmán-Mesa A, Hoeijmakers HJ, Fisher C, ao M. Mendonça J, Yurchenko SN, Tennyson J, Kurucz RL, Heng K. HELIOS-K 2.0 and an open-source opacity database for exoplanetary atmospheres. Astrophys J Suppl Ser 2021;253:30. http://dx.doi.org/10.3847/1538-4365/abd773.

[307] Hirose S, Hauschildt P, Minoshima T, Tomida K, Sano T. OPTAB: Public code for generating gas opacity tables for radiation hydrodynamics simulations. Astron Astrophys 2022;659:A87. http://dx.doi.org/10.1051/0004-6361/202141076.

[308] Marigo P, Aringer B, Girardi L, Bressan A. Updated low-temperature gas opacities with AESOPUS 2.0. Astrophys J 2022;940:129. http://dx.doi.org/10.3847/1538-4357/ac9b40.

[309] Iyer AR, Line MR, Muirhead PS, Fortney JJ, Gharib-Nezhad E. The SPHINX M-dwarf spectral grid. I. Benchmarking new model atmospheres to derive fundamental M-dwarf properties. Astrophys J 2023;944:41. http://dx.doi.org/10.3847/1538-4357/acabc2.

[310] Chubb KL, Robert S, Sousa-Silva C, Yurchenko SN, Allard NF, Boudon V, Buldyreva J, Bultel B, Coustenis A, Foltynowicz A, Gordon IE, Hargreaves RJ, Helling C, Hill C, Hrodmarsson HR, Karman T, Lecoq-Molinos H, Migliorini A, Rey M, Richard C, Sadiek I, Schmidt F, Sokolov A, Stefani S, Tennyson J, Venot O, Wright SOM, Arenales-Lope R, Barstow JK, Bocchieri A, Carrasco N, Dubey D, Egorov O, Muñoz AG, Ehsan, Gharib-Nezhad, Gkouvelis L, Grübel F, Irwin PGJ, Knížek A, Lewis DA, Lodge MG, Ma S, Martins Z, Molaverdikhani K, Morello G, Nikitin A, Panek E, Rengel M, Rinaldi G, Skinner JW, Tinetti G, van Kempen TA, Yang J, Zingales T. Data availability and requirements relevant for the ariel space mission and other exoplanet atmosphere applications. RAS Tech Instrum arXiv:2404.02188.

[311] Karlovets EV, Gordon IE, Rothman LS, Hashemi R, Hargreaves RJ, Toon G, Campargue A, Perevalov VI, Čermak P, Birk M, Wagner G, Hodges JT, Tennyson J, Yurchenko SN. The update of the line positions and intensities in the line list of carbon dioxide for the HITRAN2020 spectroscopic database. J Quant Spectrosc Radiat Transfer 2021;276:107896. http://dx.doi.org/10.1016/j.jqsrt.2021.107896.

[312] Rothman LS. History of the HITRAN database. Nat Rev Phys 2021;3:302–4. http://dx.doi.org/10.1038/s42254-021-00309-2.

[313] Rothman LS, Gordon IE, Barber RJ, Dothe H, Gamache RR, Goldman A, Perevalov VI, Tashkun SA, Tennyson J. HITEMP, the high-temperature molecular spectroscopic database. J Quant Spectrosc Radiat Transfer 2010;111:2139–50. http://dx.doi.org/10.1016/j.jqsrt.2010.05.001.

[314] Hargreaves RJ, Gordon IE, Rothman LS, Tashkun SA, Perevalov VI, Lukashevskaya AA, Yurchenko SN, Tennyson J, Müller HSP. Spectroscopic line parameters of NO, NO_2, and N_2O for the HITEMP database. J Quant Spectrosc Radiat Transfer 2019;232:35–53. http://dx.doi.org/10.1016/j.jqsrt.2019.04.040.

[315] Rey M, Nikitin AV, Babikov YL, Tyuterev VG. TheoReTS – an information system for theoretical spectra based on variational predictions from molecular potential energy and dipole moment surfaces. J Mol Spectrosc 2016;327:138–58. http://dx.doi.org/10.1016/j.jms.2016.04.006.

[316] Huang X, Freedman RS, Tashkun S, Schwenke DW, Lee TJ. AI-3000K infrared line list for hot CO_2. J Mol Spectrosc 2023;392:111748. http://dx.doi.org/10.1016/j.jms.2023.111748.

[317] Underwood DS, Tennyson J, Yurchenko SN, Huang X, Schwenke DW, Lee TJ, Clausen S, Fateev A. ExoMol line lists XIV: A line list for hot SO_2. Mon Not R Astron Soc 2016;459:3890–9. http://dx.doi.org/10.1093/mnras/stw849.

[318] Bernath PF. MoLLIST: Molecular line lists, intensities and spectra. J Quant Spectrosc Radiat Transfer 2020;240:106687. http://dx.doi.org/10.1016/j.jqsrt.2019.106687.

[319] Ryabchikova T, Piskunov N, Kurucz RL, Stempels HC, Heiter U, Pakhomov Y, Barklem PS. A major upgrade of the VALD database. Phys Scr 2015;90:054005. http://dx.doi.org/10.1088/0031-8949/90/5/054005.

[320] Kurucz RL. Including all the lines. Can J Phys 2011;89:417–28. http://dx.doi.org/10.1139/p10-104.

[321] Hrodmarsson HR, van Dishoeck EF. Photodissociation and photoionization of molecules of astronomical interest updates to the leiden photodissociation and photoionization cross-section database. Astron Astrophys 2023;675:A25. http://dx.doi.org/10.1051/0004-6361/202346645.

[322] Tennyson J, Yurchenko SN. The ExoMol atlas of molecular opacities. Atoms 2018;6:26. http://dx.doi.org/10.3390/atoms6020026.

[323] Barber RJ, Strange JK, Hill C, Polyansky OL, Mellau GC, Yurchenko SN, Tennyson J. ExoMol line lists – III. An improved hot rotation-vibration line list for HCN and HNC. Mon Not R Astron Soc 2014;437:1828–35. http://dx.doi.org/10.1093/mnras/stt2011.

[324] Barton EJ, Chiu C, Golpayegani S, Yurchenko SN, Tennyson J, Frohman DJ, Bernath PF. ExoMol molecular linelists – V. The ro-vibrational spectra of NaCl and KCl. Mon Not R Astron Soc 2014;442:1821–9. http://dx.doi.org/10.1093/mnras/stu944.

[325] Sousa-Silva C, Al-Refaie AF, Tennyson J, Yurchenko SN. ExoMol line lists - VII. The rotation-vibration spectrum of phosphine up to 1500 K. Mon Not R Astron Soc 2015;446:2337–47. http://dx.doi.org/10.1093/mnras/stu2246.

[326] Al-Refaie AF, Yurchenko SN, Yachmenev A, Tennyson J. ExoMol line lists - VIII: A variationally computed line list for hot formaldehyde. Mon Not R Astron Soc 2015;448:1704–14. http://dx.doi.org/10.1093/mnras/stv091.

[327] Patrascu AT, Tennyson J, Yurchenko SN. ExoMol molecular linelists - IX: The spectrum of AlO. Mon Not R Astron Soc 2015;449:3613–9. http://dx.doi.org/10.1093/mnras/stv507.

[328] Rivlin T, Lodi L, Yurchenko SN, Tennyson J, Le Roy RJ. ExoMol line lists X: The spectrum of sodium hydride. Mon Not R Astron Soc 2015;451:5153–7. http://dx.doi.org/10.1093/mnras/stv979.

[329] Pavlyuchko AI, Yurchenko SN, Tennyson J. ExoMol line lists XI: A hot line list for nitric acid. Mon Not R Astron Soc 2015;452:1702–6. http://dx.doi.org/10.1093/mnras/stv1376.

[330] Paulose G, Barton EJ, Yurchenko SN, Tennyson J. ExoMol molecular linelists – XII. Line lists for eight isotopologues of CS. Mon Not R Astron Soc 2015;454:1931–9. http://dx.doi.org/10.1093/mnras/stv1543.

[331] Yurchenko SN, Blissett A, Asari U, Vasilios M, Hill C, Tennyson J. ExoMol molecular linelists – XIII. The spectrum of CaO. Mon Not R Astron Soc 2016;456:4524–32. http://dx.doi.org/10.1093/mnras/stv2858.

[332] Al-Refaie AF, Polyansky OL, Ovsyannikov RI, Tennyson J, Yurchenko SN. ExoMol line lists XV: A hot line-list for hydrogen peroxide. Mon Not R Astron Soc 2016;461:1012–22. http://dx.doi.org/10.1093/mnras/stw1295.

[333] Azzam AAA, Yurchenko SN, Tennyson J, Naumenko OV. ExoMol line lists XVI: A hot line list for H_2S. Mon Not R Astron Soc 2016;460:4063–74. http://dx.doi.org/10.1093/mnras/stw1133.

[334] Underwood DS, Tennyson J, Yurchenko SN, Clausen S, Fateev A. ExoMol line lists XVII: A line list for hot SO_3. Mon Not R Astron Soc 2016;462:4300–13. http://dx.doi.org/10.1093/mnras/stw1828.

[335] Polyansky OL, Kyuberis AA, Lodi L, Tennyson J, Ovsyannikov RI, Zobov N. ExoMol molecular line lists XIX: high accuracy computed line lists for $H_2^{17}O$ and $H_2^{18}O$. Mon Not R Astron Soc 2017;466:1363–71. http://dx.doi.org/10.1093/mnras/stw3125.

[336] Mizus II, Alijah A, Zobov NF, Kyuberis AA, Yurchenko SN, Tennyson J, Polyansky OL. ExoMol molecular line lists XX: a comprehensive line list for H_3^+. Mon Not R Astron Soc 2017;468:1717–25. http://dx.doi.org/10.1093/mnras/stx502.

[337] Owens A, Yurchenko SN, Yachmenev A, Thiel W, Tennyson J. ExoMol molecular line lists XXII. The rotation-vibration spectrum of silane up to 1200 K. Mon Not R Astron Soc 2017;471:5025–32. http://dx.doi.org/10.1093/mnras/stx1952.

[338] Prajapat L, Jagoda P, Lodi L, Gorman MN, Yurchenko SN, Tennyson J. ExoMol molecular line lists XXIII. Spectra of PO and PS. Mon Not R Astron Soc 2017;472:3648–58. http://dx.doi.org/10.1093/mnras/stx2229.

[339] Yurchenko SN, Sinden F, Lodi L, Hill C, Gorman MN, Tennyson J. ExoMol molecular linelists – XXIV: A new hot line list for silicon monohydride, SiH. Mon Not R Astron Soc 2018;473:5324–33. http://dx.doi.org/10.1093/mnras/stx2738.

[340] Upadhyay A, Conway EK, Tennyson J, Yurchenko SN. ExoMol molecular linelists – XXV: A hot line list for silicon sulphide, SiS. Mon Not R Astron Soc 2018;477:1520–7. http://dx.doi.org/10.1093/mnras/sty998.

[341] Yurchenko SN, Bond W, Gorman MN, Lodi L, McKemmish LK, Nunn W, Shah R, Tennyson J. ExoMol molecular linelists – XXVI: spectra of SH and NS. Mon Not R Astron Soc 2018;478:270–82. http://dx.doi.org/10.1093/mnras/sty939.

[342] Mant BP, Yachmenev A, Tennyson J, Yurchenko SN. ExoMol molecular line lists - XXVII: spectra of C_2H_4. Mon Not R Astron Soc 2018;478:3220–32. http://dx.doi.org/10.1093/mnras/sty1239.

[343] Owens A, Yachmenev A, Tennyson J, Thiel W, Yurchenko SN. ExoMol molecular line lists XXIX: The rotation-vibration spectrum of methyl chloride up to 1200 K. Mon Not R Astron Soc 2018;479:3002–10. http://dx.doi.org/10.1093/mnras/sty1542.

[344] Polyansky OL, Kyuberis AA, Zobov NF, Tennyson J, Yurchenko SN, Lodi L. ExoMol molecular line lists XXX: a complete high-accuracy line list for water. Mon Not R Astron Soc 2018;480:2597–608. http://dx.doi.org/10.1093/mnras/sty1877.

[345] Yurchenko SN, Szabo I, Pyatenko E, Tennyson J. ExoMol molecular line lists XXXI: The spectrum of C_2. Mon Not R Astron Soc 2018;480:3397–411. http://dx.doi.org/10.1093/mnras/sty2050.

[346] Li H-Y, Tennyson J, Yurchenko SN. ExoMol molecular line lists XXXII: the rovibronic spectrum of MgO. Mon Not R Astron Soc 2019;486:2351–65. http://dx.doi.org/10.1093/mnras/stz912.

[347] McKemmish LK, Masseron T, Hoeijmakers J, Pérez-Mesa VV, Grimm SL, Yurchenko SN, Tennyson J. ExoMol molecular line lists – XXXIII. The spectrum of titanium oxide. Mon Not R Astron Soc 2019;488:2836–54. http://dx.doi.org/10.1093/mnras/stz1818.

[348] Langleben J, Yurchenko SN, Tennyson J. ExoMol line list XXXIV: A rovibrational line list for phosphinidene (PH) in its $X\,^3\Sigma^-$ and $a\,^1\Delta$ electronic states. Mon Not R Astron Soc 2019;488:2332. http://dx.doi.org/10.1093/mnras/stz1856-2342.

[349] Coles PA, Yurchenko SN, Tennyson J. ExoMol molecular line lists XXXV: a rotation-vibration line list for hot ammonia. Mon Not R Astron Soc 2019;490:4638–47. http://dx.doi.org/10.1093/mnras/stz2778.

[350] Gorman M, Yurchenko SN, Tennyson J. ExoMol molecular linelists – XXXVI. $X\,^2\Pi - X\,^2\Pi$ and $A\,^2\Sigma^+ - X\,^2\Pi$ transitions of SH. Mon Not R Astron Soc 2019;490:1652–65. http://dx.doi.org/10.1093/mnras/stz2517/5565070.

[351] Chubb KL, Tennyson J, Yurchenko SN. ExoMol molecular linelists – XXXVII: spectra of acetylene. Mon Not R Astron Soc 2020;493:1531–45. http://dx.doi.org/10.1093/mnras/staa229.

[352] Owens A, Conway EK, Tennyson J, Yurchenko SN. ExoMol molecular linelists – XXXVIII: High-temperature molecular line list of silicon dioxide (SiO_2). Mon Not R Astron Soc 2020;495:1927–33. http://dx.doi.org/10.1093/mnras/staa1287.

[353] Yurchenko SN, Mellor TM, Freedman RS, Tennyson J. ExoMol molecular line lists XXXIX: Ro-vibrational molecular line list for CO_2. Mon Not R Astron Soc 2020;496:5282–91. http://dx.doi.org/10.1093/mnras/staa1874.

[354] Yurchenko SN, Tennyson J, Miller S, Melnikov VV, O'Donoghue J, Moore L. ExoMol molecular line lists XL: Ro-vibrational molecular line list for the hydronium ion (H_3O^+). Mon Not R Astron Soc 2020;497:2340–51. http://dx.doi.org/10.1093/mnras/staa2034.

[355] Owens A, Tennyson J, Yurchenko SN. ExoMol line lists – XLI. High-temperature molecular line lists for the alkali metal hydroxides KOH and NaOH. Mon Not R Astron Soc 2021;502:1128–35. http://dx.doi.org/10.1093/mnras/staa4041.

[356] Qu Q, Yurchenko SN, Tennyson J. ExoMol molecular line lists – XLII: Rovibronic molecular line list for the low-lying states of NO. Mon Not R Astron Soc 2021;504:5768–77. http://dx.doi.org/10.1093/mnras/stab1154.

[357] Mitev GB, Taylor S, Tennyson J, Yurchenko SN, Buchachenko AA, Stolyarov AV. ExoMol molecular line lists – XLIII: Rovibronic transitions corresponding to the close-lying X $^2\Pi$ and A $^2\Sigma^+$ states of NaO. Mon Not R Astron Soc 2022;511:2349–55. http://dx.doi.org/10.1093/mnras/stab3357.

[358] Yurchenko SN, Tennyson J, Syme A-M, Adam AY, Clark VHJ, Cooper B, Dobney CP, Donnelly STE, Gorman MN, Lynas-Gray AE, Meltzer T, Owens A, Qu Q, Semenov M, Somogyi W, Upadhyay A, Wright S, Zapata Trujillo JC. ExoMol line lists – XLIV. IR and UV line list for silicon monoxide ($^{28}Si^{16}O$). Mon Not R Astron Soc 2022;510:903–19. http://dx.doi.org/10.1093/mnras/stab3267.

[359] Owens A, Dooley S, McLaughlin L, Tan B, Zhang G, Yurchenko SN, Tennyson J. ExoMol line lists – XLV. Rovibronic molecular line lists of calcium monohydride (CaH) and magnesium monohydride (MgH). Mon Not R Astron Soc 2022;511:5448–61. http://dx.doi.org/10.1093/mnras/stac371.

[360] Mellor T, Owens A, Yurchenko SN, Tennyson J. ExoMol line lists – LI. Rvibronic molecular line list for thioformaldehyde (H_2CS). Mon Not R Astron Soc 2022;520:1997–2008. http://dx.doi.org/10.1093/mnras/stad111.

[361] Yurchenko SN, Nogué E, Azzam AAA, Tennyson J. ExoMol line lists – IL. Rovibronic spectrum of aluminium monochloride (AlCl). Mon Not R Astron Soc 2023;520:5183–91. http://dx.doi.org/10.1093/mnras/stac3757.

[362] Bowesman CA, Mizus II, Zobov NF, Polyansky OL, Sarka J, Poirier B, Pezzella M, Yurchenko SN, Tennyson J. ExoMol line lists - L: High-resolution line lists of H_3^+, H_2D^+, D_2H^+ and D_3^+. Mon Not R Astron Soc 2023;519:6333–48. http://dx.doi.org/10.1093/mnras/stad050.

[363] Owens A, Wright SOM, Pavlenko Y, Mitrushchenkov A, Koput J, Yurchenko SN, Tennyson J. ExoMol line lists - LI. Molecular line list for lithium hydroxide (LiOH). Mon Not R Astron Soc 2024;527:731–8. http://dx.doi.org/10.1093/mnras/stad3226.

[364] Pearce O, Yurchenko SN, Tennyson J. ExoMol line lists – LII. Line lists for the methylidyne cation (CH^+). Mon Not R Astron Soc 2024;527:10726–36. http://dx.doi.org/10.1093/mnras/stad3909.

[365] Yurchenko SN, Brady RP, Tennyson J, Smirnov AN, Vasilyev OA, Solomonik VG. ExoMol line lists LIII. Empirical rovibronic spectra yttrium oxide (YO). Mon Not R Astron Soc 2024;527:4899–912. http://dx.doi.org/10.1093/mnras/stad3225.

[366] Bowesman CA, Qu Q, McKemmish LK, Yurchenko SN, Tennyson J. ExoMol line lists – LV: Hyperfine-resolved molecular line list for vanadium monoxide ($^{51}V^{16}O$). Mon Not R Astron Soc 2024;529:1321–32. http://dx.doi.org/10.1093/mnras/stae542.

[367] Brady RP, Yurchenko SN, Tennyson J, Kim G-S. ExoMol line lists – LVI. The SO line list, MARVEL analysis of experimental transition data and refinement of the spectroscopic model. Mon Not R Astron Soc 2024;527:6675–90. http://dx.doi.org/10.1093/mnras/stad3508.

[368] Kefala K, Boudon V, Yurchenko SN, Tennyson J. Empirical rovibrational energy levels for methane. J Quant Spectrosc Radiat Transfer 2024;316:108897. http://dx.doi.org/10.1016/j.jqsrt.2024.108897.

[369] Owens A, Yurchenko SN, Tennyson J. ExoMol line lists - LVIII. High-temperature molecular line list of carbonyl sulphide (OCS). Mon Not R Astron Soc 2024;530:4004–15. http://dx.doi.org/10.1093/mnras/stae1110.

[370] Yurchenko SN, Mellor T, Tennyson J. ExoMol line lists – LIX. High-temperature line list for N_2O. Mon Not R Astron Soc.

[371] Yurchenko SN, Bowesman CA, Brady RP, Guest ER, Kefala K, Mitev GB, Owens A, Perri AN, Pezzella M, Smola O, Solokov A, Zhang J, Tennyson J. ExoMol line lists – LX: Molecular line list for the ammonia isotopologue $^{15}NH_3$. Mon Not R Astron Soc.

[372] Mitev GB, Bowesman CA, Yurchenko SN, Tennyson J. ExoMol line lists – LXI: A trihybrid linelist for rovibronic transitions of the hydroxyl radical (OH). Mon Not R Astron Soc.

[373] Lynas-Gray AE, Polyansky OL, Tennyson J, Yurchenko SN, Zobov NF. ExoMol line lists – LXII: Ro-vibrational energy levels and line-strengths for the propadienediylidene (C_3) electronic ground-state. Mon Not R Astron Soc.

[374] Mizus II, Zobov NF, Pezzella M, Boyarkin OV, Koshelev MA, Makarov DS, Yurchenko SN, Tennyson J, Polyansky OL. ExoMol line lists – LXIII: Ro-vibrational energy levels and line-strengths HDO. Mon Not R Astron Soc.

[375] Semenov M, El-Kork N, Yurchenko SN, Tennyson J. ExoMol line lists – LXIV: Empirical rovibronic spectra of phosphorous mononitride (PN) covering the IR and UV regions. Mon Not R Astron Soc 2024. (submitted for publication).

[376] Harris GJ, Larner FC, Tennyson J, Kaminsky BM, Pavlenko YV, Jones HRA. A $H^{13}CN/HN^{13}C$ linelist, model atmospheres and synthetic spectra for carbon stars. Mon Not R Astron Soc 2008;390:143–8.

[377] Tennyson J. Accurate variational calculations for line lists to model the vibration rotation spectra of hot astrophysical atmospheres. WIREs Comput Mol Sci 2012;2:698–715. http://dx.doi.org/10.1002/wcms.94.

[378] Tennyson J, Bernath PF, Brown LR, Campargue A, Carleer MR, Császár AG, Gamache RR, Hodges JT, Jenouvrier A, Naumenko OV, Polyansky OL, Rothman LS, Toth RA, Vandaele AC, Zobov NF, Daumont L, Fazliev AZ, Furtenbacher T, Gordon IE, Mikhailenko SN, Shirin SV. IUPAC critical evaluation of the rotational-vibrational spectra of water vapor. Part I. Energy levels and transition wavenumbers for $H_2^{17}O$ and $H_2^{18}O$. J Quant Spectrosc Radiat Transfer 2009;110:573–96. http://dx.doi.org/10.1016/j.jqsrt.2009.02.014.

[379] Tennyson J, Bernath PF, Brown LR, Campargue A, Császár AG, Daumont L, Gamache RR, Hodges JT, Naumenko OV, Polyansky OL, Rothman LS, Vandaele AC, Zobov NF. A database of water transitions from experiment and theory (IUPAC technical report). Pure Appl Chem 2014;86:71–83. http://dx.doi.org/10.1515/pac-2014-5012.

[380] Bowesman CA, Akbari H, Hopkins S, Yurchenko SN, Tennyson J. Fine and hyperfine resolved empirical energy levels for VO. J Quant Spectrosc Radiat Transfer 2022;289:108295. http://dx.doi.org/10.1016/j.jqsrt.2022.108295.

[381] Császár AG, Furtenbacher T. Spectroscopic networks. J Mol Spectrosc 2011;266:99–103. http://dx.doi.org/10.1016/j.jms.2011.03.031.

[382] Flaud J-M, Camy-Peyret C, Maillard J-P. Higher ro-vibrational levels of H_2O deduced from high-resolution oxygen-hydrogen flame spectra between 2800–6200 cm^{-1}. Mol Phys 1976;32:499–521. http://dx.doi.org/10.1080/00268977600103251.

[383] Al-Derzi AR, Yurchenko SN, Tennyson J, Melosso M, Jiang N, Puzzarini C, Dore L, Furtenbacher T, Tobias R, Császár AG. An improved rovibrational linelist of formaldehyde, $H_2^{12}C^{16}O$. J Quant Spectrosc Radiat Transfer 2021;266:107563. http://dx.doi.org/10.1016/j.jqsrt.2021.107563.

[384] Germann M, Hjalten A, Tennyson J, Yurchenko SN, Gordon IE, Pett C, Silander I, Krzempek K, Hudzikowski A, Gluszek A, Sobon G, Foltynowicz A. Optical frequency comb Fourier transform spectroscopy of formaldehyde in the 1250 to 1390 cm^{-1} range: experimental line list and MARVEL analysis. J Quant Spectrosc Radiat Transfer 2024;312:108782. http://dx.doi.org/10.1016/j.jqsrt.2023.108782.

[385] Yurchenko SN, Al-Refaie AF, Tennyson J. ExoCross: A general program for generating spectra from molecular line lists. Astron Astrophys 2018;614:A131. http://dx.doi.org/10.1051/0004-6361/201732531.

[386] Zhang J, Tennyson J, Yurchenko SN. PyExoCross: a python program for generating spectra and cross-sections from molecular line lists. RAS Tech Instrum 2024;3:257–87. http://dx.doi.org/10.1093/rasti/rzae016.

[387] Lodi L, Tennyson J. Line lists for $H_2^{18}O$ and $H_2^{17}O$ based on empirically-adjusted line positions and ab initio intensities. J Quant Spectrosc Radiat Transfer 2012;113:850–8. http://dx.doi.org/10.1016/j.jqsrt.2012.02.023.

[388] Zak EJ, Tennyson J, Polyansky OL, Lodi L, Tashkun SA, Perevalov VI. A room temperature CO_2 line list with *ab initio* computed intensities. J Quant Spectrosc Radiat Transfer 2016;177:31–42. http://dx.doi.org/10.1016/j.jqsrt.2015.12.022.

[389] Bowesman CA, Shuai M, Yurchenko SN, Tennyson J. A high resolution line list for AlO. Mon Not R Astron Soc 2021;508:3181–93. http://dx.doi.org/10.1093/mnras/stab2525.

[390] Chubb KL, Min M, Kawashima Y, Helling C, Waldmann I. Aluminium oxide in the atmosphere of hot jupiter WASP-43b. Astron Astrophys 2020;639:A3. http://dx.doi.org/10.1051/0004-6361/201937267.

[391] Bol'shakov AA, Mao X, Russo RE. Spectral emission enhancement by an electric pulse for LIBS and LAMIS. J Anal Atom Spectrom 2017;32:657–70. http://dx.doi.org/10.1039/c6ja00436a.

[392] Hou H, Mao X, Zorba V, Russo RE. Laser ablation molecular isotopic spectrometry for molecules formation chemistry in femtosecond-laser ablated plasmas. Anal Chem 2017;89:7750–7. http://dx.doi.org/10.1021/acs.analchem.7b01750.

[393] Wong A, Yurchenko SN, Bernath P, Mueller HSP, McConkey S, Tennyson J. ExoMol line list XXI: Nitric oxide (NO). Mon Not R Astron Soc 2017;470:882–97. http://dx.doi.org/10.1093/mnras/stx1211.

[394] Tsurikov GN, Bisikalo DV. NO biomarker: Transmission and emission methods for its potential detection in exoplanet atmospheres with spektr-UF (WSO-UV). Astron Rep 2023;67:1123–38. http://dx.doi.org/10.1134/S1063772923110100.

[395] Pavlenko Y, Tennyson J, Yurchenko SN, Schmidt MR, Jones HRA, Lyubchik Y, Suárez Mascareño A. AlH lines in the blue spectrum of Proxima Centauri. Mon Not R Astron Soc 2022;516:5655–73. http://dx.doi.org/10.1093/mnras/stac2588.

[396] Yurchenko SN, Williams H, Leyland PC, Lodi L, Tennyson J. ExoMol line lists XXVIII: The rovibronic spectrum of AlH. Mon Not R Astron Soc 2018;479:1401–11. http://dx.doi.org/10.1093/mnras/sty1524.

[397] Falco A, Tremblin P, Charnoz S, Ridgway RJ, Lagage P-O. Hydrogenated atmospheres of lava planets: atmospheric structure and emission spectra. Astron Astrophys 2024;683:A194. http://dx.doi.org/10.1051/0004-6361/202347650.

[398] Pavlenko YV, Yurchenko SN, McKemmish LK, Tennyson J. Analysis of the TiO isotopologues in stellar optical spectra. Astron Astrophys 2020;42:A77. http://dx.doi.org/10.1051/0004-6361/202037863.

[399] Edwards B, Changeat Q, Baeyens R, Tsiaras A, Al-Refaie A, Taylor J, Yip KH, Bieger MF, Blain D, Gressier A, et al. ARES I: WASP-76 b, a tale of two HST spectra. Astrophys J 2020;160:8. http://dx.doi.org/10.3847/1538-3881/ab9225.

[400] Gorman MN, Yurchenko SN, Tennyson J. ExoMol molecular line lists XXXVI: $X^2\Pi$–$X^2\Pi$ and $A^2\Sigma$–$X^2\Pi$ transitions of SH. Mon Not R Astron Soc 2019;490:1652–65. http://dx.doi.org/10.1093/mnras/stz2517.

[401] Barton EJ, Yurchenko SN, Tennyson J. ExoMol molecular linelists – II. The ro-vibrational spectrum of SiO. Mon Not R Astron Soc 2013;434:1469–75. http://dx.doi.org/10.1093/mnras/stt1105.

[402] Ito Y, Ikoma M, Kawahara H, Nagahara H, Kawashima Y, Nakamoto T. Theoretical emission spectra of atmospheres of hot rocky super-earths. Astrophys J 2015;801:144. http://dx.doi.org/10.1088/0004-637X/801/2/144.

[403] Nguyen TG, Cowan NB, Pierrehumbert RT, Lupu RE, Moores JE. The impact of ultraviolet heating and cooling on the dynamics and observability of lava planet atmospheres. Mon Not R Astron Soc 2022;513:6125–33. http://dx.doi.org/10.1093/mnras/stac1331.

[404] Yadin B, Vaness T, Conti P, Hill C, Yurchenko SN, Tennyson J. ExoMol molecular linelists: I the rovibrational spectrum of BeH, MgH and CaH the $X^2\Sigma^+$ state. Mon Not R Astron Soc 2012;425:34–43.

[405] Darby-Lewis D, Tennyson J, Lawson KD, Yurchenko SN, Stamp MF, Shaw A, Brezinsek S. JET contributor, synthetic spectra of BeH, BeD and BeT for emission modelling in JET plasmas. J Phys B 2018;51:185701. http://dx.doi.org/10.1088/1361-6455/aad6d0.

[406] McKemmish LK, Yurchenko SN, Tennyson J. ExoMol line lists XVIII. The high-temperature spectrum of VO. Mon Not R Astron Soc 2016;463:771–93. http://dx.doi.org/10.1093/mnras/stw1969.

[407] Qu Q, Yurchenko SN, Tennyson J. A method for the variational calculation of hyperfine-resolved rovibronic spectra of diatomic molecules. J Chem Theory Comput 2022;18:1808–20. http://dx.doi.org/10.1021/acs.jctc.1c01244.

[408] Qu Q, Yurchenko SN, Tennyson J. A variational model for the hyperfine resolved spectrum of VO in its ground electronic state. J Chem Phys 2022;157:124305. http://dx.doi.org/10.1063/5.0105965.

[409] Bowesman CA, Yurchenko SN, Tennyson J. A hyperfine-resolved spectroscopic model for vanadium monoxide ($^{51}V^{16}O$). Mol Phys 2024;122:e2255299. http://dx.doi.org/10.1080/00268976.2023.2255299.

[410] Brady RP, Yurchenko SN, Kim G-S, Somogyi W, Tennyson J. An ab initio study of the rovibronic spectrum of sulphur monoxide (SO): diabatic vs. adiabatic representation. Phys Chem Chem Phys 2022;24:24076–88. http://dx.doi.org/10.1039/D2CP03051A.

[411] Brugamyer E, Dodson-Robinson SE, Cochran WD, Sneden C. Silicon and oxygen abundances in planet-host stars. Astrophys J 2011;738:97. http://dx.doi.org/10.1088/0004-637x/738/1/97.

[412] Bordiu C, Rizzo JR, Bufano F, Quintana-Lacaci G, Buemi C, Leto P, Cavallaro F, Cerrigone L, Ingallinera A, Loru S, Riggi S, Trigilio C, Umana G, Sciacca E. First detection of silicon-bearing molecules in eta Car. Astrophys J Lett 2022;939:L30. http://dx.doi.org/10.3847/2041-8213/ac9b10.

[413] Schilke P, Leurini S, Menten K, Alcolea J. Interstellar SiN. Astron Astrophys 2003;412:L15–8. http://dx.doi.org/10.1051/0004-6361:20031649.

[414] Turner JL, Dalgarno A. Chemistry of silicon in interstellar clouds. Astrophys J 1977;213:386–9. http://dx.doi.org/10.1086/155167.

[415] Feldman PA, Matthews HE, Bell MB, Herzberg G, Saito S, Endo Y, Hirota E. Limits to interstellar SiN. J R Astron Soc Can 1983;77:258.

[416] Davis DN. The spectrum of β Pegasi. Astron J 1947;106:28. http://dx.doi.org/10.1086/144938.

[417] Gratton L. Studies of the spectra of K-giants.1. A table of wave lengths and identifications of spectral lines In The Region lambda-lambda-4000 5000. Astron J 1952;115:346–401. http://dx.doi.org/10.1086/145554.

[418] Turner BE. Detection of SiN in IRC +10216. Astrophys J 1992;388:L35. http://dx.doi.org/10.1086/186324.

[419] Yousefi M, Bernath PF, Hodges J, Masseron T. A new line list for the $A^2\Sigma^+ - X^2\Pi$ electronic transition of OH. J Quant Spectrosc Radiat Transfer 2018;217:416–24. http://dx.doi.org/10.1016/j.jqsrt.2018.06.016.

[420] Furtenbacher T, Hegedus ST, Tennyson J, Császár AG. Analysis of the measured high-resolution doublet rovibronic spectra of ^{12}CH and ^{16}OH. Phys Chem Chem Phys 2022;24:19287. http://dx.doi.org/10.1039/D2CP02240K.

[421] Yorke L, Yurchenko SN, Lodi L, Tennyson J. ExoMol line lists VI: A high temperature line list for phosphorus nitride. Mon Not R Astron Soc 2014;445:1383–91. http://dx.doi.org/10.1093/mnras/stu1854.

[422] Semenov M, El-Kork N, Yurchenko SN, Tennyson J. Rovibronic spectroscopy of PN from first principles. Phys Chem Chem Phys 2021;23:22057–662. http://dx.doi.org/10.1039/D1CP02537F.

[423] Sochi T, Tennyson J. A computed line list for the H_2D^+ molecular ion. Mon Not R Astron Soc 2010;405:2345–50.

[424] Miller S, Geballe TR, Stallard T, Tennyson J. Thirty years of H_3^+ astronomy. Rev Modern Phys 2020;92:035003. http://dx.doi.org/10.1103/RevModPhys.92.035003.

[425] Barber RJ, Tennyson J, Harris GJ, Tolchenov RN. A high accuracy computed water line list. Mon Not R Astron Soc 2006;368:1087–94.

[426] Partridge H, Schwenke DW. The determination of an accurate isotope dependent potential energy surface for water from extensive ab initio calculations and experimental data. J Chem Phys 1997;106:4618–39. http://dx.doi.org/10.1063/1.473987.

[427] Melin ST, Sanders ST, Nasir EF. Comparison of ExoMol simulated spectra for H_2O to high-temperature low-pressure gas cell measurements at 1723 K in the 7321–7598 cm($-^1$) range. J Quant Spectrosc Radiat Transfer 2020;253:107079. http://dx.doi.org/10.1016/j.jqsrt.2020.107079.

[428] Furtenbacher T, Tóbiás R, Tennyson J, Polyansky OL, Császár AG. W2020: A database of validated rovibrational experimental transitions and empirical energy levels of $H_2^{16}O$. J Phys Chem Ref Data 2020;49:033101. http://dx.doi.org/10.1063/5.0008253.

[429] Furtenbacher T, Tóbiás R, Tennyson J, Polyansky OL, Kyuberis AA, Ovsyannikov RI, Zobov NF, Császár AG. W2020: A database of validated rovibrational experimental transitions and empirical energy levels part II. $H_2^{17}O$ and $H_2^{18}O$ with an update to $H_2^{16}O$. J Phys Chem Ref Data 2020;49:043103. http://dx.doi.org/10.1063/5.0030680.

[430] Voronin BA, Tennyson J, Tolchenov RN, Lugovskoy AA, Yurchenko SN. A high accuracy computed line list for the HDO molecule. Mon Not R Astron Soc 2010;402:492–6.

[431] Zobov NF, Koshelev MA, Makarov DS, Boyarkin OV, Tyuterev VG, Tennyson J, Polyansky OL. A global line list for HDO between 0 and 35000 cm^{-1} constructed using multiphoton spectra. J Quant Spectrosc Radiat Transfer 2021;271:107694. http://dx.doi.org/10.1016/j.jqsrt.2021.107694.

[432] Tennyson J, Bernath PF, Brown LR, Campargue A, Császár AG, Daumont L, Gamache RR, Hodges JT, Naumenko OV, Polyansky OL, Rothman LS, Toth RA, Vandaele AC, Zobov NF, Fally S, Fazliev AZ, Furtenbacher T, Gordon IE, Mikhailenko SN, A B. IUPAC critical evaluation of the rotational-vibrational spectra of water vapor. Part II. Energy levels and transition wavenumbers for HD^{16}O, HD^{17}O, and HD^{18}O. J Quant Spectrosc Radiat Transfer 2010;111:2160–84. http://dx.doi.org/10.1016/j.jqsrt.2010.06.012.

[433] Voronin BA, Tennyson J, Chesnokova TY, Chentsov AV, Bykov AD. The infrared absorption spectrum of the $H_2^{14}O$ radioactive isotopologue of water. Mol Phys http://dx.doi.org/10.1080/00268976.2024.2333474.

[434] Voronin BA, Tennyson J, Yurchenko SN, Chesnokova TY, Chentsov AV, Bykov AD, Makarova MV, Voronina SS, Cruz FC. The infrared absorption spectrum of radioactive water isotopologue $H_2^{15}O$. Spectrochim Acta A 2024;311:124007. http://dx.doi.org/10.1016/j.saa.2024.124007.

[435] Voronin BA, Tennyson J, Yurchenko SN, Chesnokova TY, Chentsov AV, Bykov AD, Cruz FC. The spectrum of radioactive water vapor: the $H_2^{19}O$ radio-isotopologue. J Radioanal Nucl Chem.

[436] Voronin BA, Makarova MV, Poberovskii AV, Bykov AD, Dudnikiva EA, Tennyson J. The absorption spectrum of short-lived isotopic variant of water, $H_2^{15}O$: Tentative detection at the earth's atmosphere. J Quant Spectrosc Radiat Transfer 2021;276:107929. http://dx.doi.org/10.1016/j.jqsrt.2021.107929.

[437] Huang X, Schwenke DW, Tashkun SA, Lee TJ. An isotopic-independent highly accurate potential energy surface for CO_2 isotopologues and an initial $^{12}C^{16}O_2$ infrared line list. J Chem Phys 2012;136:124311. http://dx.doi.org/10.1063/1.3697540.

[438] Polyansky OL, Bielska K, Ghysels M, Lodi L, Zobov NF, Hodges JT, Tennyson J. High accuracy CO_2 line intensities determined from theory and experiment. Phys Rev Lett 2015;114:243001. http://dx.doi.org/10.1103/PhysRevLett.114.243001.

[439] Yurchenko SN, Thiel W, Jensen P. Theoretical ROVibrational energies (TROVE): A robust numerical approach to the calculation of rovibrational energies for polyatomic molecules. J Mol Spectrosc 2007;245:126–40. http://dx.doi.org/10.1016/j.jms.2007.07.009.

[440] Balashov AA, Raj A, Wójtewicz S, Ciuryłło R, Lisak D, Bielska K. Theoretically predicted CO_2 lines near 700 nm not observed. J Quant Spectrosc Radiat Transfer 2024;108978. http://dx.doi.org/10.1016/j.jqsrt.2024.108978.

[441] Ibrahim MTI, Alatoom D, Furtenbacher T, Csaszar AG, Yurchenko SN, Azzam AAA, Tennyson J. MARVEL analysis of high-resolution rovibrational spectra of $^{13}C^{16}O_2$. J Comput Chem 2024;45:969–84. http://dx.doi.org/10.1002/jcc.27266.

[442] Alatoom D, Ibrahim MTI, Furtenbacher T, Csaszar AG, Alghizzawi M, Yurchenko SN, Azzam AAA, Tennyson J. MARVEL analysis of high-resolution rovibrational spectra of $^{16}O^{12}C^{18}O$. J Comput Chem 2024. http://dx.doi.org/10.1002/jcc.27453.

[443] Yachmenev A, Campargue A, Yurchenko SN, Küpper J, Tennyson J. Electric quadrupole transitions in carbon dioxide. J Chem Phys 2021;154:211104. http://dx.doi.org/10.1063/5.0053279.

[444] Fleurbaey H, Grilli R, Mondelain D, Kassi S, Yachmenev A, Yurchenko SN, Campargue A. Electric-quadrupole and magnetic-dipole contributions to the $\nu_2 + \nu_3$ band of carbon dioxide near 3.3 μm. J Quant Spectrosc Radiat Transfer 2021;266:107558. http://dx.doi.org/10.1016/j.jqsrt.2021.107558.

[445] Korablev OI, Belyaev DA, Dobrolenskiy YS, Trokhimovskiy AY, Kalinnikov YK. Acousto-optic tunable filter spectrometers in space missions (invited). Appl Opt 2018;57:C103–19. http://dx.doi.org/10.1364/AO.57.00C103.

[446] Wang Y, Owens A, Tennyson J, Yurchenko SN. MARVEL analysis of the measured high-resolution rovibronic spectra of the calcium monohydroxide radical (CaOH). Astrophys J Suppl Ser 2020;248:9. http://dx.doi.org/10.3847/1538-4365/ab85cb.

[447] Owens A, Clark VHJ, Mitrushchenkov A, Yurchenko SN, Tennyson J. Theoretical rovibronic spectroscopy of the calcium monohydroxide radical (CaOH). J Chem Phys 2021;154:234302. http://dx.doi.org/10.1063/5.0052958.

[448] Mitrushchenkov AO. A new general Renner-Teller (including $\varepsilon \geq 1$) spectroscopic formalism for triatomic molecules. J Chem Phys 2012;136:024108. http://dx.doi.org/10.1063/1.3672162.

[449] Reid IN, Kirkpatrick JD, Gizis JE, Dahn CC, Monet DG, Williams RJ, Liebert J, Burgasser AJ. Four nearby L dwarfs. Astron J 2000;119:369–77. http://dx.doi.org/10.1086/301177.

[450] Xu E, Tennyson J. Empirical rovibrational energy levels for carbonyl sulphide. Mol Phys 2023;e2279694. http://dx.doi.org/10.1080/00268976.2023.2279694.

[451] Esparza-Borges E, López-Morales M, Adams Redai JI, Pallé E, Kirk J, Casasayas-Barris N, Batalha NE, Rackham BV, Bean JL, Casewell SL, Decin L, Dos Santos LA, Muñoz AG, Harrington J, Heng K, Hu R, Mancini L, Molaverdikhani K, Morello G, Nikolov NK, Nixon MC, Redfield S, Stevenson KB, Wakeford HR, Alam MK, Benneke B, Blecic J, Crouzet N, Daylan T, Inglis J, Kreidberg L, Petit dit de la Roche DJM, Turner JD. Detection of carbon monoxide in the atmosphere of WASP-39b applying standard cross-correlation techniques to JWST NIRSPEC G395h data. Astrophys J Lett 2023;955:L19. http://dx.doi.org/10.3847/2041-8213/acf27b.

[452] Tsai S-M, Lee EKH, Powell D, Gao P, Zhang X, Moses J, Hébrard E, Venot O, Parmentier V, Jordan S, Hu R, Alam MK, Alderson L, Batalha NM, Bean JL, Benneke B, Bierson CJ, Brady RP, Carone L, Carter AL, Chubb KL, Inglis J, Leconte J, Line M, López-Morales M, Miguel Y, Molaverdikhani K, Rustamkulov Z, Sing DK, Stevenson KB, Wakeford HR, Yang J, Aggarwal K, Baeyens R, Barat S, de Val-Borro M, Daylan T, Fortney JJ, France K, Goyal JM, Grant D, Kirk J, Kreidberg L, Louca A, Moran SE, Mukherjee S, Nasedkin E, Ohno K, Rackham BV, Redfield S, Taylor J, Tremblin P, Visscher C, Wallack NL, Welbanks L, Youngblood A, Ahrer E-M, Batalha NE, Behr P, Berta-Thompson ZK, Blecic J, Casewell SL, Crossfield IJM, Crouzet N, Cubillos PE, Decin L, Désert J-M, Feinstein AD, Gibson NP, Harrington J, Heng K, Henning T, Kempton EM-R, Krick J, Lagage P-O, Lendl M, Lothringer JD, Mansfield M, Mayne NJ, Mikal-Evans T, Palle E, Schlawin E, Shorttle O, Wheatley PJ, Yurchenko SN. Photochemically produced SO_2 in the atmosphere of WASP-39b. Nature 2023;617:483. http://dx.doi.org/10.1038/s41586-023-05902-2.

[453] Grenfell JL. A review of exoplanetary biosignatures. Phys Rep 2017;713:1–17. http://dx.doi.org/10.1016/j.physrep.2017.08.003.

[454] Schwieterman EW, Olson SL, Pidhorodetska D, Reinhard CT, Ganti A, Fauchez TJ, Bastelberger ST, Crouse JS, Ridgwell A, Lyons TW. Evaluating the plausible range of N_2O biosignatures on exo-earths: An integrated biogeochemical, photochemical, and spectral modeling approach. Astrophys J 2022;937:109. http://dx.doi.org/10.3847/1538-4357/ac8cfb.

[455] Angerhausen D, Pidhorodetska D, Leung M, Hansen J, Alei E, Dannert F, Kammerer J, Quanz SP, Schwieterman EW, Initiative L. Large interferometer for exoplanets (LIFE). XII. The detectability of capstone biosignatures in the mid-infrared-sniffing exoplanetary laughing gas and methylated halogens. Astron J 2024;167:128. http://dx.doi.org/10.3847/1538-3881/ad1f4b.

[456] Tennyson J, Furtenbacher T, Yurchenko SN, Császár AG. Empirical rovibrational energy levels for nitrous oxide. J Quant Spectrosc Radiat Transfer 2024;316:108902. http://dx.doi.org/10.1016/j.jqsrt.2024.108902.

[457] Tennyson J. Empirical rovibronic energy levels of C_3. Mol Phys http://dx.doi.org/10.1080/00268976.2023.2276912.

[458] Furtenbacher T, Coles PA, Tennyson J, Yurchenko SN, Yu S, Drouin B, Tóbiás R, Császár AG. Empirical rovibational energy of ammonia up to 7500 cm^{-1}. J Quant Spectrosc Radiat Transfer 2020;251:107027. http://dx.doi.org/10.1016/j.jqsrt.2020.107027.

[459] Sadiek I, Fleisher AJ, Hayden J, Huang X, Hugi A, Engeln R, Lang N, van Helden J-PH. Dual-comb spectroscopy of ammonia formation in non-thermal plasmas. Comm Chem 2024;7:110. http://dx.doi.org/10.1038/s42004-024-01190-7.

[460] Coles PA, Ovsyannikov RI, Polyansky OL, Yurchenko SN, Tennyson J. Improved potential energy surface and spectral assignments for ammonia in the near-infrared region. J Quant Spectrosc Radiat Transfer 2018;219:199–212. http://dx.doi.org/10.1016/j.jqsrt.2018.07.022.

[461] Irwin PGJ, Bowles N, Braude AS, Garland R, Calcutt S, Coles PA, Yurchenko SN, Tennyson J. Analysis of gaseous ammonia (NH_3) absorption in the visible spectrum of jupiter - update. Icarus 2019;321:572–82. http://dx.doi.org/10.1016/j.icarus.2018.12.008.

[462] Yurchenko SN. A theoretical room-temperature line list for $^{15}NH_3$. J Quant Spectrosc Radiat Transfer 2015;152:28–36. http://dx.doi.org/10.1016/j.jqsrt.2014.10.023.

[463] Chubb KL, Joseph M, Franklin J, Choudhury N, Furtenbacher T, Császár AG, Gaspard G, Oguoko P, Kelly A, Yurchenko SN, Tennyson J, Sousa-Silva C. MARVEL analysis of the measured high-resolution spectra of C_2H_2. J Quant Spectrosc Radiat Transfer 2018;204:42–55. http://dx.doi.org/10.1016/j.jqsrt.2017.08.018.

[464] Mellor T, Owens A, Yurchenko SN, Tennyson J. MARVEL analysis of high-resolution spectra of thioformaldehyde (H_2CS). J Mol Spectrosc 2023;391:111732. http://dx.doi.org/10.1016/j.jms.2022.111732.

[465] Yurchenko SN, Owens A, Kefala K, Tennyson J. ExoMol line lists LVII. High accuracy ro-vibrational line list for methane (CH_4). Mon Not R Astron Soc 2024;528:3719–29. http://dx.doi.org/10.1093/mnras/stae148.

[466] Yurchenko SN, Tennyson J. ExoMol line lists IV: The rotation-vibration spectrum of methane up to 1500 K. Mon Not R Astron Soc 2014;440:1649–61. http://dx.doi.org/10.1093/mnras/stu326.

[467] Yurchenko SN, Amundsen DS, Tennyson J, Waldmann IP. A hybrid line list for CH_4 and hot methane continuum. Astron Astrophys 2017;605:A95. http://dx.doi.org/10.1051/0004-6361/201731026.

[468] Rey M, Nikitin AV, Tyuterev VG. Theoretical hot methane line list up T = 2000 K for astrophysical applications. Astrophys J 2014;789:2. http://dx.doi.org/10.1088/0004-637X/789/1/2.

[469] Rey M, Nikitin AV, Tyuterev VG. Accurate theoretical methane line lists in the infrared up to 3000 K and quasi-continuum absorption/emission modeling for astrophysical applications. Astrophys J 2017;847:105. http://dx.doi.org/10.3847/1538-4357/aa8909.

[470] Hargreaves RJ, Gordon IE, Rey M, Nikitin AV, Tyuterev VG, Kochanov RV, Rothman LS. An accurate, extensive, and practical line list of methane for the HITEMP database. Astrophys J Suppl Ser 2020;247:55. http://dx.doi.org/10.3847/1538-4365/ab7a1a.

[471] Kefala K, Yurchenko SN, Tennyson J. Assigning spectra of methane. 2024, (in preparation).

[472] Masseron T, Plez B, Van Eck S, Colin R, Daoutidis I, Godefroid M, Coheur P-F, Bernath P, Jorissen A, Christlieb N. CH in stellar atmospheres: an extensive linelist. Astron Astrophys 2014;571:A47. http://dx.doi.org/10.1051/0004-6361/201423956.

[473] Yousefi M, Bernath PF. Line lists for AlF and AlCl in the $X^1\Sigma^+$ ground state. Astrophys J Suppl Ser 2018;237:8. http://dx.doi.org/10.3847/1538-4365/aacc6a.

[474] Hou S, Bernath PF. Line list for the ground state of CaF. J Quant Spectrosc Radiat Transfer 2018;210:44–51. http://dx.doi.org/10.1016/j.jqsrt.2018.02.011.

[475] Hou S, Bernath PF. Line list for the MgF ground state. J Quant Spectrosc Radiat Transfer 2017;203:511–6.

[476] Frohman DJ, Bernath PF, Brooke JSA. Molecular line lists: The ro-vibrational spectra of NaF and KF. J Quant Spectrosc Radiat Transfer 2016;169:104–10. http://dx.doi.org/10.1016/j.jqsrt.2015.10.004.

[477] Bittner DM, Bernath PF. Line lists for LiF and LiCl in the $X^1\Sigma^+$ ground state. Astrophys J Suppl Ser 2018;235:8. http://dx.doi.org/10.3847/1538-4365/aa9846.

[478] Burrows A, Dulick M, Bauschlicher CW, Bernath PF, Ram RS, Sharp CM, Milsom JA. Spectroscopic constants, abundances, and opacities of the TiH molecule. Astrophys J 2005;624:988–1002. http://dx.doi.org/10.1086/429366.

[479] Chowdhury PK, Merer AJ, Rixon SJ, Bernath PF, Ram RS. Low-N lines of the A $^6\Sigma^+$ - X $^6\Sigma^+$ (1, 0) band of CrH. Phys Chem Chem Phys 2006;8:822–6. http://dx.doi.org/10.1039/b514188e.

[480] Wende S, Reiners A, Seifahrt A, Bernath PF. CRIRES spectroscopy and empirical line-by-line identification of FeH molecular absorption in an M dwarf. Astron Astrophys 2010;523:A58. http://dx.doi.org/10.1051/0004-6361/201015220.

[481] Bernath PF, Dodangodage R, Liévin J. S-type stars: LaO line list for the B $^2\Sigma^+$ - X $^2\Sigma^+$ band system. J Mol Spectrosc 2022;933:99. http://dx.doi.org/10.3847/1538-4357/ac731f.

[482] Li G, Gordon IE, Le Roy RJ, Hajigeorgiou PG, Coxon JA, Bernath PF, Rothman LS. Reference spectroscopic data for hydrogen halides. Part I: Construction and validation of the ro-vibrational dipole moment functions. J Quant Spectrosc Radiat Transfer 2013;121:78–90. http://dx.doi.org/10.1016/j.jqsrt.2013.02.005.

[483] Coxon JA, Hajigeorgiou PG. Improved direct potential fit analyses for the ground electronic states of the hydrogen halides: HF/DF/TF, HCl/D-Cl/TCl, HBr/DBr/TBr and HI/DI/TI. J Quant Spectrosc Radiat Transfer 2015;151:133–54. http://dx.doi.org/10.1016/j.jqsrt.2014.08.028.

[484] Li G, Gordon IE, Bernath PF, Rothman LS. Direct fit of experimental ro-vibrational intensities to the dipole moment function: Application to HCl. J Quant Spectrosc Radiat Transfer 2011;112:1543–50. http://dx.doi.org/10.1016/j.jqsrt.2011.03.014.

[485] Li G, Gordon IE, Hajigeorgiou PG, Coxon JA, Rothman LS. Reference spectroscopic data for hydrogen halides, part II: The line lists. J Quant Spectrosc Radiat Transfer 2013;130:284–95. http://dx.doi.org/10.1016/j.jqsrt.2013.07.019.

[486] Li G, Gordon IE, Rothman LS, Tan Y, Hu S-M, Kassi S, Campargue A, Medvedev ES. Rovibrational line lists for nine isotopologues of the CO molecule in the $X\ ^1\Sigma^+$ ground electronic state. Astrophys J Suppl Ser 2015;216:15. http://dx.doi.org/10.1088/0067-0049/216/1/15.

[487] Ram RS, Brooke JSA, Western CM, Bernath PF. Einstein A-values and oscillator strengths of the A $^2\Pi$ – X $^2\Sigma^+$ system of CP. J Quant Spectrosc Radiat Transfer 2014;138:107–15. http://dx.doi.org/10.1016/j.jqsrt.2014.01.030.

[488] Lodi L, Yurchenko SN, Tennyson J. The calculated rovibronic spectrum of scandium hydride, ScH. Mol Phys 2015;113:1559–75. http://dx.doi.org/10.1080/00268976.2015.1029996.

[489] Coppola CM, Lodi L, Tennyson J. Radiative cooling functions for primordial molecules. Mon Not R Astron Soc 2011;415:487–93.

[490] Amaral PHR, Diniz LG, Jones KA, Stanke M, Alijah A, Adamowicz L, Mohallem JR. Benchmark rovibrational linelists and Einstein A-coefficients for the primordial molecules and isotopologues. Astrophys J 2019;878:95. http://dx.doi.org/10.3847/1538-4357/ab1f65.

[491] Roueff E, Abgrall H, Czachorowski P, Pachucki K, Puchalski M, Komasa J. The full infrared spectrum of molecular hydrogen. Astron Astrophys 2019;630:A58. http://dx.doi.org/10.1051/0004-6361/201936249.

[492] Abgrall H, Roueff E, Launay F, Roncin J-Y. The B $^1\Sigma_u^+$ → X $^1\Sigma_g^+$ and D $^1\Pi_u$ → X $^1\Sigma_g^+$ band systems of molecular hydrogen. Can J Phys 1994;72:856–65. http://dx.doi.org/10.1139/p94-112.

[493] Owens A, Yachmenev A, Küpper J, Yurchenko SN, Thiel W. The rotation–vibration spectrum of methyl fluoride from first principles. Phys Chem Chem Phys 2018;21:3496–505. http://dx.doi.org/10.1039/C8CP01721B.

[494] Coles PA, Yurchenko SN, Kovacich RP, Hobby J, Tennyson J. A variationally computed room temperature line list for AsH_3. Phys Chem Chem Phys 2019;21:3264–77. http://dx.doi.org/10.1039/C8CP07110A.

[495] Owens A, Yurchenko SN. Theoretical rotation-vibration spectroscopy of cis- and trans-diphosphene (P_2H_2) and the deuterated species P_2HD. J Chem Phys 2019;150:194308. http://dx.doi.org/10.1063/1.5092767.

[496] Mant BP, Chubb KL, Yachmenev A, Tennyson J, Yurchenko SN. The infrared spectrum of PF_3 and the analysis of rotational energy clustering effect. Mol Phys 2019;118:e1581951. http://dx.doi.org/10.1080/00268976.2019.1581951.

[497] Adam AY, Yachmenev A, Yurchenko SN, Jensen P. A variationally computed IR line list for the methyl radical CH_3. J Phys Chem A 2019;123:22. http://dx.doi.org/10.1021/acs.jpca.9b02919.

[498] Clark VHJ, Owens A, Tennyson J, Yurchenko SN. The high-temperature rotation-vibration spectrum and rotational clustering of silylene (SiH_2). J Quant Spectrosc Radiat Transfer 2020;246:106929. http://dx.doi.org/10.1016/j.jqsrt.2020.106929.

[499] Syme A-M, McKemmish LK. Full spectroscopic model and trihybrid experimental-perturbative-variational line list for CN. Mon Not R Astron Soc 2021;505:4383–95. http://dx.doi.org/10.1093/mnras/stab1551.

[500] Perri AN, Taher F, McKemmish LK. Full spectroscopic model and trihybrid experimental-perturbative-variational line list for ZrO. Mon Not R Astron Soc 2023;524:4631–41. http://dx.doi.org/10.1093/mnras/stad2103.

[501] Perri AN, McKemmish LK. Full spectroscopic model and trihybrid experimental-perturbative-variational line list for NH. Mon Not R Astron Soc 2024;531:3023–33. http://dx.doi.org/10.1093/mnras/stae1340.

[502] Li X, Qin Z, Liu L. High-temperature molecular line list of hydroboron monoxide (hbo). Phys Chem Chem Phys 2024;26:12838–43. http://dx.doi.org/10.1039/d3cp05997a.

[503] Western CM, Carter-Blatchford L, Crozet P, Ross AJ, Morville J, Tokaryk DW. The spectrum of N_2 from 4 500 to 15 700 cm^{-1} revisited with PGOPHER. J Quant Spectrosc Radiat Transfer 2018;219:127–41. http://dx.doi.org/10.1016/j.jqsrt.2018.07.017.

[504] Campargue A, Solodov AM, Solodov AA, Yachmenev A, Yurchenko SN. Detection of electric-quadrupole transitions in water vapour near 5.4 and 2.5 μm. Phys Chem Chem Phys 2020;22:12476–81. http://dx.doi.org/10.1039/D0CP01667E.

[505] Qin Z, Bai T, Liu L. Line lists for the X $^2\Sigma^+$ – X $^2\Sigma^+$, A $^2\Pi$ – A $^2\Pi$ and A$^2\Pi$ – X$^2\Sigma^+$ transitions of CP. J Quant Spectrosc Radiat Transfer 2021;258:107352. http://dx.doi.org/10.1016/j.jqsrt.2020.107352.

[506] Bielska K, Kyuberis AA, Reed ZD, Li G, Cygan A, Ciuryło R, Adkins EM, Lodi L, Zobov NF, Ebert V, Lisak D, Hodges JT, Tennyson J, Polyansky OL. Subpromille measurements and calculations of CO (3–0) overtone line intensities. Phys Rev Lett 2022;129:043002. http://dx.doi.org/10.1103/PhysRevLett.129.043002.

[507] Balashov AA, Bielska GLK, Kyuberis AA, Wójtewicz S, Domysławska J, Ciuryło R, Zobov amd D. Lisak JTNF, Polyansky OL. Measurement and calculation of CO (7–0) overtone line intensities. J Chem Phys 2023;158:234306. http://dx.doi.org/10.1063/5.0152996.

[508] Khalil M, Mahmoud S, Brady RP, Almehairbi M, Gacesa M, Yurchenko SN, Tennyson J, Ghaferi AA, El-Kork N. Theoretical investigation of the $A^1\Pi - X^1\Sigma^+$, $B^1\Sigma^+ - X^1\Sigma^+$, $C^1\Sigma^+ - X^1\Sigma^+$, $D'^1\Sigma^+ - X^1\Sigma^+$ and $E^1\Pi - X^1\Sigma^+$. Phys Chem Chem Phys 2024. (submitted for publication).

[509] Somogyi W, Yurchenko SN, Yachmenev A. Calculation of electric quadrupole linestrengths for diatomic molecules: Application to the H_2, CO, HF, and O_2 molecules. J Chem Phys 2021;155:214303. http://dx.doi.org/10.1063/5.0063256.

[510] Somogyi W, Yurchenko SN, Kim G-S. An *ab initio* spectroscopic model of the molecular oxygen atmospheric and infrared bands. Phys Chem Chem Phys 2024. (submitted for publication).

[511] Yurchenko SN, Lodi L, Tennyson J, Stolyarov AV. Duo: A general program for calculating spectra of diatomic molecules. Comput Phys Comm 2016;202:262–75. http://dx.doi.org/10.1016/j.cpc.2015.12.021.

[512] Syme A-M, McKemmish LK. Experimental energy levels of $^{12}C^{14}N$ through MARVEL analysis. Mon Not R Astron Soc 2020;499:25–39. http://dx.doi.org/10.1093/mnras/staa2791.

[513] Brooke JSA, Ram RS, Western CM, Li G, Schwenke DW, Bernath PF. Einstein a coefficients and oscillator strengths for the A $^2\Pi$ – X $^2\Sigma^+$ (red) and B $^2\Sigma^+$ – X $^2\Sigma^+$ violet systems and rovibrational transitions in the X $^2\Sigma^+$ state of CN. Astrophys J Suppl Ser 2014;210:23. http://dx.doi.org/10.1088/0067-0049/210/2/23.

[514] McKemmish LK, Borsovszky J, Goodhew KL, Sheppard S, Bennett AFV, Martin ADJ, Singh A, Sturgeon CAJ, Furtenbacher T, Császár AG, Tennyson J. Marvel analysis of the measured high-resolution rovibronic spectra of $^{90}Zr^{16}O$. Astrophys J 2018;867:33. http://dx.doi.org/10.3847/1538-4357/aadd19.

[515] Sorensen JJ, Bernath PF. Near-infrared and visible opacities of S-type stars: The B $^1\Pi$ – X $^1\Sigma^+$ band system of ZrO. Astrophys J 2021;923:234. http://dx.doi.org/10.3847/1538-4357/ac300d.

[516] Darby-Lewis D, Shah H, Joshi D, Khan F, Kauwo M, Sethi N, Bernath PF, Furtenbacher T, Tóbiás R, Császár AG, Tennyson J. MARVEL analysis of the measured high-resolution spectra of ^{14}NH. J Mol Spectrosc 2019;362:69–76. http://dx.doi.org/10.1016/j.jms.2019.06.002.

[517] Brooke JSA, Bernath PF, Western CM, van Hemert MC, Groenenboom GC. Line strengths of rovibrational and rotational transitions within the X $^3\Sigma^-$ ground state of NH. J Chem Phys 2014;141:054310. http://dx.doi.org/10.1063/1.4891468.

[518] Brooke JSA, Bernath PF, Western CM. Note: Improved line strengths of rovibrational and rotational transitions within the X $^3\Sigma^-$ ground state of NH. J Chem Phys 2015;143:026101. http://dx.doi.org/10.1063/1.4923422.

[519] Fernando AM, Bernath PF, Hodges JN, Masseron T. A new linelist for the A $^3\Pi$ – X $^3\Sigma^-$ transition of the NH free radical. J Quant Spectrosc Radiat Transfer 2018;217:29–34. http://dx.doi.org/10.1016/j.jqsrt.2018.05.021.

[520] Jans ER. Rovibronic molecular line list for the N_2(C $^3\Pi_u \rightarrow$ B $^3\Pi_g$) second positive system. J Quant Spectrosc Radiat Transfer 2024;312:108809. http://dx.doi.org/10.1016/j.jqsrt.2023.108809.

[521] Vallon R, Richard C, Crozet P, Wannous G, Ross A. Laboratory measurements of NiH by Fourier transform dispersed fluorescence. Astrophys J 2009;696:172–5. http://dx.doi.org/10.1088/0004-637X/696/1/172.

[522] Harker H, Richard C, Tourasse G, Crozet P, Ross AJ. Zeeman spectroscopy of NiH: Lande factors of three $\Omega = \frac{3}{2}$ excited electronic states. J Mol Spectrosc 2013;292:28–34. http://dx.doi.org/10.1016/j.jms.2013.09.005.

[523] Havalyova I, Bozhinova I, Pashov A, Ross AJ, Crozet P. A coupled-channels model describing the low-lying $^2\Delta$, $^2\Sigma^+$ and $^2\Pi$ electronic states of nickel monohydride with experimental accuracy. J Quant Spectrosc Radiat Transfer 2021;272:107800. http://dx.doi.org/10.1016/j.jqsrt.2021.107800.

[524] Allard NF, Spiegelman F, Kielkopf JF. K–H_2 line shapes for the spectra of cool brown dwarfs. Astron Astrophys 2016;589:A21. http://dx.doi.org/10.1051/0004-6361/201628270.

[525] Allard NF, Spiegelman F, Leininger T, Molliere P. New study of the line profiles of sodium perturbed by H_2. Astron Astrophys 2019;628:A120. http://dx.doi.org/10.1051/0004-6361/201935593.

[526] Allard NF, Kielkopf JF, Myneni K, Blakely JN. New theoretical study of potassium perturbed by he and a comparison to laboratory spectra. Astron Astrophys 2024;683:A188. http://dx.doi.org/10.1051/0004-6361/202348711.

[527] Gamache RR, Roller C, Lopes E, Gordon IE, Rothman LS, Polyansky OL, Zobov NF, Kyuberis AA, Tennyson J, Yurchenko SN, Császár AG, Furtenbacher T, Huang X, Schwenke DW, Lee TJ, Drouin BJ, Tashkun SA, Perevalov VI, Kochanov RV. Total internal partition sums for 167 isotopologues of 53 molecules important in planetary atmospheres: application to HITRAN2016 and beyond. J Quant Spectrosc Radiat Transfer 2017;203:70–87. http://dx.doi.org/10.1016/j.jqsrt.2017.03.045.

[528] Irwin AW. Polynomial partition-function approximations of 344 atomic species and molecular-species. Astrophys J Suppl Ser 1981;45:621–33.

[529] Sauval AJ, Tatum JB. A set of partition functions and equilibrium constants for 300 diatomic molecules of astrophysical interest. Astrophys J Suppl Ser 1984;56:193–209. http://dx.doi.org/10.1086/190980.

[530] Barklem PS, Collet R. Partition functions and equilibrium constants for diatomic molecules and atoms of astrophysical interest. Astron Astrophys 2016;588:A96. http://dx.doi.org/10.1051/0004-6361/201526961.

[531] Sousa-Silva C, Hesketh N, Yurchenko SN, Hill C, Tennyson J. High temperature partition functions and thermodynamic data for ammonia and phosphine. J Quant Spectrosc Radiat Transfer 2014;142:66–74. http://dx.doi.org/10.1016/j.jqsrt2014.03.012.

[532] Tennyson J, Hill C, Yurchenko SN. Data structures for ExoMol: Molecular line lists for exoplanet and other atmospheres. In: 6th international conference on atomic and molecular data and their applications. ICAMDATA-2012, AIP conference proceedings, vol. 1545, New York: AIP; 2013, p. 186–95. http://dx.doi.org/10.1063/1.4815853.

[533] Tennyson J, Hulme K, Naim OK, Yurchenko SN. Radiative lifetimes and cooling functions for astrophysically important molecules. J Phys B 2016;49:044002. http://dx.doi.org/10.1088/0953-4075/49/4/044002.

[534] Hill C, Hanicinec M. A python package for managing simple chemical species and states. 2022, https://github.com/xnx/pyvalem, version 2.5.12.

[535] Hill C, Dipti, Hanicinec M, et al. PyValem: a machine-readable notation and python library for atomic and molecular structures and states. 2024, Manuscript (in preparation).

[536] Pezoa F, Reutter JL, Suarez F, Ugarte M, Vrgoč D. Foundations of json schema. In: Proceedings of the 25th international conference on world wide web, international world wide web conferences steering committee. 2016, p. 263–73.

[537] Furtenbacher T, Szidarovszky T, Hruby J, Kyuberis AA, Zobov NF, Polyansky OL, Tennyson J, Császár AG. Definitive high-temperature ideal-gas thermochemical functions of the $H_2^{16}O$ molecule. J Phys Chem Ref Data 2016;45:043104. http://dx.doi.org/10.1063/1.4967723.

[538] Miller S, Stallard T, Melin H, Tennyson J. H_3^+ cooling in planetary atmospheres. Faraday Discuss 2010;147:283–91. http://dx.doi.org/10.1039/C004152C.

[539] Miller S, Stallard T, Tennyson J, Melin H. Cooling by H_3^+ emission. J Phys Chem A 2013;117:9770–7.

[540] Wells DC, Greisen EW, Harten RH. FITS - a flexible image transport system. Astron Astrophys Suppl 1981;44:363.

[541] Mollière P, Wardenier JP, van Boekel R, Henning T, Molaverdikhani K, Snellen IAG. petitRADTRANS - A Python radiative transfer package for exoplanet characterization and retrieval. Astron Astrophys 2019;627:A67. http://dx.doi.org/10.1051/0004-6361/201935470.

[542] Mollière P, Nasedkin E, Blain D. petitRADTRANS. 2023, http://dx.doi.org/10.5281/zenodo.8337871.

[543] Irwin PGJ, Teanby NA, de Kok R, Fletcher LN, Howett CJA, Tsang CCC, Wilson CF, Calcutt SB, Nixon CA, Parrish PD. The NEMESIS planetary atmosphere radiative transfer and retrieval tool. J Quant Spectrosc Radiat Transfer 2008;109:1136–50. http://dx.doi.org/10.1016/j.jqsrt.2007.11.006.

[544] Fortney JJ, Robinson TD, Domagal-Goldman S, Del Genio AD, Gordon IE, ib Nezhad E, Lewis N, Sousa-Silva C, Airapetian V, Drouin B, Hargreaves RJ, Huang X, Karman T, Ramirez RM, Rieker GB, Tennyson J, Wordsworth R, Yurchenko SN, Johnson AV, Lee TJ, Dong C, Kane S, Lopez-Morales M, Fauchez T, Lee T, Marley MS, Sung K, Haghighipour N, Robinson T, Horst S, Gao P, you Kao D, Dressing C, Lupu R, Savin DW, Fleury B, Venot O, Ascenzi D, Milam S, Linnartz H, Gudipati M, Gronoff G, Salama F, Gavilan L, Bouwman J, Turbet M, Benilan Y, Henderson B, Batalha N, Jensen-Clem R, Lyons T, Freedman R, Schwieterman E, Goyal J, Mancini L, Irwin P, Desert J-M, Molaverdikhani K, Gizis J, Taylor J, Lothringer J, Pierrehumbert R, Zellem R, Batalha N, Rugheimer S, Lustig-Yaeger J, Hu R, Kempton E, Arney G, Line M, Alam M, Moses J, Iro N, Kreidberg L, Blecic J, Louden T, Molliere P, Stevenson K, Swain M, Bott K, Madhusudhan N, Krissansen-Totton J, Deming D, Kitiashvili I, Shkolnik E, Rustamkulov Z, Rogers L, Close L. The need for laboratory measurements and ab initio studies to aid understanding of exoplanetary atmospheres. 2019, arXiv:1905.07064.

[545] Barton EJ, Hill C, Czurylo M, Li H-Y, Hyslop A, Yurchenko SN, Tennyson J. The ExoMol diet: H_2 and he line-broadening parameters. J Quant Spectrosc Radiat Transfer 2017;203:490–5. http://dx.doi.org/10.1016/j.jqsrt.2017.01.028.

[546] Ma Q, Tipping R, Boulet C. Modification of the Robert–Bonamy formalism in calculating Lorentzian half-widths and shifts. J Quant Spectrosc Radiat Transfer 2007;103:588–96. http://dx.doi.org/10.1016/j.jqsrt.2006.08.001.

[547] Sokolov A, Yurchenko SN, Tennyson J, Gamache RR, Vispoel B. Calculation of collisional line-broadening and shifting of acetylene using the complex Robert–Bonamy–Ma approach. J Quant Spectrosc Radiat Transfer 2024. (in preparation).

[548] Guest ER, Tennyson J, Yurchenko SN. Modelling the rotational dependence of line broadening using machine learning. J Mol Spectrosc 2024;401:111901. http://dx.doi.org/10.1016/j.jms.2024.111901.

[549] Guest E. Predicting the rotational dependence of line broadening using machine learning. 2024, http://dx.doi.org/10.5281/zenodo.10631728.

[550] Buldyreva J, Yurchenko SN, Tennyson J. Simple semi-classical model of pressure-broadened infrared/microwave linewidths in the temperature range 200–3000 K. RAS Tech Instrum 2022;1:43–7. http://dx.doi.org/10.1093/rasti/rzac004.

[551] Buldyreva J, Stehlin K, Yurchenko SN, Guest ER, Tennyson J. Semi-classical estimates of pressure-induced linewidths for infrared absorption by hot (exo)planetary atmospheres. Astrophys. J. Suppl. Ser. 2024. (submitted for publication).

[552] Buldyreva J, Brady RP, Yurchenko SN, Tennyson J. Collisional broadening of molecular rovibronic lines. J Quant Spectrosc Radiat Transfer 2024;313:108843. http://dx.doi.org/10.1016/j.jqsrt.2023.108843.

[553] Hazi AU, Taylor HS. Stabilization method of calculating resonance energies: Model problem. Phys Rev A 1970;1:1109–20. http://dx.doi.org/10.1103/PhysRevA.1.1109.

[554] Bacic Z, Simons J. Resonance energies and lifetimes from stabilization-based methods. J Phys Chem 1982;86:1192–200. http://dx.doi.org/10.1021/j100396a027.

[555] Mandelshtam VA, Ravuri TR, Taylor HS. Calculation of the density of resonance states using the stabilization method. Phys Rev Lett 1993;70:1932–5. http://dx.doi.org/10.1103/PhysRevLett.70.1932.

[556] Pezzella M, Yurchenko SN, Tennyson J. ExoMol photodissociation cross-sections I – HCl and HF. Mon Not R Astron Soc 2022;514:4413–25. http://dx.doi.org/10.1093/mnras/stac1634.

[557] Venot O, Bénilan Y, Fray N, Gazeau M-C, Lefèvre F, Es-sebbar E, Hébrard E, Schwell M, Bahrini C, Montmessin F, Lefèvre M, Waldmann IP. VUV-absorption cross-section of carbon dioxide from 150 to 800 K and applications to warm exoplanetary atmospheres. Astron Astrophys 2018;609:A34. http://dx.doi.org/10.1051/0004-6361/201731295.

[558] Rothman LS, Gordon IE, Babikov Y, Barbe A, Benner DC, Bernath PF, Birk M, Bizzocchi L, Boudon V, Brown LR, Campargue A, Chance K, Cohen EA, Coudert LH, Devi VM, Drouin BJ, Fayt A, Flaud J-M, Gamache RR, Harrison JJ, Hartmann J-M, Hill C, Hodges JT, Jacquemart D, Jolly A, Lamouroux J, Le Roy RJ, Li G, Long DA, Lyulin OM, Mackie CJ, Massie ST, Mikhailenko S, Müller HSP, Naumenko OV, Nikitin AV, Orphal J, Perevalov V, Perrin A, Polovtseva ER, Richard C, Smith MAH, Starikova E, Sung K, Tashkun S, Tennyson J, Toon GC, Tyuterev VG, Wagner G. The *HITRAN* 2012 molecular spectroscopic database. J Quant Spectrosc Radiat Transfer 2013;130:4–50. http://dx.doi.org/10.1016/jqsrt.2013.07.002.

[559] Jack D, Hauschildt PH, Baron E. Time-dependent radiative transfer with PHOENIX. Astron Astrophys 2009;502:1043–9.

[560] Tennyson J, Mohr S, Hanicinec M, Dzarasova A, Smith C, Waddington S, Liu B, Alves LL, Bartschat K, Bogaerts A, Engelmann SU, Gans T, Gibson AR, Hamaguchi S, Hamilton KR, Hill C, O'Connell D, Rauf S, van 't Veer K, Zatsarinny O. The 2021 release of the quantemol database (QDB) of plasma chemistries and reactions. Plasma Sources Sci Technol 2022;31:095020. http://dx.doi.org/10.1088/1361-6595/ac907e.

[561] Owens A, Mitrushchenkov A, Yurchenko SN, Tennyson J. ExoMol line lists – XLVII. Rovibronic molecular line list of the calcium monohydroxide radical (CaOH). Mon Not R Astron Soc 2022;516:3995–4002. http://dx.doi.org/10.1093/mnras/stac2462.

[562] Pezzella M, Mitev GB, Yurchenko SN, Tennyson J, Mitrushchenkov AO. A variational method for studying the photodissociation of triatomic molecules. Phys Chem Chem Phys 2024. (submitted for publication).

[563] Weck PF, Schweitzer A, Stancil PC, Hauschildt PH, Kirby K. The molecular continuum opacity of ^{24}MgH in cool stellar atmospheres. Astrophys J 2003;584:459–64. http://dx.doi.org/10.1086/345524.

[564] Miyake S, Gay CD, Stancil PC. Rovibrationally resolved photodissociation of HeH^+. Astrophys J 2011;735:21. http://dx.doi.org/10.1088/0004-637X/735/1/21.

[565] el Qadi WH, Stancil PC. Photodissociation of CN. Astrophys J 2013;779:97. http://dx.doi.org/10.1088/0004-637X/779/2/97.

[566] McMillan EC, Shen G, McCann JF, McLaughlin BM, Stancil PC. Rovibrationally resolved photodissociation of SH^+. J Phys B 2016;49:084001. http://dx.doi.org/10.1088/0953-4075/49/8/084001.

[567] Pattillo RJ, Cieszewski R, Stancil PC, Forrey RC, Babb JF, McCann JF, McLaughlin BM. Photodissociation of CS from excited rovibrational levels. Astrophys J 2018;858:10. http://dx.doi.org/10.3847/1538-4357/aab5b9.

[568] Bai T, Qin Z, Liu L. Rovibrationally resolved direct photodissociation of MgO. Mon Not R Astron Soc 2021;505:2177–85. http://dx.doi.org/10.1093/mnras/stab1426.

[569] Qin Z, Bai T, Liu L. Temperature-dependent direct photodissociation cross-sections and rates of AlCl. Mon Not R Astron Soc 2021;508:2848–54. http://dx.doi.org/10.1093/mnras/stab2655.

[570] Qin Z, Bai T, Liu L. Destruction of AlF: a quantum study of its ground -state photodissociation. Mon Not R Astron Soc 2022;510:3011–8. http://dx.doi.org/10.1093/mnras/stab3598.

[571] Bai T, Yang X, Qin Z, Liu L. Photodissociation cross-sections and rates of NaO. Mon Not R Astron Soc 2023;527:3847–57. http://dx.doi.org/10.1093/mnras/stad3447.

[572] Qin Z, Hu P, Bai T, Liu L. A theoretical study of temperature-dependent photodissociation cross-sections and rates for O_2. Astrophys J Suppl Ser 2023;269:48. http://dx.doi.org/10.3847/1538-4365/ad03ed.

[573] Spake JJ, Sing DK, Evans TM, Oklopčić A, Bourrier V, Kreidberg L, Rackham BV, Irwin J, Ehrenreich D, Wyttenbach A, Wakeford HR, Zhou Y, Chubb KL, Nikolov N, Goyal JM, Henry GW, Williamson MH, Blumenthal S, Anderson DR, Hellier C, Charbonneau D, Udry S, Madhusudhan N. Helium in the eroding atmosphere of an exoplanet. Nature 2018;557:68–70. http://dx.doi.org/10.1038/s41586-018-0067-5.

[574] Hoeijmakers HJ, Seidel JV, Pino L, Kitzmann D, Sindel JP, Ehrenreich D, Oza AV, Bourrier V, Allart R, Gebek A, Lovis C, Yurchenko SN, Astudillo-Defru N, Bayliss D, Cegla H, Lavie B, Lendl M, Melo C, Murgas F, Nascimbeni V, Pepe F, Ségransan D, Udry S, Wyttenbach A, Heng K. Hot exoplanet atmospheres resolved with transit spectroscopy (HEARTS) - IV. A spectral inventory of atoms and molecules in the high-resolution transmission spectrum of WASP-121 b. Astron Astrophys 2020;641:A123. http://dx.doi.org/10.1051/0004-6361/202038365.

[575] Cont D, Yan F, Reiners A, Casasayas-Barris N, Mollière P, Pallé E, Henning T, Nortmann L, Stangret M, Czesla S, López-Puertas M, Sánchez-López A, Rodler F, Ribas I, Quirrenbach A, Caballero JA, Amado PJ, Carone L, Khaimova J, Kreidberg L, Molaverdikhani K, Montes D, Morello G, Nagel E, Oshagh M, Zechmeister M. Detection of fe and evidence for TiO in the dayside emission spectrum of WASP-33b. Astron Astrophys 2021;651:A33. http://dx.doi.org/10.1051/0004-6361/202140732.

[576] Kramida A, Ralchenko Yu, Reader J, NIST ASD Team. NIST atomic spectra database (ver. 5.6.1). Gaithersburg, MD: National Institute of Standards and Technology; 2019, [Online]. Available: https://physics.nist.gov/asd [2019, April 13].

[577] Kramida A, Ralchenko Y, Reader J, NIST ASD Team. Development of nist atomic databases and online tools. Atoms 2020;8:56. http://dx.doi.org/10.3390/atoms8030056.

[578] Wright SOM, Nugroho SK, Gibson NP, de Mooij EJW, Waldmann I, Tennyson J, Kawahara H, Kuzuhara M, Hirano T, Kotani T, Kawashima Y, Watson CA, Tamura M, Zwintz K, Harakawa H, Hodapp K, Jacobson S, Konishi M, Kurokawa T, Nishikawa J, Omiya M, Serizawa T, Serizawa T, Ueda A, Vievard S, Yurchenko SN. A spectroscopic thermometer: individual vibrational band spectroscopy with the example of OH in the atmosphere of WASP-33b. Astron J 2023;166:41. http://dx.doi.org/10.3847/1538-3881/acdb75.

[579] Sousa-Silva C, Petkowski JJ, Seager S. Molecular simulations for the spectroscopic detection of atmospheric gases. Phys Chem Chem Phys 2019;21:18970–87. http://dx.doi.org/10.1039/C8CP07057A.

[580] Tinetti G, Drossart P, Eccleston P, Hartogh P, Heske A, Leconte J, Micela G, Ollivier M, Pilbratt G, Puig L, Turrini D, Vandenbussche B, Wolkenberg P, Beaulieu J-P, Buchave LA, Ferus M, Griffin M, Guedel M, Justtanont K, Lagage P-O, Machado P, Malaguti G, Min M, Nø rgaard Nielsen HU, Rataj M, Ray T, Ribas I, Swain M, Szabo R, Werner S, Barstow J, Burleigh M, Cho J, du Foresto VC, Coustenis A, Decin L, Encrenaz T, Galand M, Gillon M, Helled R, Morales JC, Muñoz AG, Moneti A, Pagano I, Pascale E, Piccioni G, Pinfield D, Sarkar S, Selsis F, Tennyson J, Triaud A, Venot O, Waldmann I, Waltham D, Wright G, Amiaux J, Auguères J-L, Berthé M, Bezawada N, Bishop G, Bowles N, Coffey D, Colomé J, Crook M, Crouzet P-E, Da Peppo V, Sanz IE, Focardi M, Frericks M, Hunt T, Kohley R, Middleton K, Morgante G, Ottensamer R, Pace E, Pearson C, Stamper R, Symonds K, Rengel M, Renotte E, Ade P, Affer L, Alard C, Allard N, Altieri F, André Y, Arena C, Argyriou I, Aylward A, Baccani C, Bakos G, Banaszkiewicz M, Barlow M, Batista V, Bellucci G, Benatti S, Bernardi P, Bézard B, Blecka M, Bolmont E, Bonfond B, Bonito R, Bonomo AS, Brucato JR, Brun AS, Bryson I, Bujwan W, Casewell S, Charnay B, Pestellini CC, Chen G, Ciaravella A, Claudi R, Clédassou R, Damasso M, Damiano M, Danielski C, Deroo P, Di Giorgio AM, Dominik C, Doublier V, Doyle S, Doyon R, Drummond B, Duong B, Eales S, Edwards B, Farina M, Flaccomio E, Fletcher L, Forget F, Fossey S, Fränz M, Fujii Y, García-Piquer Á, Gear W, Geoffray H, Gérard JC, Gesa L, Gomez H, Graczyk R, Griffith C, Grodent D, Guarcello MG, Gustin J, Hamano K, Hargrave P, Hello Y, Heng K, Herrero E, Hornstrup A, Hubert B, Ida S, Ikoma M, Iro N, Irwin P, Jarchow C, Jaubert J, Jones H, Julien Q, Kameda S, Kerschbaum F, Kervella P, Koskinen T, Krijger M, Krupp N, Lafarga M, Landini F, Lellouch E, Leto G, Luntzer A, Rank-Lüftinger T, Maggio A, Maldonado J, Maillard J-P, Mall U, Marquette J-B, Mathis S, Maxted P, Matsuo T, Medvedev A, Miguel Y, Minier V, Morello G, Mura A, Narita N, Nascimbeni V, Nguyen Tong N, Noce V, Oliva F, Palle E, Palmer P, Pancrazzi M, Papageorgiou A, Parmentier V, Perger M, Petralia A, Pezzuto S, Pierrehumbert R, Pillitteri I, Piotto G, Pisano G, Prisinzano L, Radioti A, Réess J-M, Rezac L, Rocchetto M, Rosich A, Sanna N, Santerne A, Savini G, Scandariato G, Sicardy B, Sierra C, Sindoni G, Skup K, Snellen I, Sobiecki M, Soret L, Sozzetti A, Stiepen A, Strugarek A, Taylor J, Taylor W, Terenzi L, Tessenyi M, Tsiaras A, Tucker C, Valencia D, Vasisht G, Vazan A, Vilardell F, Vinatier S, Viti S, Waters R, Wawer P, Wawrzaszek A, Whitworth A, Yung YL, Yurchenko SN, Osorio MRZ, Zellem R, Zingales T, Zwart F. A chemical survey of exoplanets with ARIEL. Exp Astron 2018;46:135–209. http://dx.doi.org/10.1007/s10686-018-9598-x.

[581] Pascale E, Bezawada N, Barstow J, Beaulieu J-P, Bowles N, du Foresto VC, Coustenis A, Decin L, Drossart P, Eccleston P, Encrenaz T, Forget F, Griffin M, Güdel M, Hartogh P, Heske A, Lagage P-O, Leconte J, Malaguti P, Micela G, Middleton K, Min M, Moneti A, Morales JC, Mugnai L, Ollivier M, Pace E, Papageorgiou A, Pilbratt G, Puig L, Rataj M, Ray T, Ribas I, Rocchetto M, Sarkar S, Selsis F, Taylor W, Tennyson J, Tinetti G, Turrini D, Vandenbussche B, Venot O, Waldmann IP, Wolkenberg P, Wright G, Osorio M-RZ, Zingales T. The ARIEL space mission. In: Lystrup M, MacEwen HA, Fazio GG, Batalha N, Siegler N, Tong EC, editors. Space telescopes and instrumentation 2018: optical, infrared, and millimeter wave, Vol. 10698. International Society for Optics and Photonics, SPIE; 2018, 106980H. http://dx.doi.org/10.1117/12.2311838.